Classical & Quantum Chaos In a Non-Linearly Kicked Harmonic Oscillator

Mark V. Daly B Sc

A thesis submitted for the degree of Doctor Of Philosophy

Dublin City University

School of Physical Sciences

Supervisor Prof Daniel M Heffernan

August 1994

I hereby certify that this material, which I now submit for assessment on the programme of study leading to the award of PhD is entirely my own work and has not been taken from the work of others save and to the extent that such work has been cited and acknowledged within the text of my work

Signed· I.D. No.:

Candidate

Date.

In Memory of Major Thomas J. Corley

(1909 - 1985)

Requiēscās in Pace, Praeceptor Meus

ABSTRACT

The work described in this thesis is based on a detailed analysis of the classical and quantum non linear dynamics of a kicked oscillator This system belongs to a class of kicked physical systems (time dependent Hamiltonians) whose dynamics have universal properties We begin the analysis by considering the classical mapping (recursive relationship) derived from the parent system equations The analysis covers the system's phase space and its evolution as parameters are changed The detailed orbit structure is obtained and the break-up of this orbit structure in the phase space, influenced by presence of periodic orbits, is examined thoroughly We also show the existence of two types of orbital diffusion (normal diffusion and a resonance enhanced diffusion) The results from this classical analysis are then compared with the quantum mapping The complexity of this quantum mapping is considerable but, with some necessary numerical considerations, we have used it to generate the time evolution of the quantum probability amplitudes of the system's eigenfunctions These amplitudes permit the calculation of the system's energy as time progresses and enable us to compare the quasi-phase space given by the Wigner distrubution with the classical manifold structure to check for *scarring* of the quantum wavefunctions The quantum mapping we derive has not been defined in any of the literature so that all the results obtained in the quantum regime are original In the classical regime our work on periodic orbits and resonance enhanced diffusion is also original We have adopted some techniques and methods from other kicked systems and modified them for our system to complete the investigation of the kicked oscillator

ACKNOWLEDGEMENTS

The work contained in thesis cannot be justly attributed solely to myself but also to all those who in some way or other made my time as a post-graduate so much more *interesting* than it would have been without them I don't like presenting lists of who did this and that etc, etc What I want to present here is a collection of the messages I would like to pass on to those who shared these last five years with me, both in D C U and St Patrick's College, Maynooth and also to those without whom I would never have started or finished this work

This thesis is dedicated to one person who unfortunately will never see it The measure of one's greatness is not how great they consider themselves but how fortunate people think themselves to be having known such a person This can never be more true in the case of Major Thomas J Corley without whom the lives of many would have been so very much duller and without whom I would never have had the opportunity nor the ability to complete this research I hope your trust in me was not ill-placed

Laughter is such a definitive tonic that if it was possible to capture its essence and bottle it would most certainly be called *The Carter Girls* The potency of this essence is without equal as can be judged by the effect these two people have on all around them when they get started I can only say this you two have cheered me up on so many occasions that if a laugh was worth money I'd owe more than most developed countries You two are fantastic and I love you both for all you've given me over the years Cheers!

To my family, close relatives and friends I give my thanks for the times I've been encouraged and comforted by you Its good to know there's always a place called *home* waiting for you with those you love willing to help when times are bad or joining in the laughter when times are good If I had it all to do again I wouldn't change a thing Its from the mistakes I've made that I've learned so much more about people, life and loyalty than I would have known if I hadn't made any in the first place To be welcomed with open arms and not judged prematurely is surely a most blessed gift and one which I know is there for me at *home*

Life is all about taking risks and chances It was such when Professor Daniel

Heffernan took me on to do research for him back in '89 If it wasn't for his willingness to take a chance with me and take me on as a post-grad then the past five years would not have unfolded the way they did and my life would certainly be very much different now than is the case It is only fitting that I take this opportunity to personally thank Professor Daniel Heffernan for his foresight in giving me this chance to do *some real physics* Thanks Danny for all the help and guidance you've given me

I was not the only person *in the same boat* when a post-graduate in D C U and it is to my fellow past (and present) colleagues that I dedicate this paragraph The number of people I have come to know while a post-graduate precludes my presenting a complete list here so I'll just thank you all for the good times and the bad There are a few I would like to single out for special mention To Billy, for the laughs, strategy games, good conversation and all the bottles of Miller you owe me, thanks! The last few years wouldn't have been near as good as they have been without you To Catherine for all the laughs and good chats we've had To the staff of the School of Physical Sciences in D C U , especially Prof Eugene Kennedy, and the staff in the Dept of Mathematical Physics in Maynooth I want to thank you for all the help you've given me in the past I also want to single out Dr Charles Nash for giving me all the help he has both with the administration of the network in Maynooth and his help in unravelling the compexities of TEX Finally to all those, too numerous to mention (so I won't), thank you for the past five years

To my beloved Janet, without whom I would be so much less a person than I am now The time we've been together is so precious that I won't demean it with words Surely one who has the love of another is blessed but to love (and be loved) by such a special person as you is more wonderful than I could ever have imagined possible Thank you for all that you've given me, my love and I'll try not to let you down I love you

Finally, if there's anyone else out there I haven't mentioned or who doesn't fall into any of the above categories TOUGH!

TABLE OF CONTENTS

OVERVIEW OF THESIS LAYOUT & CONTENTS

The work presented in this thesis is in two parts, the classical regime of the kicked harmonic oscillator and the corresponding quantum regime The classical regime is presented first and the results from the detailed analysis are presented in chapters 3 & 4 We then proceed to the more abstract fully quantum regime and compare the results obtained, in chapters 6 & 7, with those in the earlier chapters from the classical regime Our intention is to relate the dynamics & phase space structures in the classical regime to the evolution of wavefunctions, energies & qausi-phase space distributions in the fully quantum regime Consequently, we will illustrate how remnants of the classical regime are visible in the fully quantum regime without us having to explore such limits as $\hbar \to 0$

The principle reasons for our choosing the kicked harmonic oscillator are that this system is physically real (and not mathematically motivated) and classically chaotic Furthermore, it has been postulated by Berman et al (1991) that the kicked rotator, which is known to have suppression of chaos in the quantum regime, is not a generic kicked system They argue that the presence of an extra time scale in the kicked oscillator can give rise to wavefunction de-localisation and hence non suppression of chaos in the quantum regime

In chapter 1 we review the area of Hamiltonian chaos which is pertinent to the research carried out by us The chapter also introduces the physical significance of the system we examine (Chernikov et al (1987)) and shows how the equations governing the system are obtained Some definitions are included at the end of the chapter of the more important expressions and terms used in the later analysis

Chapter 2 consists solely of the derivation of the classical mapping from the Hamiltonian describing the kicked harmonic oscillator We proceed by expressing the Hamiltonian in terms of the systems annihilation & creation operators with no specific kick potential is given Our reason for this is to show the generic nature of the mapping thus obtained through comparison with that obtained Goggin et al (1990) for their formulation of the quantum logistic map We then proceed with a specific potential so that the system corresponds to the physical system presented in section 1 3 of this chapter (Chernikov et

al (1987)) Once the final expression is arrived at, the mapping is transposed to from a quantum operator regime to a classical scalar regime and the final classical mapping is presented once the real and complex terms of the expression are separated The special case of a resonant kicking, *i e* when the kick period is commensurate with the natural period of oscillation of the free harmonic oscillator, is highlighted specifically as this is the case we are primarily considering Some phase space portraits are also included for the purpose of illustrating the diversity of dynamic behaviour present

The analysis of the derived classical mapping takes place in chapters 3 & 4 In chapter 3 we examine the structure of the phase space and use the subsequent results to highlight the mechanisms of orbit travel in the diffuse *stohcastic* layer within this phase space We also obtain an expression which allows us to predict the orders of periodic points existing on the layer boundary and show using the K A M theorem how these affect the break up of stable orbits in the invariant cells in the phase space which define the stable motion of the system Due to the fundamental importance of the stochastic layer in defining the non-linear properties of our kicked system, we examine the layer itself specifically its width variation as a function of the kick strength and the diffusion of orbits within the layer itself This latter examination is presented in chapter 4 where we undertake an analysis similar to that of Rechester & White (1890) We examine the effect of correlations, between iterates, on the diffusion of orbits and we modify the approach of Rechester & White so that it can successfully model the behaviour of our kicked system We also highlight how strong correlations between iterates can lead to a resonance effect which manifests itself as spikes on the diffusion curve A comparison is made between our expressions for this enhancement and the predictions of Ishizaki et al (1989) for their investigation of a similar phenomenon for the kicked rotator

The derivation of the quantum mapping signifies the beginning of the quantum analysis of our kicked oscillator The approach we take is similar to Fox et al ((1990), (1994)) which maps the probability amphtudes of the undriven oscillator's eigenfunctions from kick to kick This allows us to construct wavefunctions, energy evolutions, phase space distributions and quasi-energy levels The approach uses a fixed evolution matrix which multiplies a vector, consisting of the amplitude strengths of one time step, to give

a vector consisting of the amplitudes at the subsequent time step This approach allows all the analysis to be carried out, for a given set of parameter values, by just calculating a single matrix However, for each parameter change, a new matrix must be evaluated The derivation proper and the numerical short-cuts we considered when computing these evolution matrices are included in chapter 5

The results from our quantum mapping are analysed in chapter 6 & 7 We take a three-tiered approach to the analysis, namely a neghgble kick strength input, a moderate kick strength input and a large kick strength input Our reasons for this are made clear in chapter 6 The vast choice of initial distributions of probability amplitude strengths is overcome by considering two types a pure state of the undriven oscillator and a mixed state consisting of a weighted distribution of the undriven oscillator's eigenfunctions These plus our three-tiered approach constitute the scope of our quantum analysis inputs In chapter 6 we examine the amplitude distribution as it evolves in time for our three kick strengths, the energy evolution for the corresponding cases and the relevant wavefunction evolution We examine the diffusion of orbits which exhibit a linear energy increase and also the quasi-energy levels manifested in some of the results as steady state levels in the energy evolution curves The conclusions drawn are compared with the quasi-phase space portraits presented in chapter 7

Chapter 7 represents the final stage in our analysis We present, initially, a derivation of the Wigner distribution (Wigner (1932)) based on the equations given in the review by Hillery et al (1984) The resultant expression is also shown to be real valued despite the appearance of complex terms The latter half of the chapter is devoted to several pairs of figures, each consisting of an image of the wigner distribution above the corresponding contour plot of the same distribution Our intention is to illustrate how the system evolves temporally in its position-momentum space and compare it to the classical results The results of this are as startling as they are beautiful Our main conclusions are summarised in chapter 8 where inter-comparisons are made and future paths, along which research could proceed, highlighted

CHAPTER 1
HAMILTONIAN CHAOS

The pursuit of an understanding of the mechanisms behind previously indeterminable processes has been made possible with the development of fast, reliable, cost efficient solid state electronic computers Today, through the use of computers, both the scientific and engineering communities are benefiting from the research into controlling the non-linear behaviour of critical systems, the onset of turbulence and *chaos* This chapter will attempt to review briefly the main developments in non-linear dynamics which are relevant to the work being presented in this thesis Many books exist which will give the reader a much more detailed picture of this whole area of science (Cvitanovic (1989), Bergé et al (1987), Devaney (1989), Ott (1993))

1 1 Introduction

Historically, scientists, mathematicians and, more recently, engineers have attempted to impose a simplified picture on our perceptions of the world about us For hundreds of years the nature of everything about us has been explained away as *modifications on a theme of linearity* in everything from maths to astronomy It was using Euclidian geometry that astronomers & philosophers back in antiquity tried unsuccessfully to model the Universe with the earth at its center using a series of concentric circular orbits for the moon, planets & sun (Ptolemaic System) Even the most complex of systems have had attempts made on them to be *reined in* by this predilection to linearity and to be brushed off as impossible when proved unsuccessful Yet even despite this blinkering there were some observant enough to see something hidden in the nature of these systems, a complexity which defied the simple, artificial rules that were used to explain them and flaunting a rich beauty beyond the realms of the mediocrity of simple linearity Leonardo Da Vinci himself sketched the flow of water coming from a fountain in Florence in the 16^{th} century and was observant enough to include the small structure eddy currents within the larger ones as he sketched the water spewing out This structure within structure is what makes everything around us so interesting the fact that something could be there which

we've overlooked Non-linearity is the nature of our being and chaos the theory behind that nature

In classical systems chaos is considered present if the system exhibits a *sensitive dependence on initial conditions* What this means is that any two initial conditions separated by even by an infinitesimal amount diverge exponentially with time It was Hadamard (1898) who discovered this exponential divergence of nearby trajectories for a particle flow over a surface of negative curvature Not long after, Duhem (1906) and Poincaré (1908) determined that such a property in any system precludes the making of long term predictions about nature of the system's dynamics The scene was thus set for chaos All that was required was the proper impetus to bring this work out of the abstract realm of mathematics and to a wider audience (Heffernan et al (1992) & the references quoted therein)

It was not until the invention of the electronic computer in the 1950*s* and, more importantly, the further developement of these into the solid state transistorised computers of today that numerical analysis and modelling took off in a big way Many researchers then looked to using these number crunchers as means of evaluating the complex differential equations and iterative mappings It was Lorenz (1963) who, while modelling fluid flow in a simplified atmospheric model, found the *sensitive dependence on initial conditions* Smale (1967) showed that this complex nonlinear behaviour existed in a number of systems However, it was with the advent of such people as Feigenbaum (1978,1979) and his *scaling numbers* (to explain the structure in a simple iterative mapping on the unit interval), Mandelbrot (1982) and his *fractals* and Ruelle & Takens (1971) with their *strange attractors* that this area of research rapidly took off with the litany of *chaoticians* including such prominent others as Pomeau, Vidal, Manneville, Ott, York, Greobogi, Proccacia, Jensen and so on The vast number of publications on this subject over the past decade and a half is as starthng as the area is encompassing The whole dynamicism of nature itself seems contained within the influence of chaos, everything from the fluid dynamics (Libchaber and Maurer (1982)) to organic cardiac cells (Guevara et al (1981)), from non linear electronic circuits (Testa et al (1982)) to optical systems (Arrechi et al(1982)) and chemical reactions (Hudson and Mankin (1981)) All of the above systems are, of course, classical and easily

observable in experiments In fact the experiments are so varied that the time-scales and length scales of many of the chaotic systems analysed in the classical limit vary over many orders of magnitudes, from minutes for the Libchaber & Maurer experiment to tens of micro-seconds for the Testa et al experiment Classical systems were the obvious choice for examining chaos as these apply directly to the world about us and are *in the same ballpark* when it comes to our normally observable lives yet there were those who wondered about the quantum limit and the classical-quantum correspondence and this led some to ask *What happens on the quantum level when the classical system is chaotic or turbulent?* It was this thought about the quantum limit and how classical chaos might manifest itself in this limit that led to the birth of what is now referred to as *Quantum Chaology*

1 2 Conservative Systems & Chaos

The area of quantum chaos is quite different to most of the systems mentioned above because quantum systems are described by within the *Hamiltonians* framework and their phase spaces are area-conserved This property forces any analysis of such systems along different routes to the dissipative systems discussed in section 1 The previous systems were considered dissipative because structures in their phase spaces tend to contract and tend to be attracted to time invariant highly complex structures called *strange attractors* These are usually *fractal* with the dynamics of the systems being confined to the region of phase space where these attractors reside In our conservative Hamiltonian systems we do not have such dissipation or strange attractors present Any structure retains its *area* in the multi-dimensional phase space of the system We will restrict our arguments to the $1D$ case as we will only be dealing with a 1 Dimensional oscillator in what is to follow in later chapters

As we have already mentioned, the system's dynamics are determined by its Hamiltonian, $H(\mathbf{p}, \mathbf{q}, t)$ The $\mathbf{p}$ describes the momentum and $\mathbf{q}$ describes position and both are normally vectors of the same dimensionality as the number of degrees of freedom in the system, N As $N = 1$ for our system the the vectors $\mathbf{p}$ & $\mathbf{q}$ will be replaced by the scalars

p & q The time evolution of p and q is described by Hamilton's equations which relates the *trajectory* $p(t)$ & $q(t)$ trace out in the $2D$ phase space of our system

$$\frac{dp}{dt} = -\frac{\partial H(p,q,t)}{\partial q} \tag{1 2 1}$$

$$\frac{dq}{dt} = \frac{\partial H(p,q,t)}{\partial p} \tag{1 2 2}$$

If we form a vector $\tilde{\mathbf{x}}$ from the p & q (Ott (1993)) i e

$$\tilde{\mathbf{x}} = \begin{pmatrix} p \\ q \end{pmatrix}$$

we can write the two Hamilton equations as one vector equation

$$\frac{d\tilde{\mathbf{x}}}{dt} = \mathbf{F}(\tilde{\mathbf{x}}, t) \tag{1 2 3}$$

The advantage of this is not just the ease of use of one equation but that we can, by taking the divergence of $\mathbf{F}$, show how Hamilton's equations predict the conservation of area in our $2D$ phase space,

$$\frac{\partial}{\partial x}\,\mathbf{F} = \frac{\partial}{\partial p}\left(-\frac{\partial H}{\partial q}\right) + \frac{\partial}{\partial q}\left(-\frac{\partial H}{\partial p}\right) = 0 \tag{1 2 4}$$

Furthermore, it can be shown (Ott (1993)) that for any closed curve in the $2D$ phase space, S_o, the time evolved curve S_1 encompasses the same area as does S_o This follows from differentiating w r t time the area integral and showing it to be zero

$$\frac{d}{dt}\int_{S_1} d^2\tilde{\mathbf{x}} = \oint_{S_1} \frac{d\tilde{\mathbf{x}}}{dt}\, dS = \oint_{S_1} \mathbf{F}\, dS = \int_{S_1} \frac{\partial}{\partial \tilde{\mathbf{x}}}\,\mathbf{F} d^2\tilde{\mathbf{x}} = 0 \tag{1 2 5}$$

This property of having a phase space incompressibility, Liouvilles Theorem, means that attractors do not exist for Hamiltonian systems in the same sense they do for dissipative classical systems with phase space contraction We have deliberately laboured this point so that this difference is clear Despite the area conservation of the phase space, complex structures can (and do) exist there We will show later that, using the K A M theorem, the break up of orbits in our $2D$ phase space can become very complex, even *fractal*, in that the structure has detailed structure even at arbitrarily small length scales

The absence of strange attractors with infinitely complex structures, caused by successive foldings and stretchings of the phase space, in classically conservative systems

requires the existence of another mechanism to give rise to the highly non-linear behaviour that is expected from a system which is classicallly chaotic The incompressibility of the phase space also allows the system to occupy the whole of the phase space This prompts the question *can some orbits diffuse around some (or all) of the whole phase space and exhibit sensitive dependence on initial conditions in a manner analogous to the behaviour of orbits on a dissipative strange attractor?* The answer is yes if the system has a surface layer which spreads out over part of the phase space and if this layer permits orbits to diffuse over it The existence of this layer gives rise to what we now term *Hamiltonian or Conservative Chaos* In fig 1 1 we illustrate such a layer which exists in the phase space of our driven harmonic oscillator The layer is called *stochastic* because of the diffuse nature of the orbits within it One can see from the figure that the layer occupies the space between *islands* of bounded motion in the phase space Any orbits within these islands cannot leave them and are thus bounded in energy, momentum and position The orbits present in the stochastic layer are not so bounded and can diffuse freely over the entire $2D$ phase space since the web like layer connects all inter-island spaces in the phase space (a more quantitative explanation is presented in chapter 3)

The parameters used in fig 1 1 are explained in later chapters and the figure is used here for qualitative purposes only, the quantitative analysis will be undertaken in chapters 3 & 4 for the classical mapping So for classical conservative systems the existence of this layer permits complex non-linear dyanamics to exist The quantum regime is so different from the classical that methods are used which for the most part do not resemble those in the classical regime Energy is a big factor in determining how diffuse an orbit is becoming and so, as energy levels exist in the quantum, it makes sense for energy and energy levels to be scrutinised in depth Some, such as Berry & Robnik (1984) and Lewenkopf (1991), have analysed the energy level statistics of time independent Hamiltonian systems to check for a possible phase change when the corresponding classical limit is going from regular to chaotic motion Others, Israeilev (1990), tend to construct quasi-energy levels for kicked systems and analyse these levels with a hope to uncovering some of the mystery surrounding quantum chaos. Both are, to date, inconclusive, Lewenkopf (1991) proved that exceptions can exist to the change in energy level statistics proposed

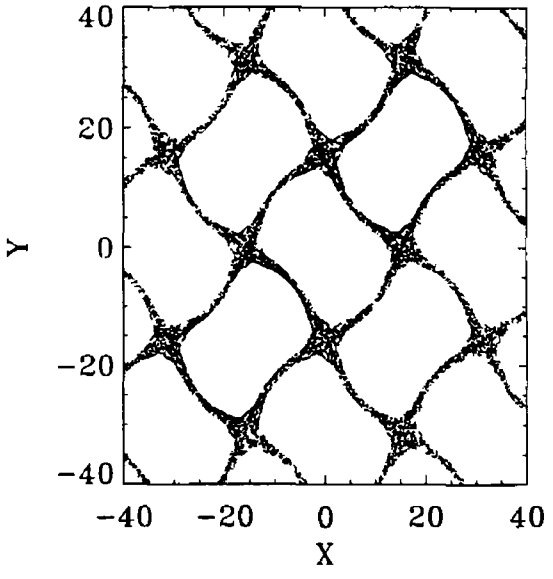

Fig 1 1 Plot of the diffuse (or stochastic) layer for the kicked harmonic oscillator for $\mu_{cl} = 6\,5$, $K = 0\,1$ & $\beta = \frac{\pi}{2}$ The meaning of the above parameters is explained in chapters 2 & 3

as a mechanism for highlighting chaos, but work is continuing The evolution of energy in time (in time dependent Hamiltonians) and the subsequent comparison with the classical limit is also used This technique was applied to the kicked rotor (Casati et al (1979)) and shown to have a natural saturation in the energy Though indicative of suppression of quantum chaos in the kicked rotator, this type of energy saturation is not universal in quantum systems In fact Berman et al (1991) have postulated that the presence of an extra time scale ($\propto ln(\hbar^{-1})$) in the quantum regime of the kicked harmonic oscillator might allow for the non suppression of chaos and that a quantum analogue of the classical crystalline phase space structure might allow for the delocalisation of wavefunctions allowing the kicked harmonic oscillator to be chaotic in the quantum regime (Daly & Heffernan (1994)) In chapter 6 of this thesis we present results which appear to show the energy increasing linearly without saturation indicating non-suppression of chaos Our matrix size and the limit of computing power available limit our time evolution but the evidence points to no suppression of chaos in the quantum limit

For quantum systems trajectories do not exist in the manner that we are accus-

tomed to dealing with in the classical regime because of the uncertainty principle Therefore a phase space as such cannot be constructed because of the uncertainty in trajectories We can however construct a quasi-phase space using the distribution introduced by Wigner (1932) and further developed by Cohen (Hillery et al (1984)) This Wigner distribution sets up a probability measure over the momentum-postion space allowing contour lines to be drawn joining regions of equal probability Thus one can construct a picture of the probability distribution in the Q-P plane and thus a quasi-phase space for these quantum systems (Hannay & Berry (1980)) To more readily compare the quantum and classical phase spaces the Husimi distribution (Husimi (1940)) is often invoked This distribution is a coherent state representation of the Wigner distirbution (c f chapter 7 and the review article by Hillery et al (1984)) As the coherent state has the least uncertainty of any wavefunction the hope is to more closely compare the two phase spaces This is the more common distribution encountered in the literature (Balazs (1990), Radons & Prange (1990), Scharf & Sundaram (1991), Kus et al (1991) and Scharf & Sundaram (1992))

The discrete nature of the ***kick*** used in periodically kicked systems permits the construction of mappings relating the system's behaviour from one kick period to the next For some of the more simple systems, the kicked quantum rotor (Scharf & Sundaram (1991)) or the Baker's map (Balazs (1990)), the methods used appear simple enough because of the simplicity of the eigenfunctions of the systems However for the more complex systems, such as our kicked harmonic oscillator, the more direct method of relating probability amplitudes, of the undriven eigenfunctions, from kick to kick (Fox & Lan (1990), Fox & Elston (1994)) is used with success We consider this latter technique more realistic as it relates physical quantities (the probability amplitudes of the eigenfunctions of the undriven harmonic oscillator) to the time evolution of the kicked system It will become apparent from the results in chapters 6 & 7 that from just the evolution of the amplitudes we can calculate the energy evolution, the quasi-energy levels & the Wigner distribution all as functions of time The usefulness of this technique depends greatly, however, on the eigenfunction of the system itself and the existence of anlaytical solutions to integrals involving such functions (c f chapter 5 eq (5 1 26)) We end with the comment that each system has its own characteristics and it is by fundamentally understanding these that the

right method for quantising the Hamiltonian can be found

The last few paragraphs were intended to highlight the differences between the quantum regime and the more familiar classical regime The conceptual difficulties associated with quantum phenomena are not eased by the complex non-linear nature of these systems but we hope that we have answered more questions in this very brief discussion of quantum chaos More detailed discussions (ones which do the subject more justice than could be attempted here) can be found m such books as *Quantum Chaos* edited by Cerdeira, Ramaswamy, Gutzwiller & Casati and Edward Ott's *Chaos in Dynamical Systems* We complete this introductory chapter with a brief outline of some of the nomenclature used in this work and how they are defined in the context of this work

1 3 The System Proper & Some Definitions

The kicked harmonic oscillator, in the form we present its Hamiltonian in chapters 2 & 5, can be motivated from physical systems Chernikov et al (1987) chose that of particle motion in an external magnetic field B_o with a disturbing plane wave packet present which propagates orthogonally to the magnetic field (which propagates along the x axis) The plane wave packet contains a very large number of plane waves

$$\frac{d^2x}{dt^2} + \omega_o^2 sin(x) = \frac{e}{m} E_o \sum_m sin(k_m x - \omega_m t) \qquad (1\ 3\ 1)$$

where $\omega_o = eB_o/mc$ is the cyclotron frequency By setting $k_m = const = k_o$ and $\omega_m = n\Delta\omega$ with $\Delta\omega$ equal to the frequency separation of neighbouring modes and $n = 0, \pm 1,$ we find that, as the number of modes m tends to infinity, the summation term can be spht to give

$$\sum_m sin(k_m x - \omega_m t) = sin(k_o x) \sum_{n=-\infty}^{\infty} cos(\frac{2n\pi t}{T}) \qquad (1\ 3\ 2)$$

The summation over n of the cosines gives a periodic train of delta pulse so that eq (1 3 1) becomes a more familiar equation

$$\frac{d^2x}{dt^2} + \omega_o^2 x = \frac{e}{m} E_o sin(k_o x) \sum_{n=-\infty}^{\infty} \delta(t - nT) \qquad (1.3\ 3)$$

From this point it is quite starightforward to reconstruct the system Hamiltonian Noting that $dq/dt = -p/m$ and that $d^2q/dt^2 = -(\frac{1}{m})dp/dt$ we find that by replacing x with q we obtain the time evolution equations of p and q

$$\frac{dp}{dt} = m\omega_o^2 x - eE_o sin(k_o x) \sum_{n=-\infty}^{\infty} \delta(t - nT) \qquad (1\ 3\ 4a)$$

$$\frac{dq}{dt} = -\frac{p}{m} \qquad (1\ 3\ 4b)$$

where, upon invoking Hamilton's equations (1 2 1) & (1 2 2) we end up with the hamiltonian we require for our analysis and that which is used from now on when referring to this system

$$H(p,q,t) = \frac{p^2}{2m} + \frac{1}{2}m\omega_o^2 q^2 + \frac{eE_o}{k_o} cos(k_o x) \sum_{n=-\infty}^{\infty} \delta(t - nT) \qquad (1\ 3\ 5)$$

Some of the more commonly used expressions and words in any area of research can very rapidly become almost *colloquial* so that their original intended definition or function takes on a much broader term or in some case is used to refer to something only vaguely related to the original meaning To prevent any misunderstanding here we will make a few *loose* definitions to essentially highlight the meaning **we intend** in this thesis for the following terms

Integrability When we refer to integrability in this system, the kicked harmonic oscillator, we mean that the Hamiltonian, $H(p,q)$, can be expressed, by means of a canonical change of variables $(p,q) \rightarrow (J,\theta)$, solely in terms of one of the variables in our system the introduction of the action-angle variables means the undriven harmonic oscillator can be expressed solely interms of J (the action variable) and is therefore integrable The kicked system cannot be so expressed and is therefore non-integrable The analysis involving integrability is carried out in chapter 3

K.A M. Theorem As we understand this very complex theorem, the tori (in our $2D$ phase space these are just orbits) in the phase space are subject to distortion and eventually break up if the rotation number of the orbit on this torus is *sufficiently commensurate with the periodicity of the perturbing term* This is how we apply this theorem to our system In

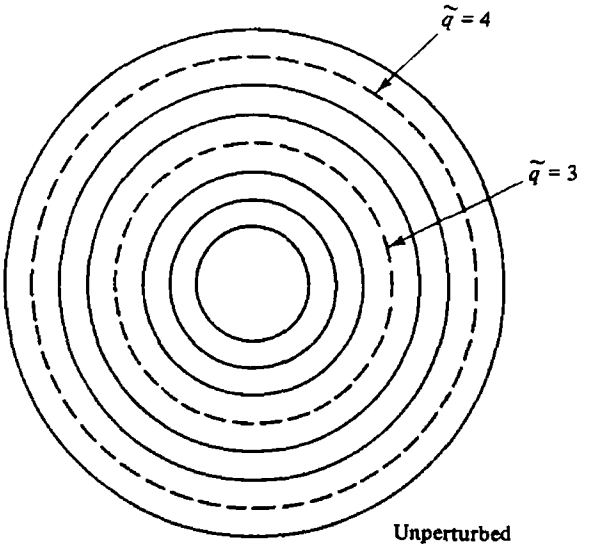

Fig 1 2 Unperturbed circular orbits of a typical integrable system The dashed orbits are the two mentioned which have rotational number of 3 & 4 and are among the first orbits to break up under K A M *From Chaos in Dynamical Systems by E Ott, Chapter 7*

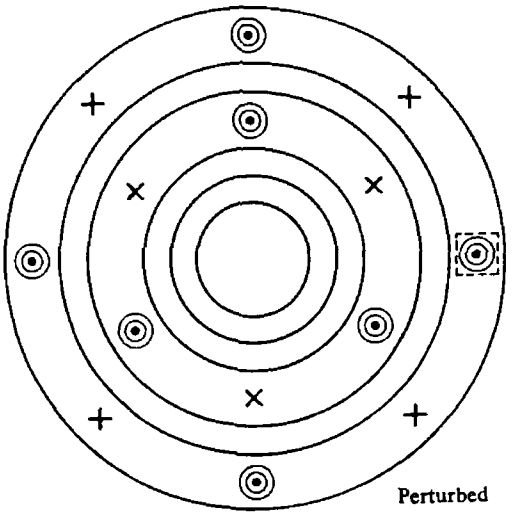

Fig 1 3 The perturbed orbits corresponding to fig 1 2 The two commensurate orbits have broken into hyperbolic & elliptic points of the order of the rotational number *From Chaos in Dynamical Systems by E Ott, Chapter 7*

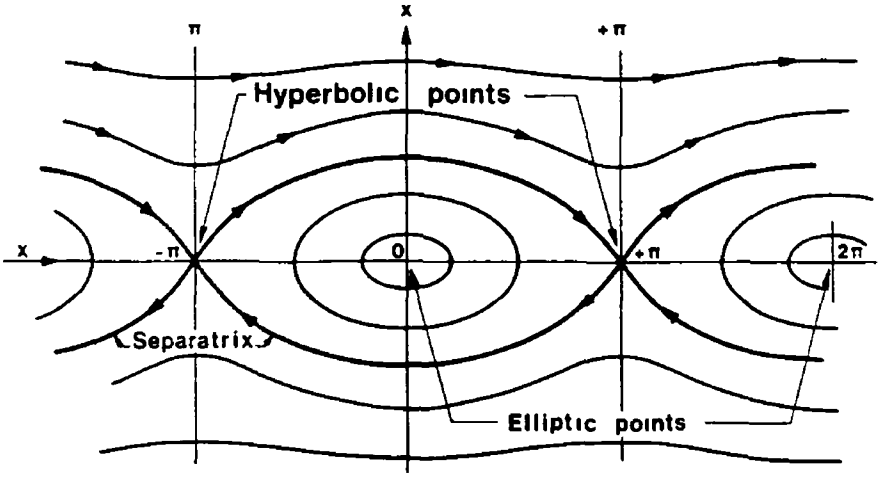

Fig 1 4 The two different types of fixed points shown here in the phase plot of the pendulum, $\ddot{x} = -sin(x)$ The separatrix is the line separating bound motion (oscillation) and unbound (rotation) *From "Self-Generated Chaotic Behaviour in Nonlinear Mechanics" by R H G Helleman in Universality in Chaos edited by P Cvitanovic*

fig 1 2 we show the circular type orbits for an integrable system (as a surface of section of a torus) and this can be compared to the case in fig 2 1 for our system with no kicking (i e integrable) In fig 1 3 we show how some orbits of rotation numbers 3 & 4 have broken up into two sets of four points (one set hyperbolic, the other elliptic) The elliptic points of these broken up orbits have a circular structure similar to the original integrable system and these too experience break up in a similar manner resulting in a highly complex structure for large kicking This is discussed in detail in chapter 3

Periodic Fixed Points What we want to discuss here is the two types of periodic fixed points encountered in the type of conservative system we're considering The first is the elliptic fixed point This is distinguished by its complex eigenvalues and by the fact that nearby points are rotated by the presence of this point into ellipses (or circles) Therefore the presence of circular concentric orbits in our phase space highlights the presence of an elliptic fixed point at the centre of these concentric orbits Hyperbolic fixed points have real eigenvalues and are distinguishable by the fact that orbits near them can be attracted

towards them along their stable directions (given by the eigenvalue less than one) and repelled along the unstable directions (given by the eigenvalue greater than one) Orbits also generally have the shape of hyperbolae near such fixed points A schematic of the two types is given in fig 1 4

This introductory chapter is just a brief review of the areas relevent to the work in this thesis and a more in depth introduction can be found in the reference books previously mentioned We will now discuss in detail the physics of the non-linearly kicked harmonic oscillator

CHAPTER 2
THE CLASSICAL MAPPING

This chapter is intended as an introduction to the classical mapping which we obtained from the quantum mechanical equations describing the kicked harmonic oscillator The ideas and methods by which we obtain the final form for the mapping are outlined along with a brief description of the the derivation itself To illustrate the complexity of the resultant mapping, we include some phase space portraits along with a plot obtained from the differential equations of the system for comparison

2 1 The Classical Derivation

As the title of this section suggests, our purpose here is to derive the classical mapping from the quantum operator equations The complete derivation is quite long and tedious so only those steps that are necessary for cohesion will be presented Furthermore, as the undriven system is a standard under-graduate problem, we will assume the reader is familiar with the operators, a & $a^\dagger$, and with the basic properties of the undriven system A more complete introduction can be found in any standard quantum mechanics book such as that by Messiah (1976) It is the classical map, resulting from this derivation, which we will use extensively in the classical analysis of the kicked quantum harmonic oscillator undertaken in chapters three and four

In order for us to proceed with this derivation it is necessary to explain briefly how we intend, here, to transpose from the quantum to the classical In quantum space the existence of wavefunctions necessitates the existence of operators to *operate* on these wavefunctions and obtain measurable quantities (once the expectation value is sought) In classical space these operators become *simple scalars* or, using a more formal notation, we simply take the *c number* representation for any operators used If some operator function, $f(a, a^\dagger)$, represents the system in the quantum limit then a scalar function $\overline{f}(\alpha, \alpha^*)$ can be defined to represent the system m the classical limit where the a & $a^\dagger$ are operators and form a Hermitian conjugate pair with the α & α^* being scalar and forming a complex conjugate pair It is by this transformation that the Hermitian conjugate operators become

simple complex conjugate numbers and hence how a *classical* system can be formed from a given quantum system (Louisell (1965))

Let us now introduce the system to be analysed It consists of a quantum harmonic oscillator, of mass M and natural frequency ω_o, which is driven by a potential $V(p,q)$ whose temporally discrete nature is brought about by its product with a periodic delta function Thus the Hamiltonian, H_T, for this system is the sum of the Hamiltonian for the undriven harmonic oscillator, H_o, and the driving (or kicking) potential term H_1 The form of the potential , $V(p,q)$, is critical for the overall system's behaviour and its exact form will be given later so as to keep the following derivation as generic as possible

The Hamiltonian, $H_o(t)$, for the isolated quantum harmonic oscillator is given below in eq (2 1 1)

$$H_o(t) = \frac{p(t)^2}{2M} + \frac{1}{2}M\omega_o^2 q(t)^2 \qquad (2\ 1\ 1)$$

where $p(t)$ signifies momentum and $q(t)$ position and both are functions of time, t (Messiah, 1976) As we will demonstrate in chapter 3, this system is integrable

To account for the kicking, the driving term, denoted $H_1(t)$, is added to $H_o(t)$, forming the hamiltonian H_T for the complete system, and the form that this kicking takes is given in eq (2 1 2)

$$H_1(t) = V(p,q) \sum_{n=-\infty}^{\infty} \delta(t - n\tau) \qquad (2\ 1\ 2)$$

As can be seen from the equation above, $H_1(t)$ is the product of a continuous potential $V(p,q)$ with a periodic train of discrete delta pulses The addition of $H_1(t)$ not only makes an integrable system, $H_o(t)$, non-integrable but also allow highly complex dynamics to exist in the system even when $H_1(t)$ is more of a perturbation than a dominant term It is this property that makes this class of system particularly interesting

To obtain the classical mapping for this system it is necessary, and preferred, to express the above equations in terms of a set of annihilation and creation operators, given by $a(t)$ and $a^\dagger(t)$ respectively Those familiar with the isolated harmonic oscillator will be aware that this substitution of $a(t)$ and $a^\dagger(t)$ for $p(t)$ and $q(t)$ makes the hamiltonian $H_o(t)$ much more manageable and this property is applied to the compound hamiltonian

$H_T(t)$ to simplify it As an intermediate step in the substitution the operators, $P(t)$ & $Q(t)$, are defined by

$$p(t) = P(t)\sqrt{M\hbar\omega_o} \qquad q(t) = Q(t)\sqrt{\frac{\hbar}{M\omega_o}} \tag{2 1 3}$$

By then defining the creation & annihilation operators as

$$a(t) = \frac{1}{\sqrt{2}}(Q(t) + \imath P(t)) \qquad a^\dagger(t) = \frac{1}{\sqrt{2}}(Q(t) - \imath P(t)) \tag{2 1 4}$$

the Hamiltonian, $H_o(t)$, for the isolated oscillator, and the Hamiltonian $H_1(t)$ for the driving term become

$$H_o(t) = \frac{\hbar\omega_o}{2}(a(t)a^\dagger(t) + a^\dagger(t)a(t)) \tag{2 1 5a}$$

and

$$H_1(t) = V(a(t), a^\dagger(t)) \sum_{n=-\infty}^{\infty} \delta(t - n\tau) \tag{2 1 5b}$$

respectively with the complete system Hamiltonian, $H_T(t)$, being just the sum of eq (2 1 5a) with eq (2 1 5b), i e

$$H_T(t) = \frac{\hbar\omega}{2}(a^\dagger(t)a(t) + a(t)a^\dagger(t)) + V(a(t), a^\dagger(t)) \sum_{n=-\infty}^{\infty} \delta(t - n\tau) \tag{2 1 6}$$

With the system hamiltonian thus expressed we will now proceed to examine the time evolution of the operators, $a(t)$ & $a^\dagger(t)$, so that a recursive mapping can be obtained The time evolution of any operator, Ψ, can be described by the equation

$$\frac{\partial\Psi}{\partial t} = -\frac{\imath}{h}(\,\Psi, H\,) \tag{2 1 7}$$

where $\Psi \equiv \Psi(t)$ is time dependent The brackets, ( ), denote the commutation of any operators contained therein As it is necessary to commute operators to obtain their time evolution then it is appropriate to review some commutation rules which are used to great advantage in the simplification of the equations resulting from the applcation of eq (2 1 7)

1 $(\,a, a\,) = 0$ (any operator commuted with itself is zero) (2 1 8a)

2 $(a, a^\dagger) = 1, \qquad (a^\dagger, a) = -1$ (2 1 8b)

3 $(a, bc) = (a, b)c + (a, c)b$ (2 1 8c)

4 $(a, b^{2n}) = \sum_{s=0}^{n-1} b^s (a, b) b^{n-s-1}$ (2 1 8d)

The a and $a^\dagger$ in the four equations above are of course functions of time, $a \equiv a(t)$ and $a^\dagger \equiv a^\dagger(t)$ For $a(t)$ & $a^\dagger(t)$, eq (2 1 8*d*) simplifies to nb^{2n-1} because the commutation of $a(t)$ with $a^\dagger(t)$, and vice versa, is scalar, *c f* eq (2 1 8*b*)

The time evolution of the operator $a(t)$ is, using rules $1 - 4$ in eqs (2 1 8a) to (2 1 8d) and eq (2 1 7)

$$\frac{\partial a(t)}{\partial t} = -\iota\omega a(t) - \frac{\iota}{\hbar}\left(a(t), V(a(t), a^\dagger(t))\right) \sum_{n=-\infty}^{\infty} \delta(t - n\tau) \qquad (2\ 1\ 9)$$

For $a^\dagger(t)$ a similar equation is obtained

$$\frac{\partial a^\dagger(t)}{\partial t} = \iota\omega a^\dagger(t) - \frac{\iota}{\hbar}\left(a^\dagger(t), V(a(t), a^\dagger(t))\right) \sum_{n=-\infty}^{\infty} \delta(t - n\tau) \qquad (2\ 1\ 10)$$

As the explicit form for the driving potential has not yet been revealed, then for convenience $-\frac{\iota}{\hbar}\left(a(t), V(a(t), a^\dagger(t))\right)$ shall be written as $f(a, a^\dagger)$ and $f^\dagger(a, a^\dagger)$ for the corresponding $a^\dagger$ commutation Putting $b \equiv \iota\omega_o$ and by integrating the equation over one kick cycle from just before the N to just before the (N+1) kick ($t = N\tau - \epsilon$ to $t = (N+1)\tau - \epsilon$) then, (as we let $\epsilon \to 0$),

$$a(N+1)e^{(b(N+1)\tau)} = a(N)e^{(bN\tau)} + f(a(N), a^\dagger(N))e^{(bN\tau)} \qquad (2\ 1\ 11)$$

Dividing across by $e^{(b(N+1)\tau)}$, to isolate the $a(N+1)$ term on the left hand side, the resulting equation is

$$a(N+1) = a(N)e^{(-b\tau)} + f(a(N), a^\dagger(N))e^{(-b\tau)} \qquad (2\ 1\ 12a)$$

with the equation for the $a^\dagger(t)$ operator similar in form to the above except for the substitution of $a(t)$ for $a^\dagger(t)$ and a few sign changes

$$a^\dagger(N+1) = a^\dagger(N)e^{(b\tau)} + f^\dagger(a(N), a^\dagger(N))e^{(b\tau)} \qquad (2\ 1\ 12b)$$

Defining β to be equal to $b\tau$, the final generic forms for the annihilation and creation operators, a & $a^\dagger$, can now be written These two equations are called *generic* because

they hold true for any temporally discrete potential of the form given in eq (2 1 2) The equations below are remarkably similar to those of Goggin et Al (1990) in his formulation of the quantum logistic map This form is quite general and can be applied to any driven oscillator system regardless of the kick term as well as other kicked systems where an annihilation - creation type operator set exists and where this set exhibits the same properties as those for our system

$$a(N+1) = \left[\, a(N) + f(a(N), a^{\dagger}(N)) \,\right] e^{-\beta} \qquad (2\ 1\ 13a)$$

$$a^{\dagger}(N+1) = \left[\, a^{\dagger}(N) + f^{\dagger}(a(N), a^{\dagger}(N)) \,\right] e^{\beta} \qquad (2\ 1\ 13b)$$

Despite having obtained such a set of generic maps it is impossible to predict the system's behaviour until a specific form for the potential is given The form of the potential we have chosen is

$$V(p,q) = \mu_q \cos(kq) \qquad (2\ 1\ 14)$$

after Berman et al (1991) In this choice of potential the parameter μ_q is the quantum kick strength and k is a characteristic length scale The importance of writing the potential like this is to enable a direct comparison to be made between the classical parameters in our current analysis and the quantum parameters in the forthcoming quantum analysis in chapters 5 and 6 This choice is also in keeping with the physcial significance of the system as explained in chapter 1 Upon substituting the operators a and $a^{\dagger}$ for q, our equation for the potential becomes

$$V(a, a^{\dagger}) = \mu_q \cos\left(K(a^{\dagger}(t) + a(t))\right) \qquad (2\ 1\ 15)$$

where for convenience K is defined to be $k\sqrt{\hbar/(2M\omega_o)}$ Using the trigonometric identity Cos($A+B$) = Cos(A)Cos(B) - Sin(A)Sin(B) with the properties of the operators, a and $a^{\dagger}$, and the series expansions of the sine and cosine functions, the operator functions $f(a, a^{\dagger})$ and $f^{\dagger}(a, a^{\dagger})$ both take on the same form

$$f(a, a^{\dagger}) = f^{\dagger}(a, a^{\dagger}) = +\imath\mu_{cl}\, \mathrm{sm}\left[\, K(a^{\dagger}(t) + a(t)) \,\right] \qquad (2\ 1\ 16)$$

where μ_{cl} is the classical kick strength and is defined to be $\mu_q K/\hbar$ A detailed step by step derivation of how we obtain eq (2 1 16) from eq (2 1 15) is included in Appendix A

It is now possible to construct the quantum operator mapping for a and $a^\dagger$ for the chosen potential These two mappings are identical in form to the generic ones defined by eqs (2 1 13$a-b$) but they are specific in the sense that the general functions $f(a,a^\dagger)$ & $f^\dagger(a,a^\dagger)$ have been replaced by their specific form as given by eq (2 1 16) The final operator maps are

$$a(N+1) = a(N)e^{-\beta} + \imath\mu_{cl}\sin\left[K(a^\dagger(N)+a(N))\right]e^{-\beta} \qquad (2\ 1\ 17a)$$

$$a^\dagger(N+1) = a^\dagger(N)e^{\beta} - \imath\mu_{cl}\sin\left[K(a^\dagger(N)+a(N))\right]e^{\beta} \qquad (2\ 1\ 17b)$$

It should be pointed out here that the $a(N)$ & $a^\dagger(N)$ constitute a Hermitian conjugate pair In order to transpose to the classical regime we multiply $a(N)$, $a^\dagger(N)$ & μ_{cl} by a parameter $K_0(\equiv k_0\sqrt{\hbar/2M\omega_0})$ defined to be equal to one Also K is divided by K_0 for consistency in the sine argument Thus no parameters or variables have any explicit dependence on $\hbar$ We can now transpose to the classical It is possible to express $a(N)$ in the *c number* representation as $\alpha(n)$ and $a^\dagger(N)$ as $\alpha^*(n)$ where the $\alpha's$ constitute a complex conjugate pair and are not operators As the $\alpha(n)'s$ and $\alpha^*(n)'s$ are just numbers then we can, quite justifiably, write $\alpha(n)$ as $x(n)+\imath y(n)$ and $\alpha^*(n)$ as $x(n)-\imath y(n)$

Therefore eqs (2 1 17a) and (2 1 17b) become

$$x(n+1)+\imath y(n+1) = \left[x(n)+\imath y(n)+\imath\mu_{cl}\sin(2Kx(n))\right]e^{-\beta} \qquad (2\ 1\ 18a)$$

for the transposition of the $a(N)$ operator mapping and

$$x(n+1)-\imath y(n+1) = \left[x(n)-\imath y(n)-\imath\mu_{cl}\sin(2Kx(n))\right]e^{+\beta} \qquad (2\ 1\ 18b)$$

for the $a^\dagger(N)$ operator mapping

It is interesting to note that the real and imaginary parts of the two above equations are identical We now split the real and imaginary parts to yield a mapping for $x(n)$(the real part) and $y(n)$(the corresponding imaginary part) The two equations we obtain are, for the real parts of eqs (2 1 18a)&(2 1 18b)

$$x(n+1) = x(n)\cos(\omega_o T) + y(n)\sin(\omega_o T) + \mu_{cl}\sin\left[2Kx(n)\right]\sin(\omega_o T) \qquad (2\ 1\ 19a)$$

and for the imaginary parts

$$y(n+1) = y(n)\cos(\omega_o T) - x(n)\sin(\omega_o T) + \mu_{cl}\sin\left[\,2Kx(n)\,\right]\cos(\omega_o T) \qquad (2.1.19b)$$

where we have replaced the parameter β with $\iota\omega_o T$ and simplified the equations. These are the equations which constitute our classical mapping as derived from the quantum mechanical operator equations. Their form is different from that normally observed in the literature such as the articles by Chernikov et al. (1989), Israilev (1990), Berman et al. (1991) and others (Schmera et al 1992, Zaslavsky and Filonenko, 1968). The reason for this is our inclusion explicitly of the K in the sine argument whereas most others re-scale their $x(n)'s$ and $y(n)'s$ such that this term is excluded. Our mapping is equivalent to that in the literature when $K = 0.5$. Our inclusion of K allows us to expand the phase space as the system's periodicity is directly proportional to the parameter K. This ability to expand the phase space allows detailed analyses to be made of the small scale structures without necessarily having to worry about computer precision. The trade off, however, is the complexity of an extra parameter.

These equations are also dimensionless as the a & $a^\dagger$ operators are themselves dimensionless from their definitions in eqs. (2.1.3) & (2.1.4) and the transposition to the classical representation adds no dimension to the variables α and α^*. Attention should also be brought to the fact that the x in the classical mappings can be traced directly back to the Q operator in quantum space and likewise the y to the P: i.e. from eq. (2.1.4) and the definitions of α and α^*

$$a = \frac{1}{\sqrt{2}}\left(\,Q + \iota P\,\right) \rightarrow \alpha = \left(\,x + \iota y\,\right) \& a^\dagger = \frac{1}{\sqrt{2}}\left(\,Q - \iota P\,\right) \rightarrow \alpha^* = \left(\,x - \iota y\,\right)$$

so that

$$\frac{Q}{\sqrt{2}} \rightarrow x \qquad \& \qquad \frac{P}{\sqrt{2}} \rightarrow y$$

with $\rightarrow$ signifying here the classical transposition.

Taking eqs. (2.1.19a) & (2.1.19b) a much simplified mapping is found for $\omega_o T = \frac{\pi}{2}$ which is the specific form chosen in the subsequent analysis as this form despite being more

manageable has one less parameter to deal with This form is given below in eqs (2 1 20) and (2 1 21) and will henceforth be referred to as the Resonant Kicked Oscillator Map (RKOM)

$$x(n+1) = y(n) + \mu_{cl} \sin\left[2Kx(n)\right] \tag{2 1 20}$$

$$y(n+1) = -x(n) \tag{2 1 21}$$

To test whether the above mappings did in fact describe the behaviour of the original Hamiltonian, eqs (2 1 1) & (2 1 2) were modelled using the time evolution approach for the p & q operators, not the a & $a^\dagger$ as before The Hamiltonian $H_T(t)$ given by the sum of eqs (2 1 1) and (2 1 2) gives the time evolution equations below for the P & Q operators (defined by eq (2 1 3))

$$\frac{\partial P}{\partial t} = -\frac{\iota}{h}\left(P, H_T\right) = \omega_o^2 Q + \mu_{cl} \sin(KQ) \sum_{n=1}^{\infty} \delta(t - n\tau) \tag{2 1 22}$$

and

$$\frac{\partial Q}{\partial t} = -\frac{\iota}{h}\left(Q, H_T\right) = -P \tag{2 1 23}$$

These were integrated numerically and the results were in agreement with the mappings above Therefore we can confidently state that the dynamics present in the classical mapping are representative of the continuous system

Some phase space plots, from the mappings in eqs (2 1 20) & (2 1 21) and from the continuous system in eqs (2 1 22) & (2 1 23), are shown in the proceeding section to illustrate how complex the phase space for this system can be and how the mapping is equivalent to the system's differential equations

2 2 Some Phase-Space Portraits

This section is solely dedicated to illustrating the phase space of the classical mapping derived in the preceding section and as such we do not intend here to analyse the phase space This section is solely demonstrative The portraits chosen are considered

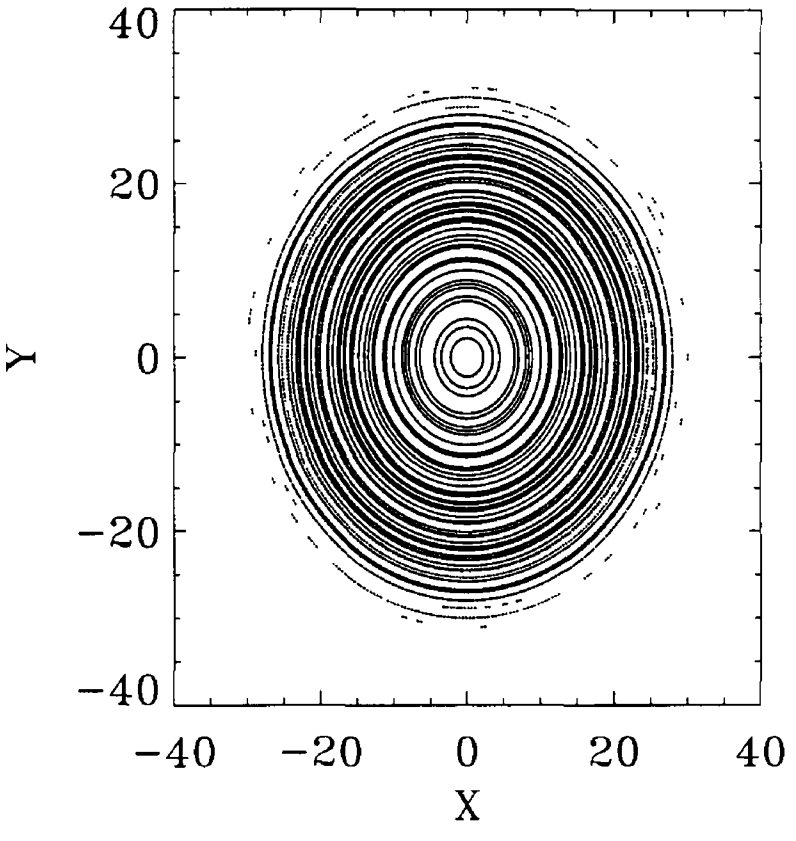

Fig 2 1 Phase space plot for $\beta = \frac{(1+\sqrt{5})\pi}{2}, K = 0\,1$ and $\mu_{cl} = 0$, i e no kicking

representative of the system at large and show how the parameters affect the structure and, subsequently, the dynamics of the kicked oscillator

Figure 2 1 shows the undriven oscillator phase space with the circular orbits characteristic of the energy levels for the isolated system The energy levels of the undriven system are given by (Messiah,1976)

$$E_n = (n + 1/2)\hbar\omega_o \equiv r_n \tag{2 2 1}$$

As the x and y are essentially the position and momentum respectively, then the energy of the system at any given point (x, y) in the phase space is directly proportional to the sum of the squares of x and y

$$E \propto x^2 + y^2 \tag{2 2 2}$$

For the undriven system the energy of any orbit, n, is constant $(= r_n)$, from eq (2 2 1), so

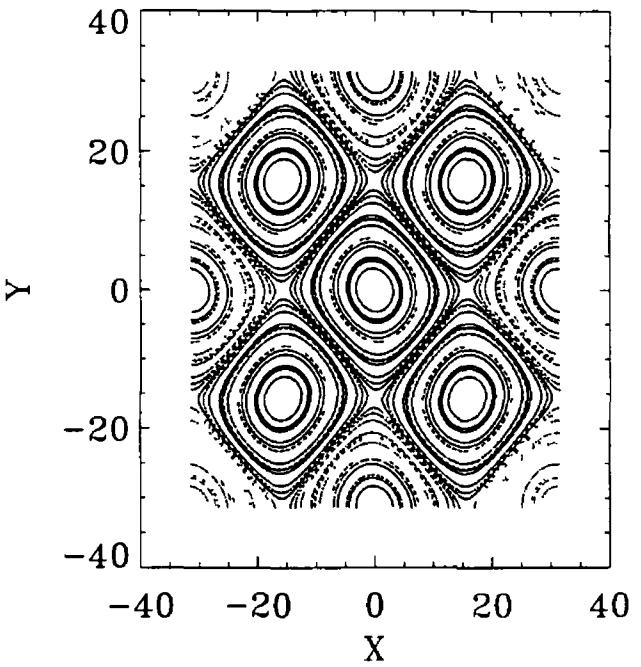

Fig 2 2 Phase space plot for $\beta = \frac{\pi}{2}, K = 0\,1$ and $\mu_{cl} = 1$,

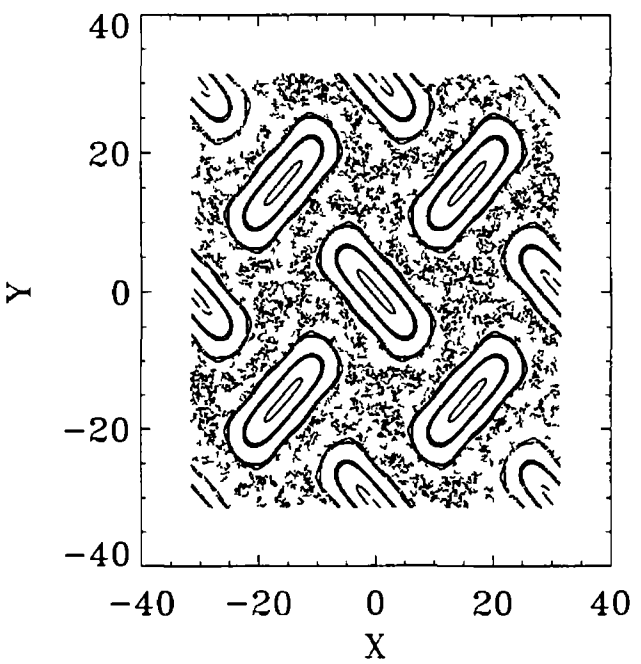

Fig 2 3 Phase space plot for $\beta = \frac{\pi}{2}, K = 0\,1$ and $\mu_{cl} = 9\,5$,

the relation between the energy and x & y is a circle hence the circular orbits The phase space properties are examined further in chapter 3

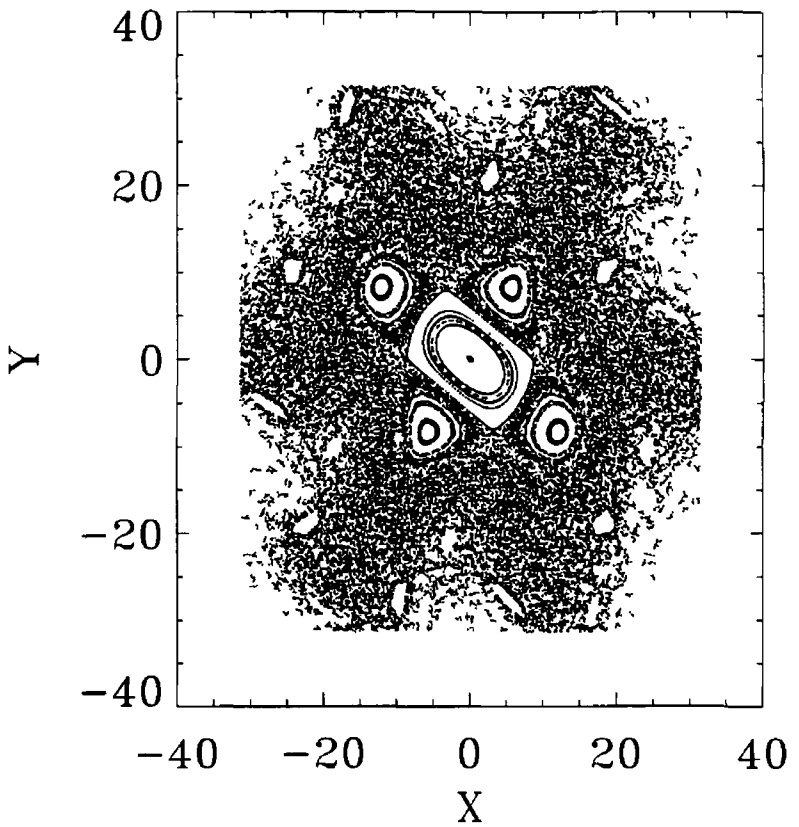

Fig 2 4 Phase space plot for $\beta = \frac{(1+\sqrt{5})\pi}{2}, K = 0\ 1$ and $\mu_{cl} = 6\ 5$ This is the off resonance case

Figs 2 2 & 2 3 show the phase spaces for two values of the kicking when the system is on resonance, i e $\beta \equiv \frac{p}{q}\pi$ where p & $q \in \mathbf{Z}$ As evident from these two figures, the higher the kicking, the wider the diffuse layer between cells A quantitative analysis of this layer is undertaken in chapters 3 & 4

The final pair of diagrams illustrate the system for non-resonant kicking, β not equal to $\frac{p}{q}\pi\ \forall p, q \in \mathbf{Z}$, and the system as modelled by the differential equations (2 1 22) & (2 1 23) The lack of symmetry in the former is striking with the diffuse layer spreading over the whole plane as the driving is increased The latter illustrates just how well the mapping represents the system and how, using some straight-forward identities, the system

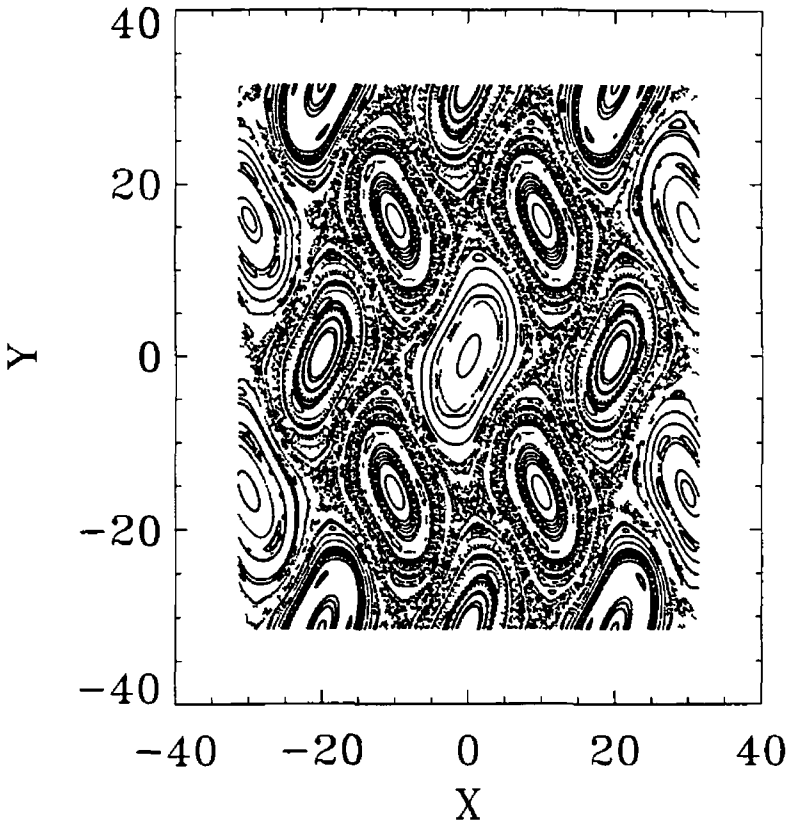

Fig 2 5 Phase space plot for the differential equations proper

can be described totally by a simple set of recursive mappings instead of a set of coupled differential equations It's these mappings, not the differential equations, that allow the following analysis to be carried out

The five phase space portraits shown in this section are only illustrative whereas, for any true characterisation to be undertaken, it is necessary to quantitatively analyse the components of the system's phase space This is the task we undertake in the following two chapters

CHAPTER 3
ANALYSIS OF THE PHASE SPACE

The phase space of the system may at first glimpse appear to be just *nice pictures* and little else However buried in these *nice pictures* is the essence of the system's behaviour and evolution both as a function of its parameters and time Therefore the principle *diagnostic tool* available is this phase space and its analysis is tantamount to understanding the system's behaviour

In this chapter we analyse the phase space of the classical mapping derived in chapter 2 and characterise it by considering its symmetry, by using the K A M theory, by looking at the effect of periodic points on invariant orbits (Cleary, 1990) and by examining the stochastic web's width and structure Through the adaptation of these well established techniques and by developing new ones it is our intention to obtain a greater understanding of the system proper using its principal diagnostic tool the phase space

3 1 The Symmetry Of The Phase Space

The symmetry of the system's phase space depends solely on the parameter β which relates the natural frequency of the undriven oscillator, ω_o, to the periodic time, τ, of the dirac delta function From the phase portraits in the last chapter it is possible to see just what an effect β has on the phase space A striking example is the difference between the phase spaces in figs 2 3 & 2 4 which show the system for $\beta = \frac{\pi}{2}$ and $\frac{1+\sqrt{5}}{2}$ respectively The former clearly shows a four fold symmetry which we attribute to the identity

$$\beta = \omega_o \tau = \frac{\pi}{2} \qquad \Leftrightarrow \qquad 4\omega_o = \frac{2\pi}{\tau} (\equiv \omega_1) \tag{3 1 1}$$

with the ratio of ω_o to ω_1 being 4 1 The latter figure (fig 2 4) shows no obvious symmetry primarily because the relationship between ω_o and ω_1 is incommensurate The advantage of using a resonance driving is that the phase space is easier to analyse using periodic orbits with their associated stabilities and manifolds However it is possible to successfully apply some of the results of the resonance case to the non-resonance case as has been done for

diffusion in the stochastic layer (Chirkov (1979), Lichtenberg and Wood (1989), Schmera et al (1992)) Our task here is to use return maps as a technique for analysing the four fold symmetry in the resonance case we are considering This technique is limited in that it is only applicable to a subset of all resonance cases

The return map is one of the principle methods for quantitatively examining and illustrating the symmetry of the system at a particular resonance value of β This technique has been widely used to analyse classically chaotic low dimensional mappings (May (1976), Feigenbaum (1980)) However, this method is restricted in that only positive integer ratios of ω_o to ω_1 (i e $\beta = \frac{1}{q}$ where $q \in \mathbf{Z}^+$) can have comparable return maps Therefore if the ratio between ω_o and ω_1 is n then the n^{th} return map is required which exists only if n is a positive integer β, in most of the analysis to follow, is fixed at $\pi/2$ This requires us to obtain an expression for the fourth return map

The fourth return map is that version of the classical mapping which relates $y(n+1)$ to $y(n-3)$ and similarly $x(n+1)$ to $x(n-3)$ Thus we can explicitly relate every fourth point The second and third return maps, denoted (2 R M) and (3 R M) respectively, must be formulated as steps to getting an exphcit form for the fourth return map (4 R M) To obtain these maps it is necessary to recall the definition of the RKOM defined in eqs (2 1 20) & (2 1 21) Taking these equations for the mapping and expressing $x(n+1)$ and $y(n+1)$ in terms of $x(n-1)$ and $y(n-1)$ respectively our expression for the second return map (2 R M) is

$$x(n+1) = -x(n-1) + \mu_{cl} \sin\Big(2Ky(n-1) + 2K\mu_{cl} \sin\Big(2Kx(n-1)\Big)\Big) \qquad (3\ 1\ 2a)$$

$$y(n+1) = -y(n-1) - \mu_{cl} \sin\Big(2Kx(n-1)\Big) \qquad (3\ 1\ 2b)$$

It follows that those points of the form $\frac{m\pi}{2K}$ constitute steady state solutions of the above equations because period two fixed points have, from their very definition, the property that $y(n-1) = y(n+1)$ and $x(n-1) = x(n+1)$ By steady state we refer to those solutions of any return map such that $x_n = x_{n-k}$ where k is the order of the return map and is an integer In what is to follow these solutions are those which set all the sine terms to zero The period one fixed points, of which they is but one the origin,

are also steady state solutions of the above as they are for all the return maps because $x(n+1) = x(n) = x(n-1) = \qquad = x(0)$

The third return map (3 R M) is obtained in a manner similar for that of 2 R M where this time $y(n+1)$ is related to $y(n-2)$ and $x(n+1)$ to $x(n-2)$ However as this return map is not required for the present analysis its form is not presented explicitly The fourth return map (4 R M) is given below

$$x(n+1) = x(n-3) - \mu_{cl} \sin\Big(\big(2Ky(n-3) + 2K\mu_{cl} \sin(2Kx(n-3))\big)\Big)$$
$$-\mu_{cl} \sin\Big(2Ky(n-3) + 2K\mu_{cl} \sin(2Kx(n-3)) + 2K\mu_{cl} \sin\Big(2Kx(n-3) -$$
$$2K\mu_{cl} \sin\Big(2Ky(n-3) + 2K\mu_{cl} \sin\big(2Kx(n-3)\big)\Big)\Big)\Big) \qquad (3\ 1\ 3a)$$

$$y(n+1) = y(n-3) + \mu_{cl} \sin\big(2Kx(n-3)\big)$$
$$+\mu_{cl} \sin\Big(2Kx(n-3) - 2K\mu_{cl} \sin\Big(2Ky(n-3) + 2K\mu_{cl} \sin\big(2Kx(n-3)\big)\Big)\Big) \qquad (3\ 1\ 3b)$$

The period four fixed points are those points satisfying the identities

$$x(n+1) = x(n-3) \qquad y(n+1) = y(n-3) \qquad (3\ 1\ 4)$$

So the steady state solutions of the above two are the fixed points of period four, two or one Any multiplier of four is a hypothetical steady state solution of the 4 R M hence the inclusion of fixed points of period two and one For a solution of the form $x(n+1) = x(n-3)$ etc to occur all terms after the first on the right hand side of eqns (3 1 3a) & (3 1 3b) must go to zero This means that all the sine arguments must all go to zero and so the period four fixed points must satisfy

$$2Kx(n+1) = 2Kx(n-3) = 2Kx = 2m\pi \qquad (3\ 1\ 5)$$

$$2Ky(n+1) = 2Ky(n-3) = 2Ky = 2n\pi \qquad (3\ 1\ 6)$$

As K has been chosen to be 0 1 for most of the analysis then it follows that the period four fixed points are given by

$$x = 5m\pi \qquad y = 5n\pi \qquad (3\ 1\ 7)$$

where $n, m \in \mathbf{Z}$ As the multipliers, n and m, can take on any integer value then the period four fixed points exist as a uniform grid over the entire $2D$ plane of the phase space This has far reaching consequences for it allows the unbounded transport of certain phase space orbits and also allows a diffuse layer to exist over the entire phase space Both of these consequences will be studied in detail in proceeding sections and chapters but suffice to say that this grid is essential for the stochastic behaviour in the system

Now that the existence of this grid of points has been established it remains for us to consider whether these fixed points are hyperbolic or elliptic The reason for this consideration is to determine in which regions of the phase space the unstable directions of the hyperbolic points exist as these determine the unbounded, diffuse behaviour previously mentioned Why this is so will become clear later The behaviour of orbits in the vicinity of elliptic and hyperbolic points determines how the phase space itself evolves both as a function of time and as a function of any of the three parameters, μ_{cl}, K and β In order for us to determine whether a periodic fixed point is elliptic or hyperbolic it is necessary to find the fixed point's eigenvalues as given by the equation

$$| J - \lambda I | = 0 \tag{3 1 8}$$

where , in this $2D$ mapping, λ is a $2D$ vector containing the eigenvalues, (λ_1, λ_2), J is the Jacobian of the n^{th}return map (where n is the periodicity of the fixed point) and is a (2×2) matrix with I being just the (2×2) identity matrix The eigenvalues of an elliptical point are in the form a complex conjugate pair such that the matrix M, containing the real and imaginary parts of the eigenvalue solutions of eq (3 1 8) for this specific fixed point, is a rotation matrix about the point itself (Bergé et al (1987)) For the $2D$ system M is of the form

$$M = \begin{pmatrix} \cos(\gamma) & -\sin(\gamma) \\ \sin(\gamma) & \cos(\gamma) \end{pmatrix} \tag{3 1 9}$$

For these elliptic fixed points the complex eigenvlaues can be expressed in terms of two real numbers α & β such that,

$$\lambda_1 = \alpha + \iota\beta \tag{3 1 10a}$$

$$\lambda_2 = \overline{\lambda}_1 = \alpha - \iota\beta \tag{3 1 10b}$$

$$\|\lambda_1\| = \|\lambda_2\| = \lambda_1\lambda_2 = \alpha^2 + \beta^2 = 1 \qquad (3\ 1\ 10c)$$

Furthermore the angle γ is $\cos^{-1}(\alpha)$, or $\sin^{-1}(\beta)$ Thus any point (x, y) in the vicinity of these elliptic points would be rotated through an angle γ at every iteration thus forming circular orbits From table 3 1 the dependence of the angle γ on μ_{cl} is shown clearly illustrating that the eigenvalues he on a unit complex circle about which they rotate anti-clockwise with increasing μ_{cl}

μ_{cl}	λ_1 $(\alpha + \iota\beta)$	λ_2 $(\alpha - \iota\beta)$	γ $\cos^{-1}(\alpha)$ or $\sin^{-1}(\beta)$	Type
1 0	0 9208 + ι0 3900	0 9208 − ι0 3900	23°4 4′	Elliptic
2 0	0 6928 + ι0 7211	0 6928 − ι0 7211	46°8 9′	"
3 0	0 3448 + ι0 9387	0 3448 − ι0 9387	69°49 8′	"
4 0	−0 0752 + ι0 9972	−0 0752 − ι0 9972	94°18 8′	"
5 0	−0 5000 + ι0 8660	−0 5000 − ι0 8660	120°	"
6 0	−0 8432 + ι0 5376	−0 8432 − ι0 5376	147°28 8′	"
7 0	−0 9992 + ι0 0399	−0 9992 − ι0 0399	177°42 5′	"
8 0	−0 8432 − ι0 5376	−0 8432 + ι0 5376	212°31 2′	"
9 0	−0 2312 − ι0 9729	−0 2312 + ι0 9729	256°34 8′	"
10	1 0000	1 0000	360°	Hyperbolic

Table 3 1 The dependence of $\lambda_1, \lambda_2$and γ on the kick strength μ_{cl} The larger μ_{cl} the faster an orbit can complete a full circuit around the fixed point once $\mu_{cl} < 100$ At this value of μ_{cl} the point becomes hyperbolic and the eigenvalues satisfy *eq* (3 1 11) rather than eqns (3 1 10a − c)

For a hyperbolic point its eigenvalues are not complex but real with the ratio between them such that their product is 1

$$\lambda_1 = 1/\lambda_2 \qquad (3\ 1\ 11)$$

In order for eq (3 1 11) to be satisfied one eigenvalue must be greater than 1 with the other less than 1 Whichever eigenvalue is greater than 1 describes the unstable direction whereas the eigenvalue less than 1 describes the stable direction

The eigenvalue equation for the period four fixed points is desired as this periodicity is the fundamental symmetry of the system To proceed further it is necessary to substitute, from eq (3 1 7), the values of the period four fixed points in order to eliminate the sin terms in the expressions for the 4 R M This substitution makes for a much simpler set of equations than those in eqs (3 1 3) and (3 1 4) The Jacobian's elements, J_{ij} where $1 \leq i, j, \leq 2$ and $i, j \in \mathbf{Z}$, are

$$J_{11} = \frac{\partial x(n+1)}{\partial x(n-3)} = 1 - 4K^2\mu_{cl}^2(-1)^{n+m} \qquad (3\ 1\ 11a)$$

$$J_{12} = \frac{\partial x(n+1)}{\partial y(n-3)} = 4K\mu_{cl}(-1)^n - 8K^3\mu_{cl}^3(-1)^{2n+m} \qquad (3\ 1\ 12b)$$

$$J_{21} = \frac{\partial y(n+1)}{\partial x(n-3)} = -4K\mu_{cl}(-1)^m + {}^{2m+n}\, 8K^3\mu_{cl}^3(-1) \qquad (3\ 1\ 12c)$$

$$J_{22} = \frac{\partial y(n+1)}{\partial y(n-3)} = 1 - 12K^2\mu_{cl}^2(-1)^{m+n} + 16K^4\mu_{cl}^4(-1)^{2(n+m)} \qquad (3\ 1\ 12d)$$

The eigenvalue equation given previously, in *eq* (3 1 8), boils down, now, to

$$(1 - \lambda - 4K^2\mu_{cl}^2(-1)^{m+n}) * (1 - \lambda - 12K^2\mu_{cl}^2(-1)^{m+n} + 16K^4\mu_{cl}^4(-1)^{2(n+m)})$$

$$-(4K\mu_{cl}(-1)^n - 8K^3\mu_{cl}^3(-1)^{2n+m}) * (-4K\mu_{cl}(-1)^m + 8K^3\mu_{cl}^3(-1)^{2m+n}) = 0 \quad (3\ 1\ 13)$$

This equation is solved on a computer using the formula for obtaining the roots of a quadratic equation to give the eigenvalues λ_1 & λ_2 for any period four fixed point ($5m\pi$, $5n\pi$) at specified values of μ_{cl} & K Remember that β is fixed now at $\frac{\pi}{2}$ It has been seen from results obtained numerically that for $\mu_{cl} > 0$ the period four fixed points with $n+m$ odd are hyperbolic with unstable and stable directions given by λ_+ and λ_- respectively Furthermore for two adjacent period four hyperbolic points A & B, with $A = (5m\pi, 5n\pi)$ and $B = (5(m+1)\pi, 5(n+1)\pi)$, the terms J_{21} & J_{22} for A are equal to $-J_{21}$ & $-J_{22}$

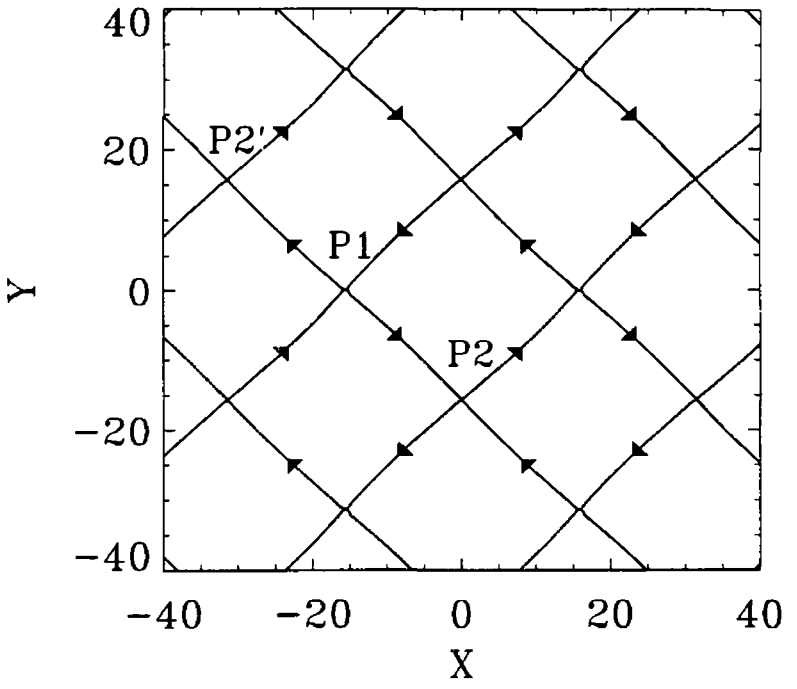

Fig 3 1 The principle directions of travel along the stochastic layer for $\mu_{cl} = 6\,5, K = 0\,1$ and $\beta = \pi/2$ The arrows indicate the directions transport takes place in Arrows pointing away from a crossover (hyperbolic fixed point) indicate unstable directions while stable point towards the fixed point

repsectively for B The result of this is to cause the unstable direction of A, given by λ_{+}^{A}, to coincide with the stable direction of B, given by λ_{-}^{B}, and vice versa A plot showing this is given in fig 3 1 From this one is able to deduce that orbits in the vicinity of the unstable manifold of any hyperbolic period four fixed point, denoted $P1$, can be shoved away from it to one of two of its neighbours, $P2$ & $P2'$, because their stable directions are coincident with the unstable directions of $P1$ Once in the vicnity of $P2$ or $P2'$ the orbit is then pushed away along their unstable manifolds to one of two of their neighbours and so the process can continue until the orbit has visited all the period four hyperbolic fixed points in the $2D$ plane of the phase space (Lowenstein, (1991), Radons & Prange (1990))

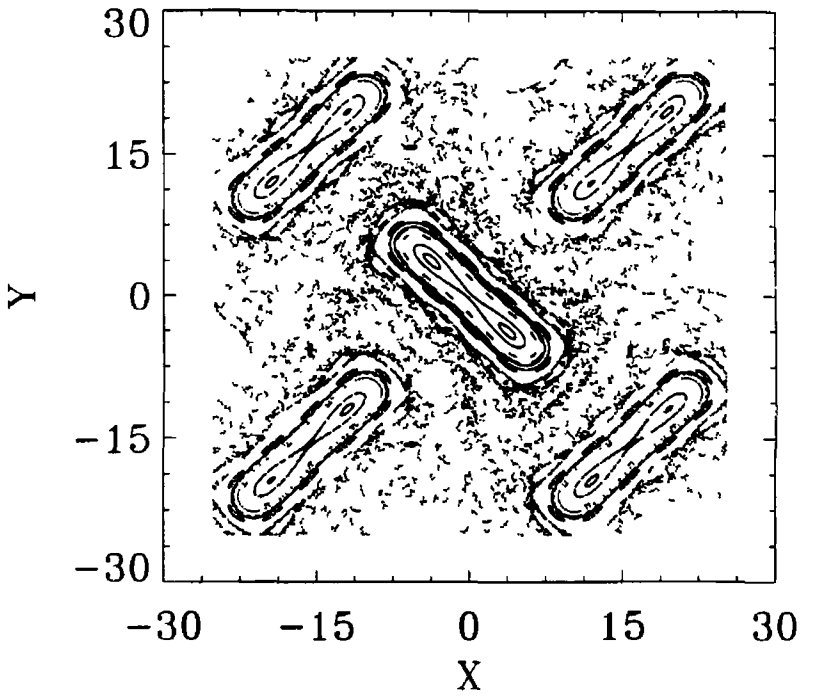

Fig 3 2 This phase plot shows the dumb bell type separatrix about the newly formed hyperbolic points in the cells' centers for $\mu_{cl} = 11\ 0, K = 0\ 1$ and $\beta = \pi/2$ The cell eventually breaks into two pieces whose centers correspond to the centers of the loops These smaller cells eventually break up in a similar way

As the period four fixed points with $n + m$ odd are hyperbolic then naturally it is safe to presume those with $n + m$ even are elliptic This is in fact the case up to the value of μ_{cl} equal to 10 At this value and for values above these elliptic points become hyperbolic with their manifolds taking on a dumb bell shape as evident from fig 3 2 The implication of this dumb bell shape is that the unstable manifolds of these points coincide with the stable manifolds at the extreme of each loop with the result that orbits near the unstable manifold get repelled only to be attracted along the stable manifold further on This causes the orbits to remain localised within the cell. Eventually, as the kicking strength is increased, the outer orbits of the cell break up and the localised orbits become de-localised

and diffuse Furthermore, as will be shown later in the chapters relating to the quantum mapping, this dumbbell type structure and the subsequent break-up of the period four invariant cells into two smaller cells is very fortunate for us This property allows us to analyse the quantum behaviour at the origin (using low order eigenfunctions) knowing that it will become unstable and that this stability can be measured by examining the evolution of energy and the probability amphtudes This is done in detail in chapter 6, sections 6 1 and 6 2

Also apparent are other separatrices bordering the diffuse region These separatrices are initially sharply defined but as the kick strength is increased they become diffuse and eventually indistinguishable from the surrounding layer At this point all that remains are the small island cells in the layer These cells contain an elliptic point at their center with invariant orbits surrounding them As the kick strength is further increased the measure of the cells reduces due to orbit breakup at the cell boundary with the stochastic layer As the kick strength increases further separatrices form in some of the orbits with small cells surrounding higher order elliptic fixed points As before these separatrices become diffuse and the small cells break away from the larger mother cell which is getting smaller Eventually the elliptic points in the center of these cells become hyperbolic and all invariant cells tend to measure zero with the stochastic layer occupying the whole of the $2D$ phase space except for the locations of the periodic points which have measure zero (Helleman (1980)) These break-ups can be best described by the following diagram

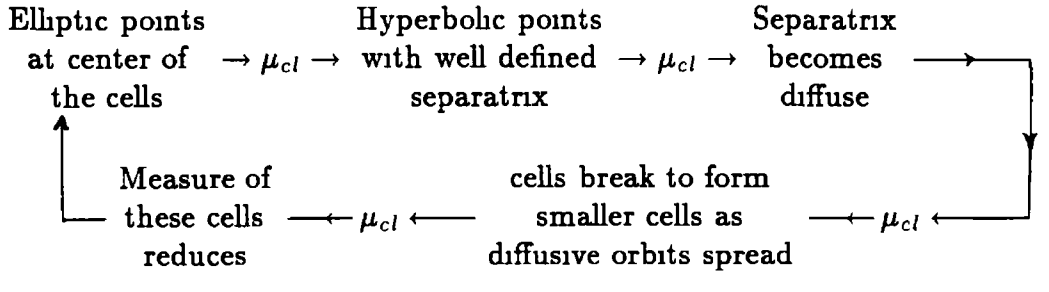

where μ_{cl} denotes increasing μ_{cl} This form of break up is predicted by the Kolmogorov Arnold Moser (K A M) theorem which is used in the following section to analyse the phase space in a more quantitative manner

3 2 Of Action-Angles & K A M

Recall how, in chapter 2, we showed how circular orbits should arise naturally in the phase space of the undriven harmonic oscillator As these circular orbits hint at an underlying circular symmetry it is prudent for us to consider expressing the a & $a^\dagger$ operator variables in terms of a set of circularly symmetric operators variables These variables are referred to as Action-Angle $(A-A)$ variables denoted J(action) and θ(angle) Once J and θ are defined with respect to a and $a^\dagger$ they can be substituted into the original system Hamiltonian, H_T The advantage of this change of variables is to readily allow us check the influence of the non-integrability of the kick term on the original integrable undriven system Our definition of integrability is that if the hamiltoman can be expressed as a function of J only then it is integrable We proceed by defining J and θ according to

$$a = \sqrt{J} * \exp(\iota\theta) \qquad \textit{and} \qquad a^\dagger = \sqrt{J} * \exp(-\iota\theta) \tag{3 2 1}$$

The action-angle variables can be expressed directly in terms of the P and Q operators with the purpose for this being our ability to directly compare the classical x and y to the classical equivalent of the action-angle variables

$$Q = \sqrt{J} * \cos(\theta) \qquad \textit{and} \qquad P = \sqrt{J} * \sin(\theta) \tag{3 2 2}$$

When the Hamiltonian for the undriven oscillator, H_o, given in *eq* (2 1 5*a*) is expressed in this new set of variables it becomes independent of θ and is a function of J only

$$H_o\,(\,J,\theta\,) \equiv H_o\,(\,J\,) = J\hbar\omega_o \tag{3 2 3}$$

such that the energy of the system is related directly to the variable J not θ This is essentially a canonical form of the original H_o The variables J and θ are also dimensionless as is apparent from eqs (3 2 1) and (3 2 3) When this Hamiltoman is transposed to the classical representation we define a new set of variables such that the following identities holds

$$x = \rho * \cos(\phi) \qquad \textit{and} \qquad y = \rho * \sin(\phi) \tag{3 2 4}$$

where ρ and ϕ are our classical equivalents of J and θ so that our transposition takes $\sqrt{J/2}$ to ρ and θ to ϕ We can now *directly* identify the circular orbits in the classical space to

these new variables As has been previously pointed out, the phase space of H_0 consists of concentric circular orbits which, in the ρ, ϕ representation, are given by

$$\rho^2 \sin^2(\theta) + \rho^2 \cos^2(\theta) = \rho^2 \tag{3 2 5}$$

where ρ is essentially the *radius* of the orbits The larger the value of ρ the larger the circle and the higher the energy of the orbit

Such a system as that represented by the Hamiltonian in eq (3 2 3) is considered integrable because the Hamiltonian can be written as a function of J solely and has no direct dependence on θ A non-integrable system can be considered to be one where the hamiltonian cannot be so written

Our interest here is in the kicked system so let us now proceed by expressing the complete system Hamiltonian, H_T, defined in eq (2 1 6) in terms of J and θ

$$H_T(J, \theta) = H_o(J) + \mu_q H_1(J, \theta) \tag{3 2 6}$$

This shows H_T to consist of an integrable term, H_o, and a non-integrable term H_1 The integrable term is that for the undriven system as described above whereas the non-integrable term is that for the driving term We have for clarity removed the kick strength variable, μ_q, from the hamiltonian H_1 so that the proceeding analysis will be easier to understand The classical equivalent of eq (3 2 6) would be the corresponding energy equation which depends on ρ and ϕ

$$E_T(\rho, \phi) = E_o(\rho) + \mu_{cl} E_1(\rho, \phi) \tag{3 2 7}$$

where E_T, E_0 and E_1 are the corresponding classical terms to H_T, H_0 and H_1 respectively The remainder of this section is devoted to explaining what effect μ_q has on the integrability of H_T and by consequence μ_{cl} on E_T The K A M theorem is also invoked to help explain why some orbits in the classical phase space break up quicker than others

For large values of kicking potential, $\mu_{cl} E_1$, the system is certainly non- integrable due to a domination by this term over the E_o term The fundamental question, however, is *To what level is the system non-integrable for small non- zero values of the kicking potential and how does this level of non-integrability affect the invariant orbits in the phase space?*

This is the question that the K A M theorem addresses According to this theorem if the non-integrable term is sufficiently small to behave more as a perturbation on the integrable term than as a major contributory term then the invariant orbits remain if the orbits have sufficiently incommensurate frequencies ω_i Those with commensurate frequencies or frequencies nearly commensurate do not remain and are distorted to a lesser or greater extent with some even being destroyed

For small μ_{cl} we can see from the phase space portrait in fig 3 3(a) that the majority of the orbits are circular in shape and are thus largely unaffected by the kicking term Subsequent enlargements (figs 3 3(b),(c)&(d)) about the hyperbolic fixed point at $(0, 5\pi)$ show that the stochastic layer is very small indeed being confined very tightly to the manifold structure resulting from the hyperbolic fixed points of period four (c f fig 3 1) The only orbits with any noticeable distortion are those whose non-integrable contribution is comparable, or greater, to their integrable term As μ_{cl} is small then those orbits with large $E_1(\rho, \phi)$ can have non-integrable contributions which can not be considered as vanishingly small Indeed it is only these orbits which have some level of discernible distortion Therefore we can conclude that for small μ_{cl} the level of non-integrability in the system as a whole is so small as to be negligible

Having addressed the problem for small μ_{cl} we now concentrate on the problem for μ_{cl} finite and beyond the perturbation realm We would expect that if $E_1(\rho, \phi)$ was of a sufficient size to be capable of distorting phase space orbits when μ_{cl} was small, and merely perturbing the system, then as μ_{cl} is increased the distortion would increase and orbital (toral in higher dimensions) breakup would arise probably through an overlapping of higher resonance separatrices This will be examined in detail in the next section

It is worth noting that as $E_1(\rho, \phi)$ is not constant then it can negate, or even reverse, the effect of an increasing μ_{cl} if it is sufficiently small In this case the non-integrable term becomes more of a perturbation and the orbits remain essentially undistorted as we can see around the elliptic point at the origin In conclusion, the higher $E_1(\rho, \phi)$ for any μ_{cl}, the greater the distortion and the sooner the break up of the orbits For our system we will show that the magnitude of $E_1(\rho, \phi)$ determines how many terms in the series expansion of its cosine term are needed to accurately describe the behaviour. More terms

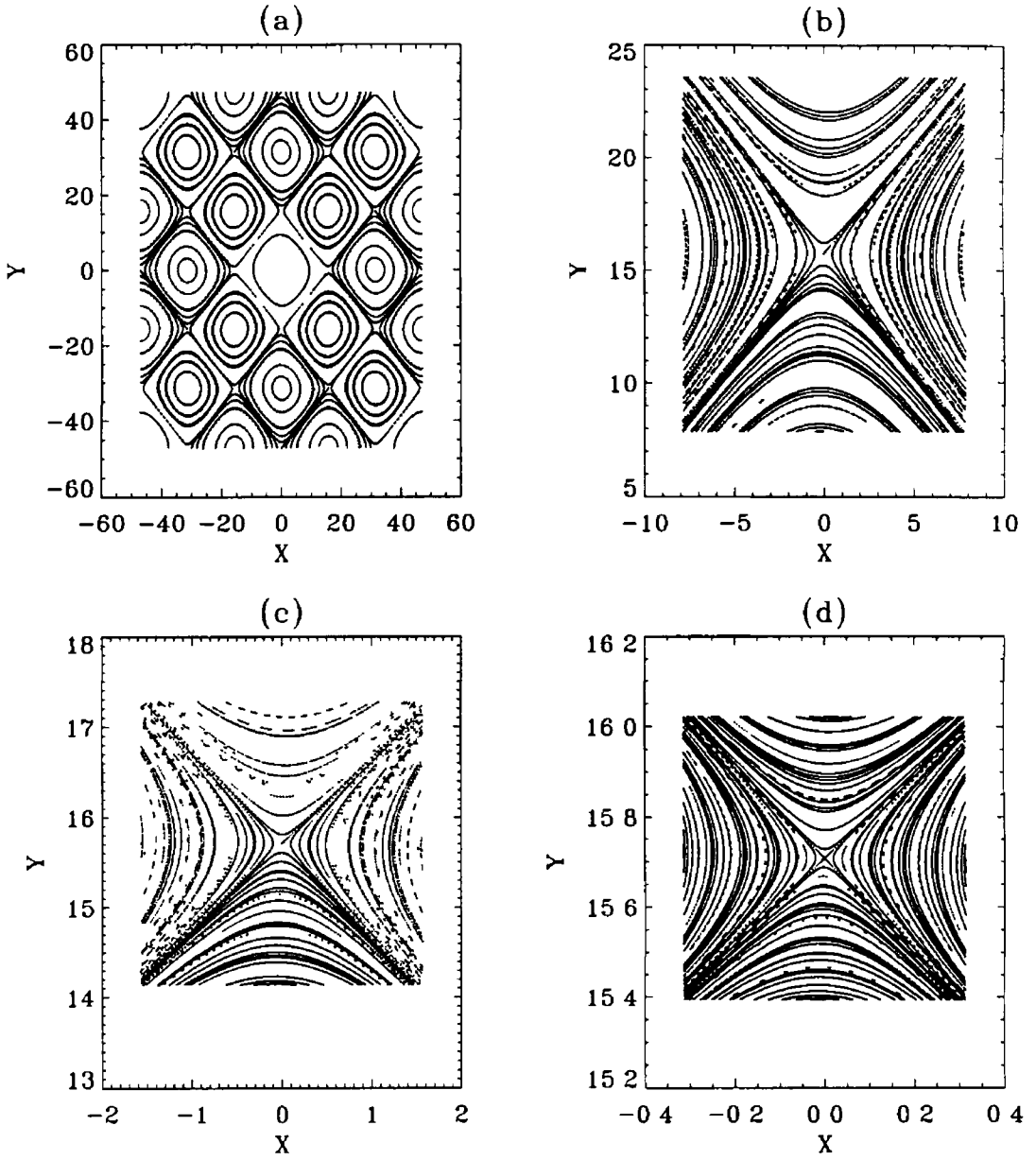

Fig 3 3 The phase space of the kicked oscillator for $\beta = \frac{\pi}{2}, K = 0\,1$ & $\mu_{cl} = 0\,5$ The enlargements in parts (b), (c) & (d) about the hyperbolic fixed point at $(0, 5\pi)$ show how confined the stochastic layer is but that it does exist nevertheless

allow for higher order periodic points and hence an earlier break up of the orbits than for orbits with less terms and hence a smaller $E_1(\rho, \phi)$ In the above analysis the classical terms, E_1, μ_{cl} and E_0, were used However their effects on the system can be related di-

rectly back to their quantum counterparts and the arguments presented above could quite easily have been presented in terms of H_1, μ_q and H_0 This inter-relating of quantum and classical is important to the analysis using the quantum mapping in chapters 6 & 7

3 3 Periodic Orbital Analysis

It is our intention here to quantitatively analyse what was stated in the previous section To accomplish this we intend to construct a form of the non- integrable term which will allow us to predict which orbits should be present given the type of potential we are using to drive the system

Let us start by examining the driving term $H(J,\theta)$ expressed as a function of the Action-Angle variables J & θ

$$H_1(J,\theta) \equiv \cos\left(\sqrt{\frac{J\hbar k^2}{M\omega_o}}\sin(\theta)\right)\sum_{n=0}^{\infty}\delta(t-n\tau) \qquad (3\,3\,1)$$

We have deliberately substituted K for its constituents as defined in chapter 2 as this will permit us to explicitly equate the ω_o term to the driving frequency $\omega_1(\equiv 2\pi/\tau)$ The cosine term is now replaced by its series expansion to give

$$H_1(J,\theta) \equiv \sum_{m=0}^{\infty}\left(\frac{-\hbar k^2}{M\omega_1}J\right)^m \frac{\sin^{2m}(\theta)}{(2m)!}\sum_{n=0}^{\infty}\frac{\delta(t-n\tau)}{r^m} \qquad (3\,3\,2)$$

where ω_o has been replaced by $r\omega_1$ and r is the ratio between ω_o and ω_1 The above can now be expressed in the more readable form

$$H_1(J,\theta) = \sum_{m=0}^{\infty}(-1)^m f_m(J,\theta,\omega_1)\sum_{n=-\infty}^{\infty} g_{mn}(\omega_1,r) \qquad (3\,3\,3)$$

The classical equivalent for the above is identical m form but has of course the classical equivalents of the quantum operators and variables The classical form is the one we shall use in the following analysis as this analysis requires comparisons between the predicting equation and results obtained from numerical simualtions in the classical phase space Our classical form is

$$E_1(\rho,\phi) = \sum_{m=0}^{\infty}(-1)^m \bar{f}_m(\rho,\phi,\omega_1)\sum_{n=-\infty}^{\infty}\bar{g}_{mn}(\omega_1,r) \qquad (3\,3\,4)$$

To analyse the behaviour of this system we need to consider the relationship between ω_o and ω_1 Remember that $\beta = \frac{\pi}{2}$, that is $r = 1/4$ Therefore we have, in the function $g_{mn}(\omega_1, r)$, a way of describing the affect the relationship between ω_o and ω_1 has on the existence of resonances in the complete system It is evident from eq (3 3 1) that not only is the cosine term sampled by the delta function at a frequency ω_1 but also that this term has an infinite set of intrinsic frequencies, $\omega^m (\equiv r^m \omega^m)$, and that the ratio between these frequencies and ω_1 allows the various resonances to exist We can use these resonances to predict the periodic points m the system's phase space Thus, depending on the values chosen for m, the resonances allowed can be various and not just multiples of four It is these resonances that cause the breakup of orbits in the phase space because only those orbits which are sufficiently incommensurate will survive an increase in the non-integrability of the system (as predicted by K A M theory)

How sufficient is sufficient? This condition of sufficiency may become more apparent by examining the resonances at some low values of m Table 3 2 shows how for a given value of m, the number of expected resonaces is dependent on the number of factors of r^m Furthermore, the statement '*maybe all factors which almost divide evenly into 256*' implies that while there are multiples of 4 which do divide into its higher powers evenly there can nevertheless exist periodic orbits which have a periodicity close enough to a divisor of 256, or any power of 4^m $\forall m \in \mathbf{Z}$, with a small remainder These constitute the quasi-commensurate orbits which accelerate the destruction of orbits with small E_1 whose resonances otherwise would be of insufficient number to break up the orbits at the same value of μ_{cl} The periodic points actually seen in the system to date have been 1,3,4,5,6,7,8,12,16,21,24,32,48,72 The inherent difficulty of locating, numerically, fixed points of a specific periodicity is well known especially if the points have small lyapunov exponents as this results in slow convergence to the points themselves (Auerbach et al (1987)) Therefore the list presented above is as complete as permitted by the limit on computing time and by the resolution of the search grid used to locate the points

The non-integrable cosine term, E_1, in the system equation can only be described by its first few series terms when its argument ($\propto \rho \sin(\phi)$) is small As the ρ can be considered, in the undriven oscillator, to be analogous to the radii of orbits then in the

m	resonances	$r^m \equiv \omega_1/\omega^m$
0	$1-1$	ω_1
1	$1-4\&1-1$	4
2	$1-16, 1-8, 1-4, 1-1$ *maybe a 1-5 & 1-3*	16
3	$1-64, 1-32, 1-16, 1-8, 1-4, 1-1$ *maybe 1-21,1-13,1-12,1-9,1-7,1-5,1-3*	64
4	all multiple of 4 up to 256 *maybe all factors which almost divide into 256 with small remainders*	256

Table 3 2 The first few terms in the expansion of the driving term in *eq* (3 3 3) showing what resonances would be expected to be present Those resonances shown in italics are those which nearly divide into the number given r^m

driven case, for those orbits near the origin, we can make a similar identification As the phase space has a definite four-fold symmetry then all invariant cells centred about a period four elliptic point satisfying the condition in Eq (3 1 7) can be transformed to the origin Therefore we can presume that the contribution from the non-integrable term E_1 about each of these elliptic fixed points is small So $\rho \sin(\phi)$ tends to zero in the vicinity of the elliptic points of period four The number of possible resonances in this region is small because of the small number of terms, in the cosine expansion of E_1, needed to adequately describe the system's behaviour (see table 3 2) Thus the possibility of orbital breakup is small for small values of the parameter μ_{cl}, but becomes increasingly more probable as the kick strength μ_{cl} is increased The system is essentially integrable in these regions for small μ_{cl}

However the further out we go from the elliptic fixed points at each invariant cell's centre then the more terms we require to satisfactorily describe the system's behaviour and

hence the greater the number of possible resonances. There is a constant multiplier (K) in the E_1 term which takes on the value 0.1 in the case being considered here. As a consequence of this the $x's$ and $y's$ have prominent fixed points every 5π (as in Eq. (3.1.7)) with hyperbolic fixed points of period four at specific multiples of 5π (as previously explained in section 1 of this chapter). The regions of the orbits nearest these hyperbolic points have largest non-integrability and hence require the most terms in the cosine expansion of E_1. The most terms implies the greatest resonance overlap and for large μ_{cl} their contributions can be very significant.

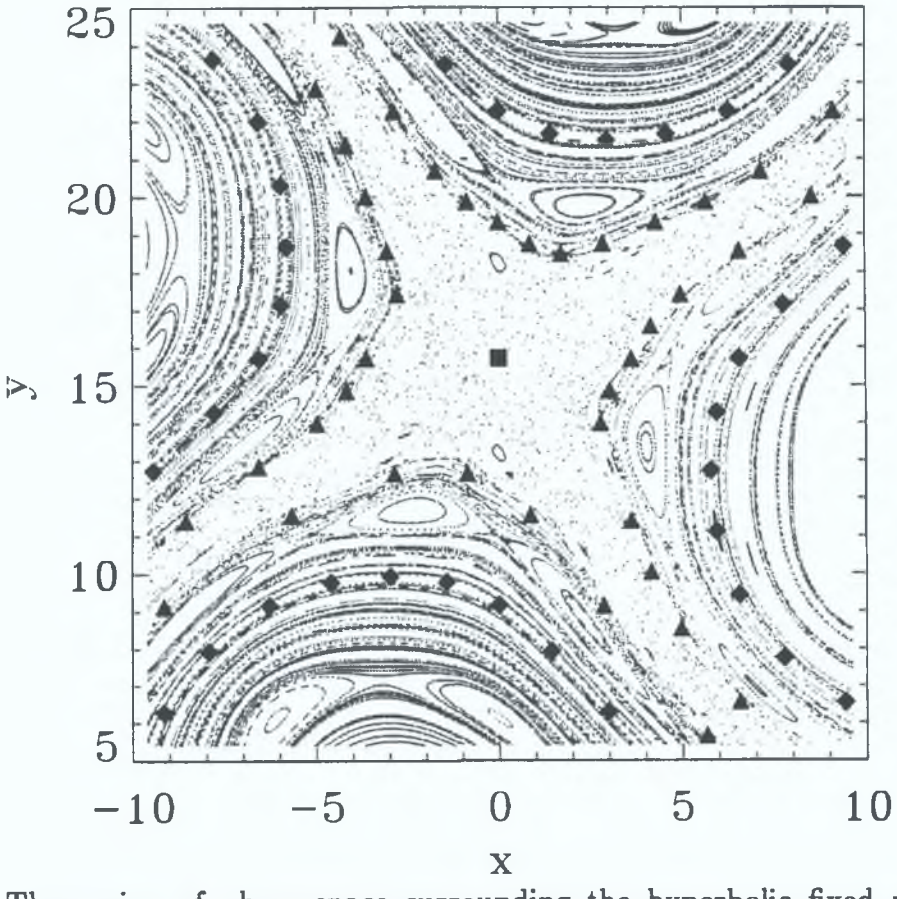

Fig.3.4 The region of phase space surrounding the hyperbolic fixed point at $(0, 5\pi)$ for $\beta = \frac{\pi}{2}, K = 0.1$ & $\mu_{cl} = 6.5$. Fixed points (both hyperbolic and elliptic) of various periodicities are shown: period 4 are denoted by squares, period 16 by diamonds & period 24 by triangles

So the break up of the orbits occur in the region most non-integrable (that is regions where $K\rho\sin(\phi)$ is not small) For small μ_{cl} the driving term (regardless of how many terms are in the cosine factor) is small and the system follows the scenario of commensurate orbital breakdown as described by the K A M theorem As μ_{cl} is increased the regions following this scenario contract about the elliptic fixed points described earlier The outer regions for these large μ_{cl} have many overlapping separatrices from each of the boundaries of the resonances These overlapping separatrices break up and form stochastic regions around the unbroken, albeit distorted, orbits The width of the stochastic region increases with increasing μ_{cl} due to the contraction of the K A M regions about the elliptic fixed points These are evident from the phase portraits shown in fig 3 3

We should expect even for very small μ_{cl} the existence of a stochastic region around the hyperbolic points as these regions are the most non-integrable for any value of μ_{cl} It may occur that a stochastic region doesn't exist below a particular value of μ_{cl} due to the small nature of the the kicking However as this region contains the greatest number of possible resonances (due to the large ρ value) it follows that separatrix break-up into stochastic layers is very probable at small μ_{cl} values The width of such a layer would be extremely thin and consequently would be very hard to locate numerically as the boundary would be quite sharp requiring high numerical precision

Fig 3 4 shows an enlargement of the phase space about the hyperbolic fixed point at $[0, 5\pi]$ for $K = 0\ 1, \mu_{cl} = 6\ 5$ and $\beta = \pi/2$ The stochastic layer is clear in the figure as are some small invariant cells within the mother cells of the period four elliptic fixed points Superimposed on this phase space are various opaque geometrical objects at the positions of the period 4 hyperbolic fixed point, the period 16 fixed points and the period 24 fixed points The points on the layer boundary are the period 24 pomts whose separatrix surrounding the invariant cells are now diffuse leaving an island chain of cells with period 24 elliptic pomts at their centers

3 4 The Stochastic Layer

One of the important features of the phase space in this classical mapping is the

existence of a layer between elliptical cells which allows the unbounded growth of energy in the system In this *stochastic* layer (so named because of its diffusive nature) the successive iterates of the mapping can wander around the whole of phase space with the effect that the energy of the diffuse orbit can increase without any limit This aspect of the layer is examined in detail in chapter four What we are going to analyse here is the width of the stochastic layer and also to compare the largest Lyapunov exponent to the stability of nearby periodic points

So let us proceed with a detailed examination of the variation of the stochastic layer width as a function of the kick parameter, μ_{cl} Generally it is accepted that for small values of the driving parameter the width increases in an exponential manner (Zaslavsky and Filonenko (1968), Zaslavsky et al (1986) and Chernikov et al (1989)) To illustrate this we present four phase plots of the layer for different values of μ_{cl} (1 0,3 0,5 0,7 0) showing both the increasing size and complexity of the layer boundary This increase in boundary complexity caused problems with the program used to measure the width as will be explained later

To measure the width, a program was written which sampled points on the main $x = 0$ axis through the hyperbolic fixed point $(0, 5\pi)$ about which the layer exists The initial guess was to see if before N iterations of the mapping the initial condition caused the n^{th} iterate (where $n \leq N \; \forall n \in \mathbf{Z}$) to leave the region of the bounded orbits and wander about the phase space If so then the distance from this point to the fixed point at $(0, 5\pi)$ was measured and this was the measure of the layer width The previous four plots show how, at the boundary layer, periodic points of increasing order, with their elliptic islands about elliptic points and separatrices through hyperbolic points, abound at high values of μ_{cl} but are noticeably absent for low values Obviously the driving term $H_1(J, \theta)$ has a lesser degree of influence at low values whereas at higher values the resonance overlaps and potential for orbital break-up by said resonances bring about this prevelence of periodic islands in the layer These islands greatly affect the layer width measurement and give rise to noticeable dips in the layer width curve

The width variation, for μ_{cl} increasing from 1 0 to 3 0 inclusively, is shown in fig 3 6 The general trend seems to indicate an exponential increase with the data from the

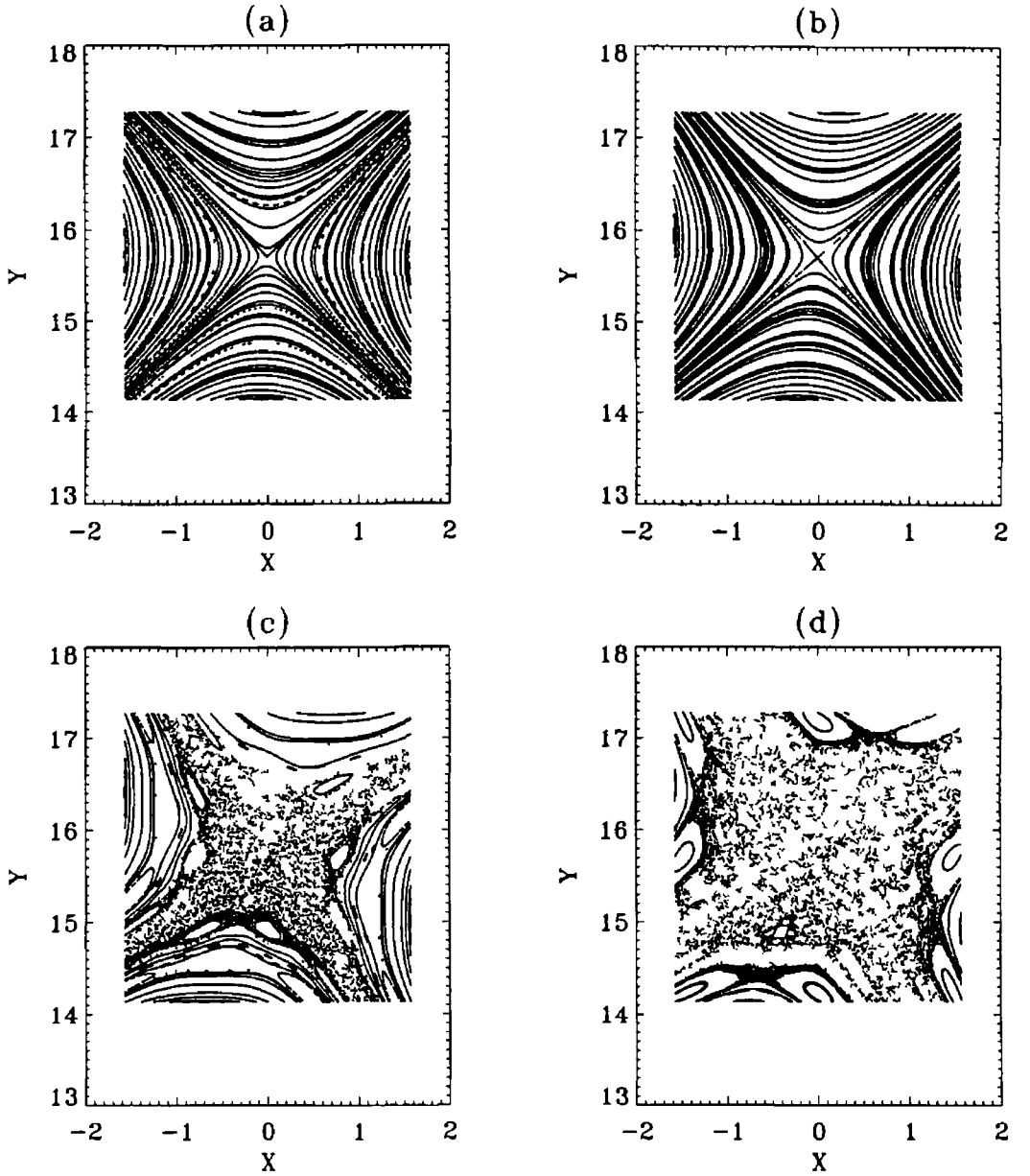

Fig 3 5 Four plots of the stochastic layer about a hyperbolic fixed point for $\beta = \frac{\pi}{2}, K = 0\,1$ & four different kick strengths In (a) $\mu_{cl} = 0\,5$, in (b) $\mu_{cl} = 1\,5$, in (c) $\mu_{cl} = 4\,5$ & in (d) $\mu_{cl} = 5\,0$

simulation fitting an exponential curve of the form

$$\Delta W = \frac{8\pi^3}{\mu_{cl}} \exp\left(-\sqrt{5}\frac{\pi^2}{\mu_{cl}}\right) \tag{3 4 1}$$

This form agrees exactly with that analytically predicted (for kicking strengths $\ll 1$) by

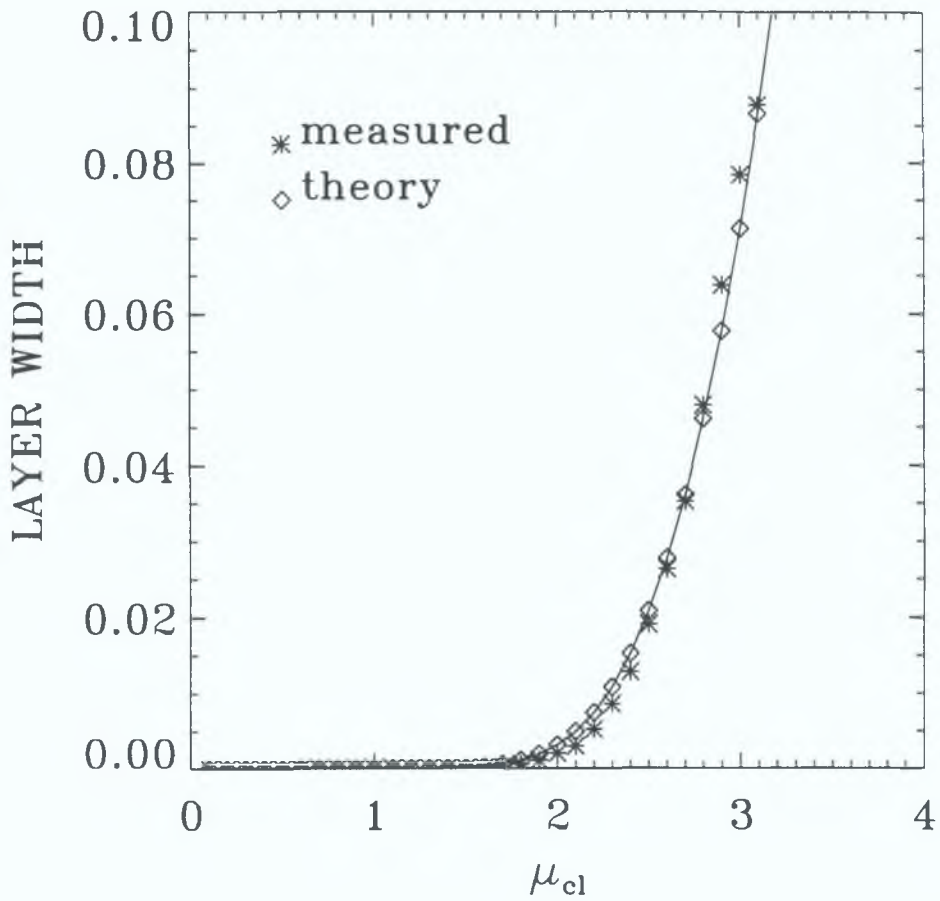

Fig.3.6 The stochastic layer width vs. the kick strength, μ_{cl}. The line corresponds to the theoretical curve while the points correspond to the measured width. The agreement is very good considering the time it takes for each measurement to converge. For values higher then $\mu_{cl} = 3.0$ we measured dips in the measured width attributed to the growth of islands on the stochastic layer boundary.

Chernikov et al. ((1989),(1987)). (Note that the $\sqrt{5}$ in the argument of the exponential arises from our explicit inclusion of K in our initial definition of μ_{cl}. See chapter two for our justification of this.)

For values of μ_{cl} greater than 3.4, dips occur in the curve probably due to the presence of the periodic islands growing about high order periodic points on the boundary where orbital break up occurs due to resonance overlap. These islands are evident only

at values of μ_{cl} greater than 3 0 and are considered by me to be the cause of the dips How a dip occurs could be as follows as the line along which the initial points for each set of iterations passes from the bounded orbital region to the stochastic region, it may encounter separatrices and periodic islands in its way The separatrices may initially be bounded and hence non-stochastic but at some value μ_{cl} become stochastic giving rise to a jump in the width curve However the islands may also increase in size pinching these regions and causing a dip with respect to the previous value if the program takes initial points that skip this region The only way to measure the layer for the higher values is to plot the phase space, enlarge the boundary region and manually measure the region's width

The *chaos* in such a conservative system as this (conservative because the Jacobian is 1 always) is attributed to this layer's existence This is true because in this layer nearby points separate exponentially and have a positive Lyapunov exponent In fig 3 7 we show this sensivity to initial conditions by measuring the separation between two points initially close to one another The initial points taken were $(x_1, y_1) = (1\ 0, 15\ 707963)$ and $(x_2, y_2) = (1\ 000001, 15\ 707964)$ i e an addition of 0 000001 to both x_1 and y_1 As can be seen from the plot in fig 3 7 the separation varies widely and this with the previously mentioned positive Lyapunov exponent confirms the presence of chaos (in the classical sense) in this layer

Furthermore we can trace the exponential divergence of nearby orbits back to the manifolds for the period four fixed points (see fig 3 1 and the discussion following it) along which orbits can diffuse over the whole phase space Furthermore depending on how near to, or on which side of, an unstable manifold an orbit is, determines on which unstable manifold it moves along at the next period four hyperbolic point Thus nearby orbits can separate exponentially along this manifold structure We have found that the calculated positive Lyapunov exponent (for a specific orbit in the stochastic layer) vs μ_{cl} follows a weighted average of the eigenvalues of the hyperbolic fixed points the orbits visits The weighting depends on which point is visited and on which unstable manifold it leaves For large μ_{cl} the complexity of the layer and the proliferation of higher order hyperbolic fixed points (brought about by invariant orbit break up by overlapping resonances) brings about

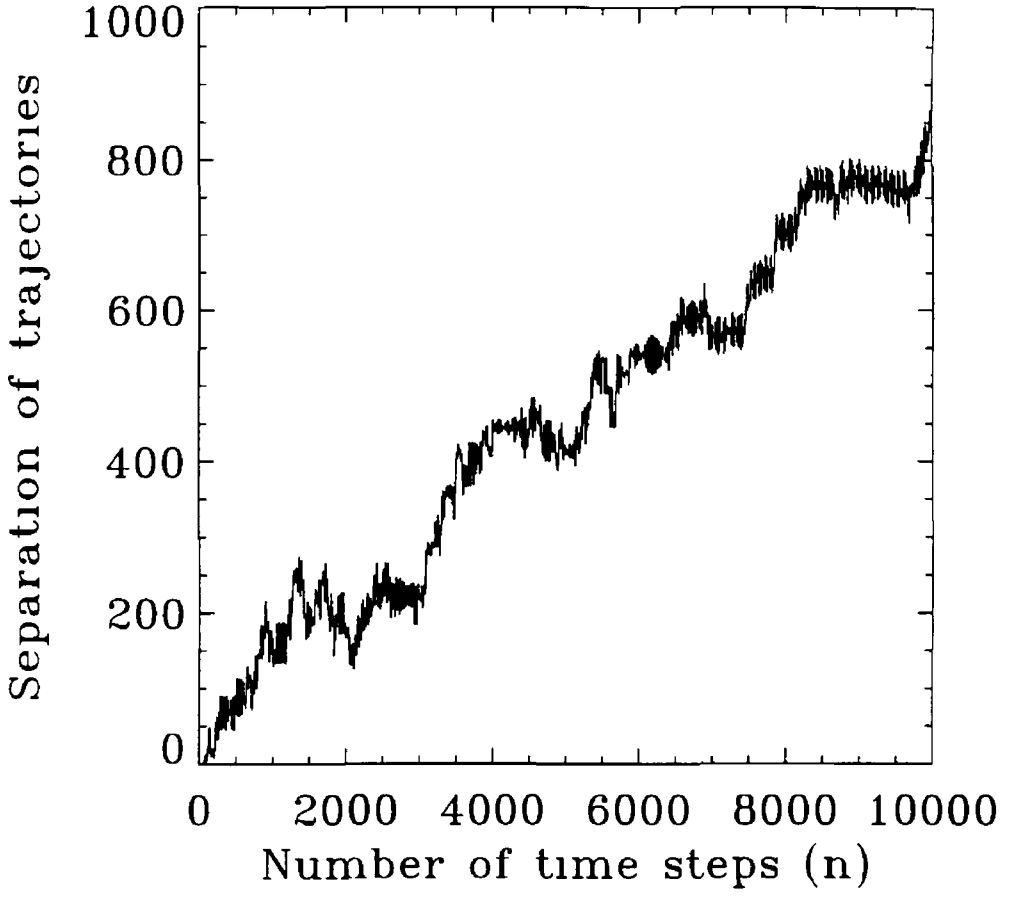

Fig 3 7 The separation of two nearby trajectories in the stochastic layer Initially very close together, they diverge very rapidly showing clearly the *sensitive dependence on initial conditions*, the hallmark of classical chaos

a variance in the above relationship between the Lyapunov exponent and the eigenvalues of the hyperbolic points This variance is put down to the increased number of unstable manifolds from these higher order hyperbolic fixed points bringing about a more complex motion in the layer than before To our knowledge most of the analytical approaches to date have not taken into account these compexities

CHAPTER 4
DIFFUSION IN THE STOCHASTIC LAYER

The stochastic layer has been shown in the last chapter to hold the key to the non-linear characteristics of the system Therefore this layer is the focus of much of the preceding and proceeding analysis The unbounded nature of phase space orbits within the layer proper points to the ability of unbounded energy growth in these orbits as shown in the last chapter Furthermore as these orbits are unbounded the method of diffusion of collections of orbits is important as in any physical system it is more usual to experience the ensemble properties rather than an individual In this chapter the diffusion of a large number of orbits is examined and some analytical arguments presented whose results fit the numerically obtained data remarkably well

4 1 Green's Function & Diffusion

The following approach is based on the analysis done by Rechester and White (1980) which led to an analytical form for the diffusion in the stochastic layer of the Chirikov-Taylor system (Chirikov et al, 1979) Their analysis was based on the use of a Green's function solution to the Vlasov equation for turbulent system with an added diffusion term The approach taken here is similar in form We will show how the extra potential term for the kicked oscillator doesn't affect the analysis for the strength of kicking we are considering To justify any approximations we are going to make it is necessary to consider the contribution of the stable orbits to the system at large over a range of kick strengths, μ_{cl}

We have already shown by illustration how the stochastic layer increases exponentially with increasing kick strength, μ_{cl}, and how the invariant cells break up by resonant overlap according to the K A M theorem (see chapter 3) We would therefore expect the area occupied in the phase space by the invariant (stable) cells to diminish as μ_{cl} is increased tending to zero as μ_{cl} tends to infinity In fact as this limit is approached the cells contract about any remaining elliptic fixed points until they become measure zero As will be shown later, this limit also tends to obliterate any correlations between any iterates of

the mapping (Chirikov, (1987)) and a random phase approximation can be used for the system

We do not have to go to such extremes to neglect the contributions of the stable orbits, however We can define a critical kick strength, μ^C, above which the stable orbits' contributions are ignored as the area of phase space occupied by them has diminished below a set level (say 10%) (This choice is arbitrary once the dominant term is the unstable kick term) The periodicity of the phase space (π/K) implies that the dynamical information contained in any region of side π/K centred on an invariant cell of order four (or one for the origin) is indicative of the system at large Therefore we may restrict q and p to $\pm\pi/(2K)$ Then the normalised momentum, P, evolving according to eq (2 1 22) can be modified to

$$\frac{\partial P}{\partial t} = \omega^2 Q + \mu_{cl} \sin(2KQ) \sum_{n=1}^{\infty} \delta(t - n\tau) \cong \mu_{cl} \sin(2KQ) \sum_{n=1}^{\infty} \delta(t - n\tau) \qquad (4\ 1\ 1)$$

which is valid only when $\mu_{cl} > \mu^C$ This can then be simplified, by normalising the time between kicks to 1, to the following

$$\Delta P \cong \mu_{cl} \sin(2KQ) \qquad (4\ 1\ 2)$$

which is a vital identity for the calculation of the diffusion coefficient D_{cl} which is defined according to (Chirikov (1987))

$$D_{cl} \propto \lim_{t \to \infty} \frac{< (\Delta P)_t^2 >}{2t} \qquad (4\ 1\ 3)$$

where <> is an ensemble average and t is the time (for the mapping $t \equiv n$ the iteration counter) *So what value of μ_{cl} is the critical value for the above to be valid?* To see this we include a table of the area occupied by both the invariant cells and the stochastic layer as a function of μ_{cl} (Refer back to chapter 2 when we defined μ_{cl} for eq (2 1 16) to recall its explicit dependence on K)

From table 4 1 we can guess at a value for μ^C which for our constraint (occupation $< 10\%$) would place it close to 14 for $K = 0\ 1$, 7 0 for $K = 0\ 2$ and so on We will show how this dependence on K affects the diffusion curves later We will now begin the analysis proper

μ_{cl} $(K = 0\,1)$	μ_{cl} $(K = 0\,2)$	μ_{cl} $(K = K_{\mathrm{arb}})$	% area occupied (invariant cells)	% area occupied (stochastic)
0 0	0 0	0 0	100	0
2 0	1 0	$2\,0 * k$	99 96	0 04
4 0	2 0	$4\,0 * k$	92 10	7 90
6 0	3 0	$6\,0 * k$	73 61	26 39
8 0	4 0	$8\,0 * k$	32 85	67 15
10 0	5 0	$10\,0 * k$	23 23	76 77
12 0	6 0	$12\,0 * k$	15 89	84 11
—	—	—	—	—
15 0	7 5	$15\,0 * k$	6 15	93 85
20 0	10 0	$20\,0 * k$	0 5 - 1	99 – 99 5

Table 4 1 Occupied area of the phase space vs the kick strength for the invariant cells and the stochastic layer when $\beta = \pi/2$ k above is just $(0\,1/K_{\mathrm{arb}})$ allowing us to express the kick strength at arbitrary $K(K_{\mathrm{arb}})$ in terms of $K = 0\,1$ The dashed line represents the cut-off below which we can neglect the stable component of the motion for the acceleration (dP/dt) equation Beyond $\mu_{cl} = 20\,0 * k$ we can consider the system's phase space to be completely stochastic

The main thrust is to obtain an expression for the probability which satisfies the Vlasov equation and then to use this to form an expression for the diffusion coefficient, D_{cl} We begin by considering the Vlasov Equation with diffusion added

$$\frac{\partial P}{\partial t} + v\frac{\partial P}{\partial Q} + \frac{dv}{dt}\frac{\partial P}{\partial v} - \frac{\sigma}{2}\frac{\partial^2 P}{\partial Q^2} = 0 \qquad (4\,1\,4)$$

where the probability distribution function is $P(Q, v, t)$ Noting that the time is quantised because of the periodic delta function then the system evolves across a kick as

$$P(Q,v,n\tau+0) = \left\{ \quad P(Q,v+\omega^2 Q+\xi\mu_{cl}\sin(Q),n\tau-0) \quad \right\}_{Q\equiv Q_{t=n\tau}} \tag{4 1 5}$$

where we have re-cast the Q to eliminate the $2K$ before it in the sine term This has the effect of changing the kick strength to $\xi\mu_{cl}$ where $\xi = K/K_0$with $K_0 = 0\,5$ This re-casting also has the affect of changing the system's periodicity from π/K to 2π allowing important identities to be made later in this analysis Between kicks the system evolves by the formula

$$P(Q,v,t) = \int_{-\infty}^{\infty} dv_1 \int_0^{2\pi} dQ_1 G(Q-Q_1,v,v_1,t-t_1)P(Q_1,v_1,t_1) \tag{4 1 6}$$

where the function $G(Q-Q_1,v,v_1,t-t_1)$ is a Green's function and satisfies the equation

$$\frac{\partial G}{\partial t} + v\frac{\partial G}{\partial Q} - \frac{\sigma}{2}\frac{\partial^2 G}{\partial Q^2} = \delta(x-x_1)\delta(t-t_1)\delta(v-v_1) \tag{4 1 7}$$

The Green's function is used as an evolution operator between kicks and because the velocity changes only across a kick (see eq (4 1 2) for dP/dt) the dv/dt is zero between kicks Hence the Vlasov equation in eq (4 1 4) becomes that in eq (4 1 7) between kicks The solution to the above can be found in books on partial differential equations with boundary conditions This specific solution can be found by considering the Green's function solution to the diffusion equation $u_t - u_{xx} = \delta(x-\xi)\delta(t-\tau)$ (Kervorkian (1990)) Our solution is of the form

$$G(Q-Q_1,v,v_1,t-t_1) = \frac{\theta(t-t_1)\delta(v-v_1)}{\sqrt{2\pi\sigma(t-t_1)}} \sum_{n=-\infty}^{\infty} \exp\left[-\frac{(Q-Q_1-v(t-t_1)+2n\pi)^2}{2\sigma(t-t_1)}\right] \tag{4 1 8}$$

The initial value chosen for the probability function $P(Q,v,t)$ is

$$P(Q,v,0) = \delta(v-v_o)$$

The velocity integral is non-contributory and is omitted from now on The position variable Q has a constant derivative between kicks as the velocity is constant and varies

only across a kick The integral over a kick just gives us the next Q position in terms of the previous one so that the probability at a time T for a position Q_T, where Q_T is the value of Q at a time T, is the product of the probabilities at each time step so that

$$P(Q,v,T) = \sum_{n_T=-\infty}^{\infty} \sum_{n_1=-\infty}^{\infty} \prod_{i=0}^{T-1} \int_0^{2\pi} dQ_i \frac{1}{\sqrt{2\sigma\pi}} \delta(v - v_o - S_T)$$
$$\exp\left[\frac{-1}{2\sigma}\sum_{j=1}^{T}(Q_j - Q_{j-1} - v_o - S_{j-1} + 2n_j\pi)^2\right] \qquad (4\ 1\ 9)$$

where

$$S_j = \sum_{p=0}^{j} \omega^2 Q_p + \xi\mu_{cl}\sin(Q_p) \qquad (4\ 1\ 10)$$

The diffusion rate is calculated from the formula

$$D_{cl} = \lim_{T\to\infty} (2T)^{-1} \int_{-\infty}^{\infty}\int_0^{2\pi} (v - v_o)^2 P(Q,v,T)dQdv \qquad (4\ 1\ 11)$$

Note the similarity to eq (4 1 3) which is that equation used by Chirikov (1987) Noting that the system has a stochastic component which is dominant at the values of μ_{cl} we are considering and that the system is formed by gaussians (brought about by the Green's function solution to the diffusion equation (Kervorkian (1990))) then the process can be considered gaussian with the following density function

$$\frac{1}{\sqrt{2\pi\sigma}} \exp\left[\frac{(y+2\pi)^2}{2\sigma}\right] \qquad (4\ 1\ 12a)$$

and characteristic function

$$\exp\left[\imath m(y + 2n\pi) - \tfrac{1}{2}m^2\sigma\right] \qquad (4\ 1\ 12b)$$

with the identity

$$\frac{1}{\sqrt{2\pi\sigma}} \sum_{n=-\infty}^{\infty} \exp\left[\frac{(y+2n\pi)^2}{2\sigma}\right] = \frac{1}{2\pi} \sum_{m=-\infty}^{\infty} \exp\left[\imath m(y + 2n\pi) - \tfrac{1}{2}m^2\sigma\right] \qquad (4\ 1\ 12c)$$

This changes the above diffusion expression to

$$D_{cl} = \lim_{T\to\infty} (2T)^{-1} \sum_{m_T=-\infty}^{\infty} \sum_{m_1=-\infty}^{\infty} \prod_{i=0}^{T-1} \int_0^{2\pi} \frac{dQ_i}{2\pi} S_T^2$$

$$\exp\left[\sum_{j=1}^{T} \frac{-1}{2} m^2\sigma + \imath m_j(Q_j - Q_{j-1} - v_o - S_{j-1})\right] \qquad (4\,1\,13)$$

We now make the approximation that, for the turbulent diffusion to occur, the kick term has to be such that it dominates over the stable term Remember that the phase space has less than 1% occupied by stable orbits at $\mu_{cl} = 20{*}\mathbf{k}$ Thus S_{j-1} can now be considered to be a summation over just the sine terms The number, n, of $m_j's$ used in any calculation determines the correlation $C(n)$ of the diffusion For all the $m_j's$ at zero we have the effective quasi-linear diffusion denoted D_{QL} and, by Rechester & White (1980), the S_T^2 can be approximated by an integral over 2π (the effective periodicity of the system) which gives $\xi^2\mu_{cl}^2/2$ then the quasi-linear diffusion is

$$D_{QL} = \frac{1}{4}\xi^2\mu_{cl}^2 \qquad (4\,1\,14)$$

If we set the problem up so that just one m_j is not zero we find that the integral term is

$$\exp\left[-\tfrac{1}{2}m^2\sigma - \imath m_i v_0\right] \int_0^{2\pi} \frac{dQ_i}{2\pi} \exp\left[\imath m_i Q\right] = 0 \qquad (4\,1\,15)$$

So the correlation term $C(1)$ is zero as predicted by Chirikov for the standard mapping (Chirikov (1987))

In formulating the higher correlations we must remember that any expression for the diffusion coefficient D_{cl} has to be independent of the velocity used as the initial probability distribution function In order for this to be satisfied the sum of all $m_j's$ for the v_0 term must come to zero Furthermore as the sum of the square of the $m_j's$ times σ tend to zero very quickly then we have chosen to keep the $m_j's$ within the bounds ± 2 If we set two consecutive $m_j's$ not equal to zero and all the rest zero then we are effectively calculating the $C(2)$ correlation (Chirikov (1987)) For this correlation we choose $m_i = \pm 1$ and $m_{i+1} = -m_i$) Our integral in the diffusion equation can now be re-arranged to remove all terms independent of the $Q_i's$

$$\exp\left[-\sum_{j=1}^{T}(\tfrac{1}{2}m_j^2\sigma + \imath m_j v_o)\right] \int_0^{2\pi} \frac{dQ_i}{2\pi} S_T^2 \exp\left[\sum_{j=1}^{T} \imath m_j(Q_j - Q_{j-1} - S_{j-1})\right] \qquad (4\,1\,16)$$

The integral now becomes

$$\exp\left[-\tfrac{1}{2}(m_{i+1}^2+m_i^2)\sigma-\iota(m_i+m_{i+1})v_o-\iota(m_i+m_{i+1})S_{i-1}\right]$$

$$\int_0^{2\pi}\frac{dQ_i}{2\pi}S_T^2\exp\left[\iota((m_i-m_{i+1})Q_i-m_{i+1}\sin(Q_i))\right] \qquad (4\ 1\ 17)$$

From the definition of $m_i$and m_{i+1}we can determine that $m_i+m_{i+1}=0$, $m^2+m^2=2$ and $m_i-m_{i+1}=2m_i$ Therefore the diffusion term for this $C(2)$ approximation is independent of v_0, as we wanted it to be

$$D_{C(2)}=\lim_{T\to\infty}\mp\frac{1}{2}\exp\left[-\sigma\right]\left\{\int_0^{2\pi}\frac{dQ_i}{2\pi}S_T^2\exp\left[+\iota(-2Q_i+\sin(Q_i))\right]\right.$$

$$\left.+\int_0^{2\pi}\frac{dQ_i}{2\pi}S_T^2\exp\left[+\iota(2Q_i-\sin(Q_i))\right]\right\} \qquad (4\ 1\ 18)$$

The integral can now be replaced by the second order Integer Bessel Function, $J_2(z)$ (see Gradshteyn and Ryzhik (1965) eq 8 411(1)) So our diffusion term becomes

$$D_{C(2)}=-\frac{1}{2}\xi^2\mu_{cl}^2J_2\left(\xi\mu_{cl}\right)e^{-\sigma} \qquad (4\ 1\ 19)$$

This term is added to the quasi-linear term in eq (4 1 14)

$$D_{cl}=D_{QL}+D_{C(2)}=\frac{1}{4}\xi^2\mu_{cl}^2\left[1-2J_2\left(\xi\mu_{cl}\right)\right] \qquad (4\ 1\ 20)$$

It is also possible to equate m_{i-2} with m_i (effectively a $C(3)$ correlation) We again set $m_{i-2}=\pm1$ and $m_i=-m_{i-2}$ This has the effect of squaring a sum of two identical integrals

$$D_{C(3)}^{(1)}=\lim_{T\to\infty}-\frac{1}{2}\exp\left[-\sigma\right]\left\{\int_0^{2\pi}\frac{dQ_i}{2\pi}S_T^2\exp\left[+\iota(-Q_i+\sin(Q_i))\right]\right.$$

$$\left.+\int_0^{2\pi}\frac{dQ_i}{2\pi}^2S_T^2\exp\left[+\iota(Q_i-\sin(Q_i))\right]\right\} \qquad (4\ 1.21)$$

The superscript on the D denotes it is the first part of the $C(3)$ correlation Again using the identity from Gradshteyn and Ryzhik (1965) we can substitute integer order Bessel functions of the first kind for these integrals The result is a J_1^2 term

$$D_{C(3)}^{(1)} = -\frac{1}{2}\xi^2\mu_{cl}^2 J_1^2(\xi\mu_{cl})\, e^{-\sigma} \tag{4 1 22}$$

Again the above is in agreement with half of the $C(3)$ correlation term put forward by Chirikov (1987), the other half we will obtain now by considering a wider range of m_j's This second half of the $C(3)$ correlation relates not two iterates but three such that m_i is correlated to both m_{i-1} and m_{i-2}, unlike the previous term where $m_i$was related to just m_{i-2} Again we need to keep the $m_j's$ small as the $\Sigma m_j^2\sigma$ term tends to zero very quickly Accounting for the v_0 constraint ($\Sigma m_j = 0$) we follow the example of Rechester and White (1980) and choose the following values for the $m_j's$ $m_i = \pm 1, m_{i+1} = -2m_i$ and $m_{i+1} = m_i$ One can see immediately that Σm_j is indeed zero satisfying our v_0 independence constraint The Σm_j^2 is six giving an $\exp(-3\sigma)$ weighting for this term Furthermore the integrals obtained from the substitution of these $m_j's$ are of a similar form to the previous correlation terms but yield a J_3 term i e

$$D_{C(3)}^{(2)} = \lim_{T\to\infty} \frac{1}{2}\exp[-3\sigma]\left\{ \int_0^{2\pi} \frac{dQ_i}{2\pi} S_T^2 \exp[+\imath(-3Q_i + \sin(Q_i))] \right.$$

$$\left. + \int_0^{2\pi} \frac{dQ_i}{2\pi}^2 S_T^2 \exp[+\imath(3Q_i - \sin(Q_i))] \right\} \tag{4 1 23}$$

which gives using the integral identity

$$D_{C(3)}^{(2)} = \frac{1}{2}\xi^2\mu_{cl}^2 J_3^2(\xi\mu_{cl})\, e^{-3\sigma} \tag{4 1 24}$$

The complete diffusion term is now the sum of all the correlation terms thus obtained

$$D_{cl} = D_{QL} + D_{C(2)} + D_{C(3)}^{(1)} + D_{C(3)}^{(2)} =$$

$$\frac{1}{4}\xi^2\mu_{cl}^2[1 - 2J_2(\xi\mu_{cl})\, e^{-\sigma} - 2J_1^2(\xi\mu_{cl})\, e^{-\sigma} + 2J_3^2(\xi\mu_{cl})\, e^{-3\sigma}] \tag{4 1 25}$$

This equation accounts for the correlations up to and including $C(3)$ We can add part of another correlation, $C(4)$, which has been shown by Chirikov (1987) to tend to zero slower than the $C(3)$ correlation To obtain this term we use choose values for the $m_j's$ satisfying our constraints for σ and v_0 The values chosen are $m_i = m_{i+3} = \pm 1$ and $m_{i+1} = m_{i+4} = -m_i$ As before $\Sigma m_j = 0$ and $\Sigma m^2 = 4$ We end up with a product of two sets of integrals identical to eq (4 1 18) (except in the multipher before the σ term) This $C(4)$ term gives us

$$D_{C(4)} = \frac{1}{2}\xi^2\mu_{cl}^2 J_2^2(\xi\mu_{cl})\, e^{-2\sigma} \tag{4 1 26}$$

Our diffusion equation now takes on the form

$$D_{cl} = D_{QL} + D_{C(2)} + D_{C(3)}^{(1)} + D_{C(3)}^{(2)} + D_{C(4)} =$$

$$\frac{1}{4}\xi^2\mu_{cl}^2[1 - 2J_2(\xi\mu_{cl})\, e^{-\sigma} - 2J_1^2(\xi\mu_{cl})\, e^{-\sigma} + 2J_3^2(\xi\mu_{cl})\, e^{-3\sigma} + 2J_2^2(\xi\mu_{cl})\, e^{-2\sigma}] \tag{4 1 27}$$

Chirikov has shown (Chirikov (1987)) that the the $C(3)$ component decays as $|\xi\mu_{cl}|^{-2}$ whereas the $C(4)$ component decays as $|\xi\mu_{cl}|^{-1}$ Thus for large $\xi\mu_{cl}$ the diffusion equation is best described by

$$D_{cl} = \frac{1}{4}\xi^2\mu_{cl}^2[1 - 2J_2(\xi\mu_{cl}) + 2J_2^2(\xi\mu_{cl})] \tag{4 1 28}$$

where we can neglect the σ term decay due to the fact that σ is usually kept very small (the value chosen by Rechester and White (1980) being just 1×10^{-4}) This is exactly the form given by Chirikov (1987) using his simplified argument based on correlations and by Israeilev (1990)

We will now show how remarkably well the above fits that data obtained from numerical simulations To numerically evaluate the diffusion coefficient we use the expression in eq (4 1 3) To accomplish this we calculate the mean energy for an ensemble of points in the stochastic layer The results showed us that the growth in energy is increasing linearly with increasing n (n being the iteration counter and hence time) and so can be written as

$$E_n(\mu_{cl}, n) \equiv B(\mu_{cl})n \equiv B(\mu_{cl})\tau \tag{4 1 29}$$

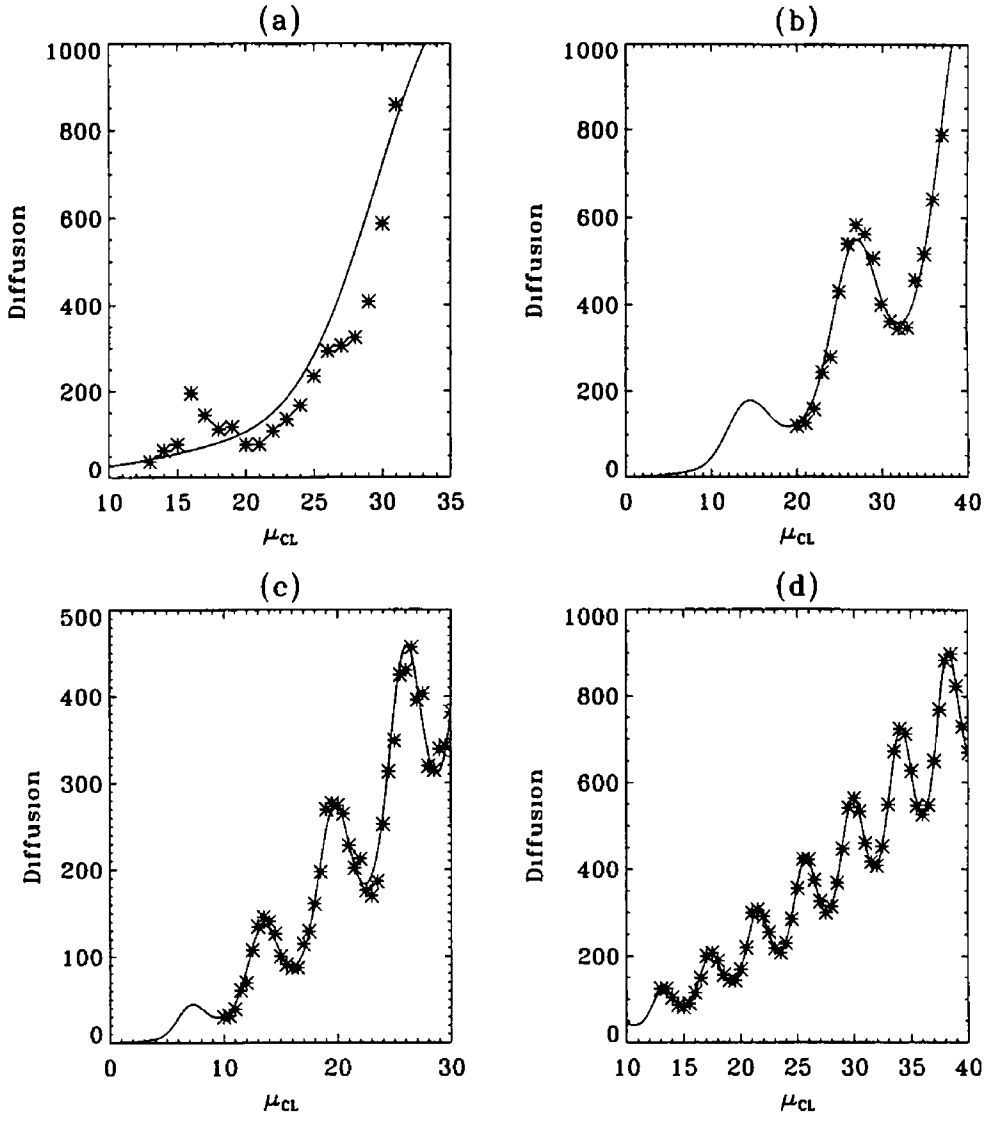

Fig 4 1 Four plots of the diffusion coefficient, $D_{cl}(\mu_{cl})$, vs the kick strength, μ_{cl} for various values of the parameter K $K = 0\ 1$ in (a), $0\ 25$ in (b), $0\ 5$ in (c) and $0\ 75$ in (d) The solid line is the theoretical curve predicted by eq (4 1 28) and the asterisks are the calculated points The fit is very good except for small values of $K\mu_{cl}$ as can be seen from (a) where the fit is the worst It was the deviations in (a) which led us to discover the anomalous diffusion peaks discussed later

Care was taken in the above calculation to avoid using periodic points or quasi- periodic points as these points' non-diffuse behaviour would affect the result These points were

numerically filtered out The next step was to obtain the best fit line to this linear graph of energy vs time (i e its derivative) This derivative is equal to twice the diffusion coefficient *Why twice?* The reason for this is that we calculated the energy of the system with time not the change in momentum squared The energy depends on p and q (or x and y for the mapping) and as one can show very easily that x and y can be interchanged without compromise then the energy is twice that value of the change in momentum So the theoretical solid curve shown in each of the figures in fig $4.1(a)-(d)$ is twice that of the diffusion coefficient expressed in eq (4 1 28) To alleviate problems associated with individual orbits and not the global nature of the system a set of 60000 initial points were taken in the stochastic region close to one of the hyperbolic period four fixed points All points were tested for quasi-periodicity and filtered out if found to be such The resultant set was iterated for 20000 time steps The four figures in fig 4 1 show the diffusion coefficient, D_{cl}, as a function of the kick strength, μ_{cl}, for a range of the parameter K The fit is remarkable except at small values of μ_{cl} where the stable component of the motion affects the assumptions made in deriving eq (4 1 28)

Despite our success with the expression above for the diffusion coefficient we nevertheless found this coefficient to diverge from the predicted value at certain regularly spaced values of the kick strength, μ_{cl} These divergences manifested themselves in the form of delta function like *spikes* on the normal turbulent diffusion predicted above with the values of the kick strength corresponding to a positive integer times the system's periodicity This discovery led to a revision of the system's behaviour when the kick strength corresponded to these *periodicity related* values We dubbed these spikes in the diffusion coefficient *Resonant Enhanced Diffusion* We now present our argument to explain these periodic spikes

4 2 Resonance Enhanced Diffusion

To proceed any further with our argument for the resonant enhanced diffusion we need to consider the nature of the effect of the system's periodicity on the dynamics of the system

We have already pointed out at the beginning of the last section that the p and q can be *effectively* restricted to region of $\pm\pi/(2K)$ This can be clearly illustrated as follows In showing why the stable component of the motion can be ignored in the preceding section we stated that when μ_{cl} is much greater than the stable component then the turbulent analysis of Rechester and White (1980) can be used However as p and q effectively visit the whole phase space then they can, for a fixed value of μ_{cl}, take on any value in the whole $2D$ real plane seemingly negating our argument of the previous section This would imply that the previous argument would not describe the diffusion correctly This would be true if the dynamics in one region were unique to that region and no other However we have shown that the system is periodic and the dynamics in any periodic cell is representative of the system at large Therefore the *effective* values of p and q are restricted to the bounds imposed by the system's periodicity Thus a point (q',p') in the phase space related to (q,p) by the relation $p' = p+n\pi/K$ and $q' = q+m\pi/K$ will have identical dynamics to the points (q,p) except its energy will be greater by an amount dependent on the $n\pi/K$ and $m\pi/K$ As a result of this, there is a strong dynamic correlation between the points (q,p) and (q',p') This reasoning is the very heart of the argument we present here We will use the correlations between sets of (q',p') to show how they give rise to these anomalous peaks in the diffusion coefficient and why these peaks correspond to a kick strength equal to a positive integer times the system's periodicity

We have shown in the previous section how the turbulent diffusion (which is that when the stable component is negligible) is derived by considering correlations between iterates at different times and relating them to the iterate we are interested in Here we will show, using the observation in the previous paragraph, how large summations over identical arguments give rise to the anomalous diffusion

Let us recall our equation for the diffusion coefficient, D_{cl}

$$D_{cl} = \lim_{T\to\infty} (2T)^{-1} \sum_{m_T=-\infty}^{\infty} \sum_{m_1=-\infty}^{\infty} \prod_{i=0}^{T-1}$$

$$\exp\left[-\sum_{j=1}^{T}(\tfrac{1}{2}m^2\sigma + \imath m_j v_o)\right] \int_0^{2\pi} \frac{dQ_i}{2\pi} S_T^2 \exp\left[\sum_{j=1}^{T} \imath m_j (Q_j - Q_{j-1} - S_{j-1})\right] \quad (4\,2\,1)$$

Now if we have strong dynamic correlations the term S_T, which is a summation up to T of the $\xi\mu_{cl}\sin(KQ_i)$, will consist of a summation of the same value again and again, i e if the Q_i are related by the expression

$$Q_i = Q_o + j\pi/K \tag{4 2 2}$$

(where $0 \leq |j| \leq |i|, j \in \mathbf{Z}$) then the summation gives us $T(\xi\mu_{cl}\sin(KQ_i))^2$ We would expect this summation to tend to infinity quicker than the summation over random Q_i This is indeed the case as we found by taking the summations of the S_T^2 term for various values of the kick strength Once properly scaled, the result followed the numerically evaluated result remarkably well so we conclude that strong correlations of the Q_i bring about the enhanced diffusion at the observed values of the kick strength Furthermore, the rapidity at which the coefficient D_{cl} would tend to infinity could also depend on the behaviour of the other terms in the expression in *eq* (4 2 1) For the D_{QL} in the previous section the $m_j's$ are all zero so we have no $e^{-\sigma}$ terms to worry about This term we would expect to tend quickest to infinity whereas the $D_{C(2)}, D_{C(3)}$ and the $D_{C(4)}$ terms would tend to infinity slower due to the presence of non zero $m_j's$ in the σ term As the number of non-zero $m_j's$ is increased (while still accounting for the restriction, $\Sigma m_j = 0$ for the v_o term to be omitted) infinity is approached slower but we see no reason why it would not be acheived eventually So the overall result is that *if points in the phase space exist so that they are highly dynamically correlated* then we would expect their contribution to the diffusion coefficient to be such that D_{cl} would tend to infinity

We have seen this anomalous diffusion to arise when the kick strength is very close or equal to a positive integer times the system's periodicity This type of diffusion has been known to exist for this type of system since the work of Carey et al (1981a & 1981b) on periodic area preserving maps and Karney et al (1982) on the effect of noise on the standard map We will here refer to a more recent analysis by Ishizaki et al (1989) which deals with the specific case of the kicked rotator In this paper they refer to accelerator modes islands which they found to exist in the stochastic layer of the kicked rotator The crux of their argument is that these islands impart an integer number of 2π (their system had a periodicity of 2π) to the momentum of stochastic layer orbits which reside close to

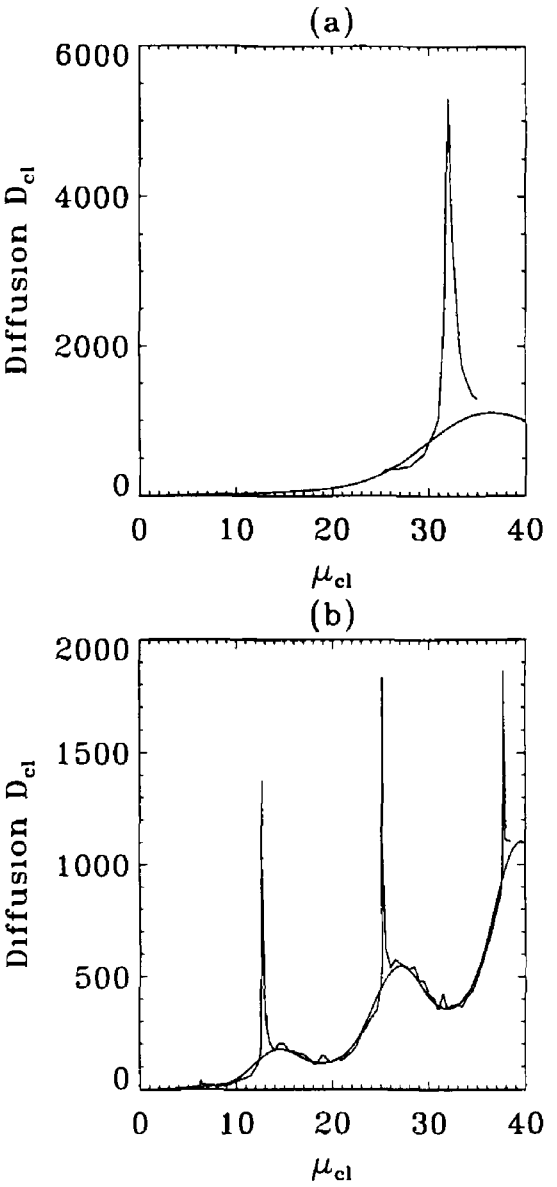

Fig 4 2 The resonance enhanced diffusion for (a) $K = 0\ 1$ and (b) $K = 0\ 25$ The spikes can be seen to occur at positive integer multiples of the system's periodicity (10π for $k = 0\ 1$ & 4π for $K = 0\ 25$)

these islands This increase of 2π translates points (q,p) to their corresponding cousins (q',p') whose dynamics are identical Furthermore these accelerator islands were found by Ishizaki et al (1989) to be of the same periodicity as the system This results in some orbital points (q,p) being highly dynamically correlated to each other and to have a much higher overall mean energy than other un-accelerated orbits The stability of these islands

is crucial to the accelaration and Ishizaki et al (1989) found them to be stable for a small range of kick strengths very close to a positive integer times the system's periodicity

Their results are applicable here because of the periodicity of our phase space and because like the kicked rotator the dynamics of one periodic cell are identical to that of another Furthermore by varying K we can change our phase space periodicity and hence show that any kicked system which has a periodic phase space will have this anomalous diffusion when the kick strength is in the vicinity of the system's periodicity

We end our analysis of the system's diffusion here with the point that this resonant enhanced diffusion has, to our knowledge after searching the relevant literature, not been reported at all for any system outside the kicked rotator This fact, despite exhaustive studies of this system by many distinguished researchers (Israilev, Berman, Chernikov etc), highlights that our present knowledge of this system is still very much incomplete

CHAPTER 5
THE QUANTUM MAPPING

Having described the classical limit of the Hamiltonian we now proceed to analyse the fully quantum limit, i e when $\hbar$ is finite and non-zero Our system Hamiltonian is time-dependent and therefore the approach taken will be different from that for time independent systems such as the quantum billiards problem (Berry et al (1986)) and others (Robnik et al (1986), Tomsovic et al (1993)) The quantum mapping derived in this chapter is obtained using an approach similar to that of Fox et al (Fox & Lan (1990), Fox & Elston (1994)) in their analysis of the kicked rotator This is, to our knowledge, the first time this has been done for the kicked harmonic oscillator and the resultant mapping is therefore unique in this regard

5 1 Derivation Of The Quantum Mapping

This section essentially deals with the derivation of the Fully quantum mapping from the system hamiltonian The general approach here is very similar to Fox & Lan (1990) in their derivation for the kicked rotator but the added potential in our problem results in a much more complex system and final mapping Initially we will examine the undriven harmonic oscillator and look at its eigenfunctions and their properties because these will be needed for the driven harmonic oscillator As such we call on much of the information contained in chapter 12 of *Quantum Mechanics Volume 1* by Messiah (1976)

Again we start off with the Hamiltonian of the Quantum Harmonic Oscillator driven (or Kicked) by a temporally discrete potential

$$H_T(p,q) = \frac{p^2}{2M} + \frac{1}{2}M\omega_o^2 q^2 + \mu_q Cos(kq)\sum_{n=1}^{\infty}\delta(t-n\tau) \qquad (5\,1\,1)$$

We need to recall from chapter 2 our definition of the integrable hamiltoman $H_o(p,q)$ for the undriven system

$$H_o(p,q) = \frac{p^2}{2M} + \frac{1}{2}M\omega_o^2 q^2 \qquad (5\,1\,2)$$

Our task now is to find a function $\psi(q,t)$ which satisfies the time dependent Schrodinger wave equation Through this equation we can obtain a form for the wavefunctions of the system The equation is given below

$$H\left(\tfrac{d}{dq},q\right)\psi(q,t) = \imath\hbar\frac{\partial\psi}{\partial t}(q,t) \qquad (5\,1\,3)$$

The functions which solve the above are many and varied but we are interested in a subclass of these solutions which have the property that $H_o\psi_n = E_n\psi_n$ where E_n is the energy of the system's n^{th} energy level These functions ψ_n are called the *eigenfunctions* of the hamiltonian H_o and will be denoted henceforth as $\phi_n(q)$ It should also be observed that the $\phi_n(q)$ are linearly independent and form a complete basis for the system Thus any other function $\psi(q,t)$ satisfying eq (5 1 3) is made up of a superposition of the $\phi_n(q)$ with coefficients $A_n(t)$ as multipliers and can be written

$$\psi(q,t) = \sum_{n=1}^{\infty} A(t)\,\phi_n(q) \qquad (5\,1\,4)$$

where the modulus of the A_n's gives the probability amplitudes for the ϕ_n in the function ψ This way we can solve for the eigenfunctions, ϕ_n, and use them to find any other function, ψ, which satisfies the wave equation So our first hurdle is to obtain an expression for the eigenfunctions To do this it is necessary to recall some of the definitions from chapter 2, namely those of eq (2 1 3), i e

$$q = Q\sqrt{\frac{\hbar}{M\omega_o}} \qquad \& \qquad p = P\sqrt{M\hbar\omega_o} \qquad (5\,1\,5)$$

We now express the momentum operator as a function of Q as per its definition The normal p operator is defined as $p = \frac{\hbar}{\imath}\frac{d}{dq}$ which allows us, employing the definitions in eq (5 1 5), to express P as $\frac{1}{\imath}\frac{d}{dQ}$ Furthermore we can now to introduce a new set of eigenfunctions $u_n(Q)$ defined to be $\sqrt[4]{\frac{\hbar}{M\omega_o}}\phi_n(q)$ where the fourth root term is to allow Q to be substituted for q (Messiah (1976)) The effect of introducing this latter set of eigenfunctions is to change our expression of H_o to

$$H_o\left(\tfrac{d}{dQ},Q\right)u_n(Q) = \frac{1}{2}\left(Q^2 - \tfrac{d^2}{dQ^2}\right)u_n(Q)\,\hbar\omega_o = E_n u_n(Q) \qquad (5\,1\,6)$$

Our next step is necessary for our formulation of the undriven system's eigenfunctions Our previous definitions (in chapter 2) of the annihilation and creation operators, a and $a^\dagger$, are extended to include the explicit form of P in terms of Q

$$a(P,Q) = \frac{1}{\sqrt{2}}(Q + \imath P) = \frac{1}{\sqrt{2}}\left(\frac{d}{dQ} + Q\right) \qquad (5\ 1\ 7a)$$

and

$$a^\dagger(P,Q) = \frac{1}{\sqrt{2}}(Q - \imath P) = \frac{1}{\sqrt{2}}\left(Q - \frac{d}{dQ}\right) \qquad (5\ 1\ 7b)$$

The form we have chosen for $a^\dagger$, the creation operator, is such that when $a^\dagger$ operates on the n^{th} eigenfunction (with the system thus being solely in the n^{th} state) it raises the system to the $(n+1)^{\text{th}}$ level with the $(n+1)^{\text{th}}$ eigenfunction being that wavefunction describing the system now, i e $a^\dagger|n> = \sqrt{n+1}|(n+1)>$ Thus it *creates* a state and hence the name *creation operator* The annihilation operator, a, does the opposite in that it lowers the state of the system from the n^{th} level to the $(n-1)^{\text{th}}$ level, i e $a|n> = \sqrt{n}|(n-1)>$ Like the creation operator, the designation *annihilation operator* for a mirrors its affect on the system's state The justification for the above properties is given in Appendix B where we also show that $(a, a^\dagger) = 1$ when operating on any pure eigenstate n Therefore the state remains unchanged It also follows that $a|0> = 0$ (you can't go lower than the zeroth level or ground state) and $|n>$, the n^{th} level, is given by the recursion relationship $\frac{1}{\sqrt{n!}}(a^\dagger)^n|0>$ These are two definitive results that we will use to obtain the form of the eigenfunctions From the action of the annihilation operator on the zeroth level we get

$$a|0> \equiv \frac{1}{\imath\sqrt{2}}\left(\frac{d}{dQ} + Q\right)u_o(Q) = 0 \qquad (5\ 1\ 8a)$$

or equivalently

$$\left(\frac{d}{dQ} + Q\right)u_o(Q) = 0 \qquad (5\ 1\ 8b)$$

The solution of eq (5 1 8b) is $u_0(Q) = C * \exp(-\frac{1}{2}Q^2)$ with the constant C being evaluated using the property $< u_0, u_0 >= 1$ and that the solution to the integral $\int_0^\infty \exp(-Q^2)dQ = \frac{\sqrt{\pi}}{2}$ C is found to be $\frac{1}{\sqrt[4]{\pi}}$ So $u_o(Q) = \frac{1}{\sqrt[4]{\pi}}\exp(-\frac{1}{2}Q^2)$ We now substitute this solution into our recursion relationship to obtain the general solution for all $u_n(Q)$, i e

$$\frac{\iota^n}{\sqrt{2^n\sqrt{\pi}(n!)}}\left(Q-\tfrac{d}{dQ}\right)^n u_o(Q)=u_n(Q) \qquad (5\,1\,9)$$

where we find, after replacing $u_0(Q)$ with explicit its form, $u_n(Q)$ takes the form

$$\frac{\iota^n}{\sqrt{2^n\sqrt{\pi}(n!)}}\left(Q-\tfrac{d}{dQ}\right)^n \exp\left(-\tfrac{1}{2}Q^2\right)=u_n(Q) \qquad (5\,1\,10)$$

We can now indentify part of the above expression with a type of orthogonal polynomial called Hermite Polynomials, $H_n(Q)$ We can do this because of the following recursion relationships (Gradshteyn & Ryzhik (1965))

1 $\quad \frac{dH_n(x)}{dx}=2nH_{n-1}(x)$

2 $\quad H_{n+1}(x)=2xH_n(x)-2nH_{n-1}(x)$

Combining these two identities gives

3 $\quad H_{n+1}(x)=\left(2x-\frac{d}{dx}\right)H_n(x)$

with the one we seek being the continued substitution of $H_{n-k}(x)$ down to $H_o(x)$

4 $\quad H_{n+1}(x)=\left(2x-\frac{d}{dx}\right)^n H_o(x)\equiv\left(2x-\frac{d}{dx}\right)^n$

because $H_o(x)=1$ It is easy to show that the Hermite polynomials, H_n, can be formed not just by $\left(2x-\frac{d}{dx}\right)^n H_o(x)$ but also by the relationship $\left(Q-\frac{d}{dQ}\right)^n \exp\left(-\frac{1}{2}Q^2\right)$ (see eq 8 950 in *Table of Integrals, Series and Products* by Gradshteyn and Ryzhik (1965) and section III in Appendix B of *Quantum Mechanics Volume 1* by Messiah (1976) We can thus substitute the hermite polynomials, $H_n(Q)$, into our equation for the eigenfunctions

$$\frac{\iota^n}{\sqrt{2^n\sqrt{\pi}(n!)}} * H_n(Q)\exp\left(-\tfrac{1}{2}Q^2\right)=u_n(Q) \qquad (5\,1\,11)$$

This completes our expression for the eigenfunctions of the undriven integrable hamiltonian Our task now is to see how the eigenfunction probability amplitudes vary in time for the complete non-integrable hamiltonian We are going to formulate the problem in such a way as to keep the eigenfunctions for the undriven osillator but generate a mapping which relates the probability amplitudes for these eigenfunction from one kick to the next

Between *kicks* the system hamiltonian is essentially the integrable hamiltonian described above Thus any wavefunction $\psi(q,t)$ can be written as a superposition of the

$u_n(Q)$ or $\phi_n(q)$ depending on the phase space being considered The wave equation for driven (kicked) harmonic oscillator is

$$\iota\hbar\frac{\partial}{\partial t}\psi(q,t) = -\frac{\hbar^2}{2M}\frac{\partial}{\partial q}\psi(q,t) + \frac{1}{2}M\omega_o^2 q^2\psi(q,t) + \mu_q Cos(k_o q)\sum_{n=-\infty}^{\infty}\delta(t-n\tau)\psi(q,t) \qquad (5\ 1\ 12)$$

As the delta *kick* is of infinitesimal duration the integrable part of the hamiltonian changes by a negligible amount and can be neglected over a kick duration Therefore the $\psi(q,t)$ change discontinuously across the delta *kicks* by the amount $\mu_q \mathrm{Cos}(k_o q)$

$$\psi(q,(N\tau)^+) = \psi(q,(N\tau)^-)\exp(\iota\mu_q \mathrm{Cos}(k_o q)) \qquad (5\ 1\ 13)$$

The wavefunction between *kicks* is just that of the undriven oscillator and can be written in the form given by eq (5 1 4) Thus from just before the N^{th} kick, when time $t = N\tau^-$, to just after it, when time $t = N\tau^+$, we have

$$\psi(q,(N\tau)^+) = \sum_{p=1}^{\infty} A_p(N\tau)^-\phi_p(q)\exp(\iota\mu_q \mathrm{Cos}(k_o q)) \qquad (5\ 1\ 14)$$

The exponential term above can be substituted for an equivalent expression which includes a summation over bessel functions of integer order This identity, $\exp(\iota\mu_q \mathrm{Cos}(k_o q)) = \sum_{s=-\infty}^{\infty}\iota^s J_s(\mu_q)\exp(\iota s k_o q)$, can be found in *Table of Integrals, Series and Products* by Gradshteyn and Ryzhik (1965) as eq 8 511(4) Our expression for the wavefunction changes to

$$\psi(q,(N\tau)^+) = \sum_{p=1}^{\infty} A_p(N\tau)^-\phi_p(q)\sum_{s=-\infty}^{\infty}\iota^s J_s(\mu_q)\exp(\iota s k_o q) \qquad (5\ 1\ 15)$$

The time evolution from $(N\tau)^+$to $((N+1)\tau)^-$is that of the evolution of the harmonic oscillator itself Because each eigenfunction gives its corresponding energystate when operated on by H_o, $H_o\phi_n = E_n\phi_n$, then the evolution between the kicks is given by

$$\psi(q,t) = \sum_{p=1}^{\infty} A_p(t)\phi_n(q)\exp(-\iota\tfrac{E_n}{\hbar}t) \qquad (5\ 1\ 16)$$

where t is restricted to $N\tau^{+}$to $(N+1)\tau^{-}$and N is an integer Furthermore $E_n = (n+\frac{1}{2})\hbar\omega_o$ The evolution from just before the N^{th} kick to just before the $(N+1)^{\text{th}}$ kick of the wavefuntion $\psi(q,t)$ can now be formally expressed It is the product of the eq (5 1 16) (the evolution from the N^{th} kick to just before the next) with eq (5 1 15) (the change over a kick) Thus we have

$$\psi(q,((N+1)\tau)^{-}) =$$

$$\sum_{p=1}^{\infty} A_p(N\tau)^{-}\phi_p(q)\sum_{s=-\infty}^{\infty}\iota^s J_s(\mu_q)\exp(\iota s k_o q)\exp(-\iota(p+\tfrac{1}{2})\omega_o\tau) \qquad (5\ 1\ 17)$$

However, we should also point out that we can express the wavefuntion $\psi(q,t)$ just before the $(N+1)^{\text{th}}$ kick in terms of the $\phi_n(q)$ and the probability amplitudes at this later time

$$\psi(q,((N+1)\tau)^{-}) = \sum_{r=1}^{\infty} A_r(((N+1)\tau)^{-})\phi_r(q) \qquad (5\ 1\ 18)$$

This last equation allows us to express the probability amplitude coefficients at time $((N+1)\tau)^{-}$ as a function of the amplitude coefficients at time $(N\tau)^{-}$ Thus

$$\textstyle\sum_{r=1}^{\infty} A_r(((N+1)\tau)^{-})\phi_r(q) =$$

$$\sum_{p=1}^{\infty} A_p(N\tau)^{-}\phi_p(q)\sum_{s=-\infty}^{\infty}\iota^s J_s(\mu_q)\exp(\iota s k_o q)\exp(-\iota(p+\tfrac{1}{2})\omega_o\tau) \qquad (5\ 1\ 19)$$

The problem with this expression is that it gives the relationship between the summation over all the probability amplitudes times the eigenfunctions and does not give any information about individual probability amplitudes To rectify this we are going to take the expectation value of the above with each eigenfunction in turn This has the effect of giving us an explicit relationship between the amplitudes at time $((N+1)\tau)^{-}$to those at time $N\tau^{-}$ We know that the expectation value of ϕ_m with ϕ_n, $<\phi_m|\phi_n>$, is δ_{nm} After taking the expectation value of the left hand side with an arbitrary eigenfunction $\phi_m$we get

$$\sum_{r=1}^{\infty} A_r(((N+1)\tau)^{-}) <\phi_m(q)|\phi_r(q)> = A_m(((N+1)\tau)^{-}) \qquad (5\ 1\ 20)$$

The right hand side does not simplify so easily when taking its expectation value with ϕ_m All terms which are functions of q have to be brought together *in the correct order* inside the Bra-Ket symbolising the expectation value

$$\sum_{p=1}^{\infty} A_p(N\tau)^- \sum_{s=-\infty}^{\infty} \iota^s J_s(\mu_q)$$

$$\exp(-\iota(p+\frac{1}{2})\omega_o\tau) < \phi_m(q)|\phi_p(q)\exp(\iota s k_o q) > \qquad (5\ 1\ 21)$$

As you can see from this expression the expectation is not between two othogonal eigenfunctions but between more compound expressions This renders void the δ_{nm} property used for the left hand side of eq (5 1 19) So by combining eqs (5 1 20) and (5 1 21) we can now obtain the expression we require to relate the amplitude coefficients at time $(N+1)\tau^-$to those at time $t = N\tau^-$

$$A(((N+1)\tau)^-) = \sum_{p=1}^{\infty} A_p(N\tau)^- \sum_{s=-\infty}^{\infty} \iota^s J_s(\mu_q) *$$

$$\exp(-\iota(p+\frac{1}{2})\omega_o\tau) < \phi_m(q)|\phi_p(q)\exp(\iota s k_o q) > \qquad (5\ 1\ 22)$$

The question now is *What does the expression* $< \phi_m(q)|\phi_p(q)\exp(\iota s k_o q) >$ *in (5 1 22) break down to and how does it affect the summation over p in (5 1 22)?* To answer this we need to refer back to eq (5 1 11) and express the eigenfunctions' explicit form for $u_n(Q)$ in terms of $\phi_n(q)$, i e

$$\phi_p(q) = \frac{\iota^p}{\sqrt{2^p\sqrt{\pi}(p!)}} * H_p(\gamma q)\exp(-\tfrac{1}{2}\gamma^2 q^2)$$

and with this explicit form we are going to evaluate the expectation values by integrating the wavefunctions over the whole of space thay occupy This space is effectively from $q = -\infty$ to $q = +\infty$ Remember that q = real and that any polynomial in q with real coefficients is also real With this in mind we can write H_p^* as just H_p

$$< \phi_m(q)|\phi_p(q)\exp(\iota s k_o q) >=$$

$$A_{mp}\iota^{m+p}\int_{-\infty}^{\infty} H_m(\gamma q)\exp(-\frac{1}{2}\gamma^2 q^2)H_p(\gamma q)\exp(-\frac{1}{2}\gamma^2 q^2)\exp(\iota s k_o q)dq \qquad (5\ 1\ 23)$$

where $H_m(\gamma q)$ is the m^{th} order Hermite polynomial and $A_{mp} = \frac{1}{\sqrt{\pi 2^{m+p}(p!)(m!)}}$ The additional term of $\exp(\iota s k_0 q)$ can be accommodated into the other terms by multiplying

the equation by $\exp(-s^2k^2/4\gamma^2)\exp(s^2k^2/4\gamma^2)$ with the result that the sk_oq term and the γq term can be grouped as a single perfect square The next step is to write $z = \gamma q - \iota\xi$ where $\xi = \frac{k_o s}{2\gamma}$ and is made up of system constants except for the summation counter s Hence the Hermite polynomials $H_n(\gamma q)$ go to $H_n(z + \iota\xi)$ whose argument is still real but is now expressed as a complex number Using this notation, the integral term becomes

$$A_{mp}\iota^{m+p}\exp(-s^2k^2/4\gamma^2)\int_{-\infty}^{\infty} H_m^*(z+\iota\xi)\,H_p(z+\iota\xi)\exp(-z^2)\frac{dz}{\gamma} \qquad (5\ 1\ 24)$$

What is the solution to this integral? How does the exponential term affect the orthogonality of the hermite polynomials in integral term? The answer to these questions can be found in Gradshteyn and Ryzhik's book *Table of Integrals, Series and Products*, eqn (7 377) The form of the integral given is almost identical

$$\int_{-\infty}^{\infty}\exp(-x^2)\,H_m(x+y)\,H_n(x+z)\,dx = 2^n\sqrt{\pi}(m!)z^{n-m}L_m^{n-m}(-2yz) \qquad (5\ 1\ 25)$$

$(m \le p)$ We found that if y and z are replaced by $\iota\xi$ and x by z then we get the solution for eq (5 1 24)

$$\int_{-\infty}^{\infty}\exp(-z^2)\,H_m(z+\iota\xi)\,H_p(z+\iota\xi)\,dz = 2^p\sqrt{\pi}(m!)(\iota\xi)^{p-m}\,L_m^{p-m}(2\xi^2) \qquad (5\ 1\ 26)$$

$(m \le p)$ where $L_m^{p-m}(x)$ is the Laguerre polynomial defined as $\sum_{r=0}^{m}(-1)^r\binom{m+(p-m)}{m-r}\frac{x^r}{r!}$ In order to be completely confident with this solution we had to evaluate numerically the integral above for sets of parameters and then substitute these parameters into the analytical form given This was done because we have a complex argument in the exponential and Gradshteyn and Ryzhik's solution does not specify if the solution holds for this We found, using Mathematica for the numerical simulations, that the solution is indeed valid for our integral! Furthermore if we stick with our original form, namely

$$\int_{-\infty}^{\infty} H_m^*(\gamma q)\,H_p(\gamma q)\exp(-(\gamma q - \iota\xi)^2)\,dq$$

we can use another identity from Gradshteyn and Ryzhik namely eq (7 374(7)) which is

$$\int_{-\infty}^{\infty} \exp\left(-\left(x-y\right)^2\right) H_m\left(x\right) H_n\left(x\right) dx = 2^n \sqrt{\pi}(m!) y^{n-m} L_m^{n-m}\left(-2y^2\right) \qquad (5\ 1\ 27)$$

$(m \leq p)$ where by replacing x by γq and y by $\iota\xi$ we get

$$\int_{-\infty}^{\infty} \exp\left(-\left(\gamma q - \iota\xi\right)^2\right) H_m\left(\gamma q\right) H_p\left(\gamma q\right) dq = 2^p \sqrt{\pi}(m!) \left(\iota\xi\right)^{p-m} L_m^{p-m}\left(2\xi^2\right) \quad (5\ 1\ 28)$$

$(m \leq p)$ which is the exactly the same result as from that in eq (5 1 26) However these solutions are only defined for $m \leq$ p So our equation for $A_m((n+1)\tau^-)$ now takes on a more complete form

$$A_m(((N+1)\tau)^-) = \sum_{p=1}^{\infty} A_p\left(N\tau\right)^- \sum_{s=-\infty}^{\infty} \iota^s J_s\left(\mu_q\right) \exp\left(-\iota\left(p+\tfrac{1}{2}\right)\omega_o\tau\right) *$$

$$\frac{\iota^{m+p}}{\sqrt{\pi 2^{m+p}(p!)(m!)}} \exp\left(-s^2k^2/4\gamma^2\right) 2^p\sqrt{\pi}(m!) \left(\iota\tfrac{k_o s}{2\gamma}\right)^{p-m} L_m^{p-m}(s^2k_o^2/2\gamma^2) \qquad (5\ 1\ 29)$$

Some of the terms above cancel and others simplify for example the inner summation over s can be halved to contain just the positive integers because $\iota^{-s}J_{-s}\left(\mu_q\right)$ is equal to $\iota^s J_s\left(\mu_q\right)$ (the $s=0$ term is zero hence its exclusion) Furthermore only one other term in this summation depends on an odd power of s (all the others depend on s^2 and are thus independent of the sign of s) With these simplifications the final form is

$$A_m(((N+1)\tau)^-) = \sum_{p=m}^{\infty} A_p\left(N\tau\right)^- \sqrt{\frac{(m!)}{(p!)}} \sum_{s=1}^{\infty} \iota^{s+2p} J_s\left(\mu_q\right) \exp\left(-\iota\left(p+\tfrac{1}{2}\right)\omega_o\tau\right)$$

$$* \exp\left(-s^2k_o^2/4\gamma^2\right) L_m^{p-m}(s^2k_o^2/2\gamma^2) \left\{ \left(\tfrac{sk_o}{\sqrt{2}\gamma}\right)^{p-m} + \left(\tfrac{-sk_o}{\sqrt{2}\gamma}\right)^{p-m} \right\} \qquad (5\ 1\ 30)$$

which holds only for $m \leq p$ hence the lower limit on the outer summation with p now only summed from $m \leq p \leq \infty$ The complex conjugate of A_m denoted A^* is expected to be of a similar form but with the signs before the ι opposite to those above

To obtain the energy level spectrum as a function of time it is necessary to find the norm of the probability amplitudes as these are the multipliers in the summation over the energy levels of the undriven system Hence the energy of any $\psi\left(q,t\right)$, where $\psi\left(q,t\right)$

was defined in eq (5 1 4), is given by $\sum_{r=1}^{\infty} \|A_r(t)\|^2 E_r$ As the E_r are the energy levels of the undriven system then the energy evolves as

$$E_\phi(N\tau^-) = \sum_{r=1}^{\infty} \left\| A_r(N\tau)^- \right\|^2 (r + \frac{1}{2})\hbar\omega_0 \qquad (5\ 1\ 31)$$

and as we can explicitly evaluate the A_r over any kick we can calculate the energy of the system at any time for any set of parameters

We should bring the reader's attention to some remarkable coincidences between this mapping and the classical Firstly the presence of $\omega_o\tau$ which is just β in the classical mapping (see chapter 2) Secondly we defined γ to be the factor between q and Q such that $1/\gamma = \sqrt{\hbar/M\omega_0}$ Therefore k_o/γ is just our classical K Thirdly we can relate μ_q to the classical μ_{cl} via the relationship defined in chapter 2 We can make comparisons quite easily now between our classical mapping and our fully quantum mapping above This we will do in the following two chapters

5 2 Numerical Considerations

Our purpose here is to highlight the approach taken when numerically evaluating the mapping in eq (5 1 30) Such an evaluation is necessary when one considers the compexity of the mapping itself Futhermore by considering how functions within the mapping behave and interact with each other we intend to justify certain assumptions made Let us begin by describing the technique we use to iterate the mapping forward in time

If you examine closely the form of the mapping in eq (5 1 30) then you can see that only the A_p on the right hand side is time dependent All other terms are time invariant and this useful observation will drastically reduce computing time in the evaluation of the mapping We can re-formulate the mapping as follows

$$A_m(((N+1)\tau)^-) = \sum_{p=1}^{\infty} U_{mp} A_p(N\tau)^- \qquad (5\ 2\ 1)$$

where U_{mp} is the mp element of an infinite time-independent square matrix, U, which performs the task of stepping the system forward in time However we have a problem in

that only those elements of the matrix for $p \geq m$ are defined (from the identity used in Gradshteyn and Ryzhik (1965) in eq (5 1 24) and (5 1 26)) To overcome this we present an argument to define those missing elements of the matrix U

We have already shown in the previous section that the Hermite polynomials are real as q itself is real Therefore we substituted H for H^* in eq (5 1 23) because of the real valuedness of these polynomials As the integral in eq (5 1 23) is a product of two polynomials then we can swap these polynomials around in the integral to give us the solution for $p \leq$m We checked, using Mathematica, the correctness of the above and found the numerically that the two are identical Furthermore one can easily check that

$$U_{mp} = U_{pm} \tag{5 2 2}$$

This symmetry allows us to calculate just one half of the matrix greatly reducing computer run time

Our task numerically is to evaluate this matrix for a finite size and then use the relation in eq (5 2 1) to obtain the probability amplitudes at each time step As both the amplitudes, $A_m(t)$, and the evolution matrix, U, are complex then we have to split the matrix into two parts (real and complex) and similarly for the amplitudes Then we split the evolution in eq (5 2 1) into the real and imaginary parts

$$A_{m_{\rm re}}(((N+1)\tau)^-) = \sum_{p=0}^{\infty} (U_{mp_{\rm re}} A_{p_{\rm re}}(N\tau)^- - U_{mp_{\rm im}} A_{p_{\rm im}}(N\tau)^-) \tag{5 2 3a}$$

for the real

$$A_{m_{\rm im}}(((N+1)\tau)^-) = \sum_{p=0}^{\infty} (U_{mp_{\rm re}} A_{p_{\rm im}}(N\tau)^- + U_{mp_{\rm im}} A_{p_{\rm re}}(N\tau)^-) \tag{5 2 3b}$$

for the imaginary parts with, naturally, the sum being the complete complex probability amplitude at the specific kick

$$A_m(((N+1)\tau)^-) = A_{m_{\rm re}}(((N+1)\tau)^-) + \iota A_{m_{\rm im}}(((N+1)\tau)^-) \tag{5 2 3c}$$

The real and imaginary U matrices are calculated first using a C code program with a software link to Mathematica allowing high order Laguerre Polynomials to be evaluated

whereas a set of amphtude programs calculate the time evolution using the expressions in eqs (5 2 3a) and (5 2 3b) The complex conjugate of A_m is then that of A_m with the sign of ι changed We can then calculate the energy of the system at a specific time knowing that

$$E((N+1)\tau^-) = \sum_{n=0}^{\infty} \{ \ A^2_{n_{\rm re}}(((N+1)\tau)^-) + A^2_{n_{\rm im}}(((N+1)\tau)^-) \ \} (n+1/2)\hbar\omega_o \quad (5\ 2\ 4)$$

This energy calculation is fundamental to understanding the system's evolution and the possible existence of *chaos*

The numerical evaluation of the evolution matrix, U, is hampered by the infinite summation over s (see eq (5 1 30)) Therefore we need to approximate this by a truncated sum (if possible) It is well known (Israilev (1990)) that Integer Order Bessel functions ($J_n(z)$) tend to zero if the order of the function is greater than twice the argument Therefore for any fixed argument, z, there exists a cutoff for the Bessel functions at $2z$ Our inner summation over s could be given upper and lower limits of $2\mu_{cl}$ and $-2\mu_{cl}$ respectively if no other functions exited in the summation which depended on s However we do have others which we need to consider The magnitude of the complex term could, if s got large enough, hypothetically dominate but as $J_s(z)$ tend to zero if $|s| \gg z$ quicker than the complex term tends to ∞ then their product would not diverge at large s That still leaves us with a guess at the upper bound on s The answer comes from the exponential term with the $-s^2$ argument This term dominates at large $|s|$ even over the Laguerre polynomials to the extent that the summation over s can be truncated after about 20 to 30 terms (well within the scope of any computer) These properties were examined using Mathematica and we found that after 15 terms the decrease in magnitude was between 8 to 20 orders depending on the orders of the functions

All these precautions went into the numerical programming to ensure that the results obtained would accurately mirror the matrix itself Further precautions will be outlined as necessary during the detailed analysis undertaken in the next chapter

CHAPTER 6
ANALYSIS OF THE QUANTUM MAPPING

This chapter is one of the more interesting for us in that it covers the results we obtained from our quantum mapping As this mapping has been derived using an approach never adopted for this system we presume the following analysis to be both novel and unique In this chapter we present the results obtained from the mapping obtained in chapter 5 and compare its results with those from the classical mapping in chapters 2, 3 and 4 The results presented are the time evolution of the probability amplitudes, the energy of the system for various kick strengths, μ_q, and the corresponding wavefunctions These results will be used along with those for the Wigner distribution in the following chapter to develop a correspondence between the quantum mapping and the classical mapping

6 1 Probability Amplitudes In Time

The quantum mapping in chapter 5 relates the probability amplitudes from one time step to the next Consequently, as the probability amplitudes consist the primary data from the approach we're taking, then it is appropriate to begin our quantum analysis by examining how they vary in time As previously discussed in chapter 5 section 2 (under Numerical Considerations) we have set the problem up so that the evolution matrix is time invariant and the size of this square matrix sets a limit on the order of the highest probability amphtude (and hence eigenfuncton) we can consider This will become important when iterating the quantum mapping over time

The diversity of our approach becomes clear when choosing which time evolutions to present as *typical* of the system's behaviour in this section We could, for example, choose a pure (in the sense of the undriven oscillator) even parity or odd parity eigenstate to begin with and examine its time evolution However, we have chosen a mixed state with a gaussian profile across the probability amplitudes centred on a low order undriven oscillator eigenstate, i e $m = 10$ Our reasons for venturing so low were driven by practical considerations concerning the finite size of our evolution matrix, U We restricted U to a 350×350 matrix, for computational feasibility, with the result that, if the initial state

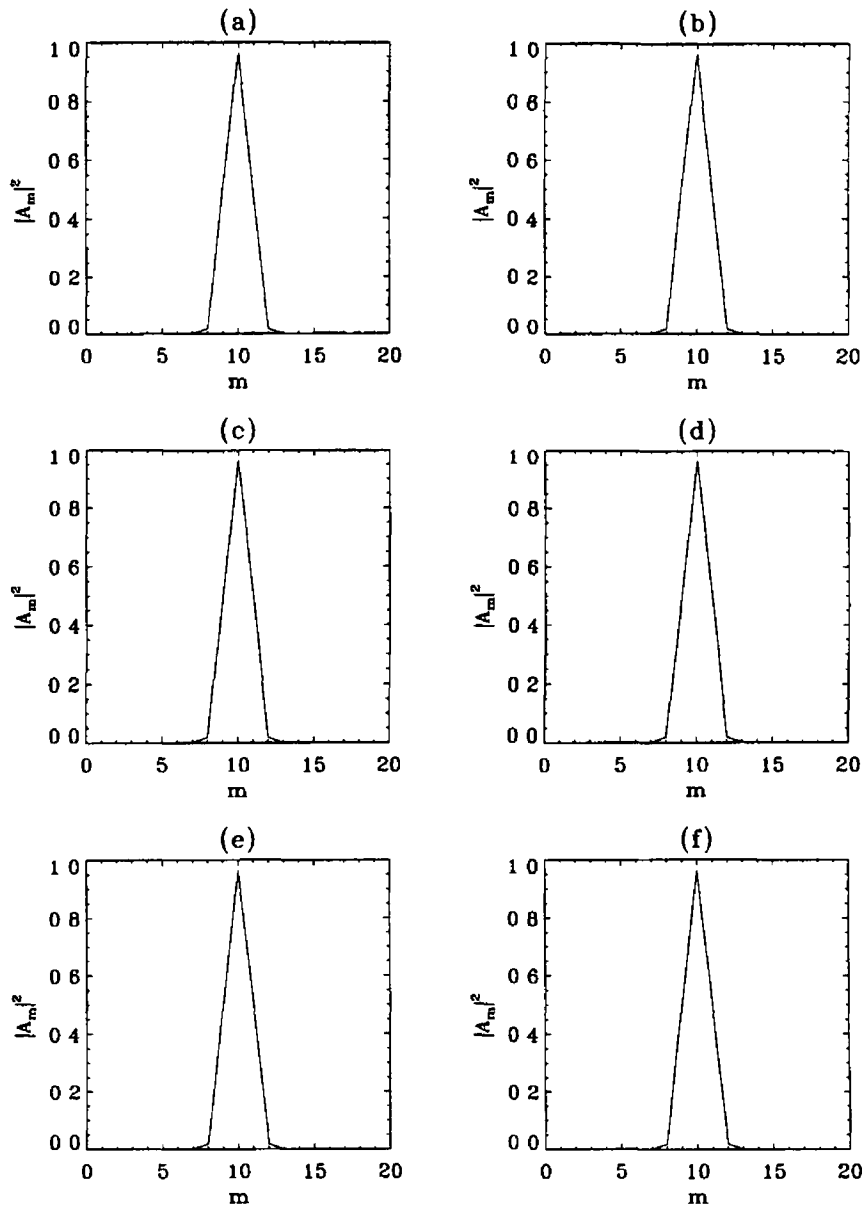

Fig 6 1 The probability amplitudes for the mixed parity state of a gaussian centred on m=10 with $\mu_q = 0\ 00005$ Each of the successive plots (b)-(f) shows the system 300 time steps later The system remains essentially unchanged regardless of the kicking

spreads, or diffuses, so that the amplitudes near the $m = 350$ boundary are becoming increasingly significant, there is an artificial time limit imposed beyond which the results are boundary influenced and therefore untrustworthy

We would expect that if the kick strength, μ_q, was so small as to be negligible then

its influence would be correspondingly weak In this case the spread over the amplitudes would be very small if at all noticeable and the energy of the system would be constant This is the case for $\mu_q = 0\ 00005$ where the gaussian profile is retained for the duration of the time sample (2000 iterations) We present in figs $6\ 1(a) - (f)$ the probability amplitudes every 300 time steps The variation from the original is slight and, as will be shown later, its energy varies little from the initial state's energy This is what we see classically for those orbits near the origin at low, near negligible, kick strengths (refer to fig 2 2 in chapter 2) Classically, those orbits would remain circular in shape and vary little from the unkicked state

If, however, the kicking is modest but not dominant, we would expect, classically, that those orbits very close to the origin to remain essentially undisturbed forming an island which is invariant (the invariant cells of chapter 3) but that the orbits further out would become increasing disturbed and distorted (*re* Chapter 3) In the quantum case we find that the system's probability amplitudes settle down to specific patterns after a period of time The settling down time being dependent on the kick strength and how far away from the steady state distribution of amplitudes the initial state was We show such a case in figs $6\ 2(a) - (f)$ for $\mu_q = 0\ 5$ Again the intervals between $(a), (b),\quad ,(f)$ is 300 iterations The stable configuration is clear in figs $6\ 1(d), (e)\&(f)$ We will show in the next section how this configuration affects the energy and how similar steady configurations give rise to *quasi-energy levels*, levels whose periodicity matches that of the kick period and thus appear constant to the mapping (Israelev (1990))

Lastly we present the amplitudes' evolution when the kick strength is such that it dominates the system's behaviour We saw in Chapter3 (fig 3 2 and table 3 1) how the elliptic fixed points of order four and the origin become hyperbolic at $\mu_{cl} = 10\ 0$ This very fortunate result means that the origin can become unstable and that orbits in its vicinity can become diffuse as they spread into the stochastic layer In the quantum case we would expect this to manifest itself as a continual spreading over all the orders of the probability amplitudes and a subsequent linear increase in energy For our third figure we present six snapshots of the evolution for $\mu_q = 1\ 5$ The spreading out is evident and so rapid that after forty, or so, mterations we had to stop the calculations as the upper boundary on the

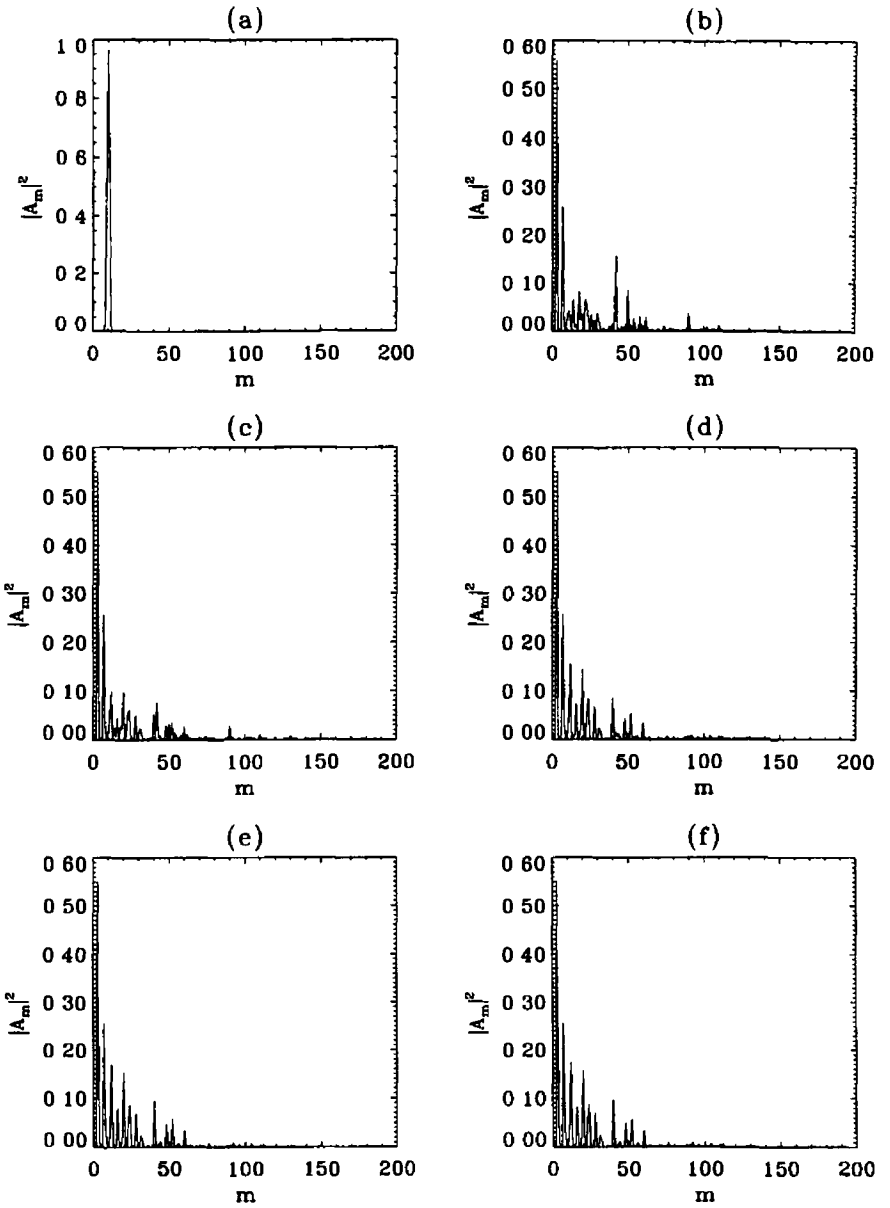

Fig 6 2 The probability amplitudes for the same state in fig 6 1 except this time $\mu_q = 0\ 5$ The interval between each plot is as before and it is worthwhile pointing out that the distributions in (d)-(f) are quite similar, i e the system is saturating naturally and the state is becoming localised

probability amplitudes had been reached The energy increase was linear and also without saturation (within this time sample) The probability amplitudes are presented in figs 6 3$(a) - (f)$

It can sometimes be difficult to compare successive iterations of the amplitudes

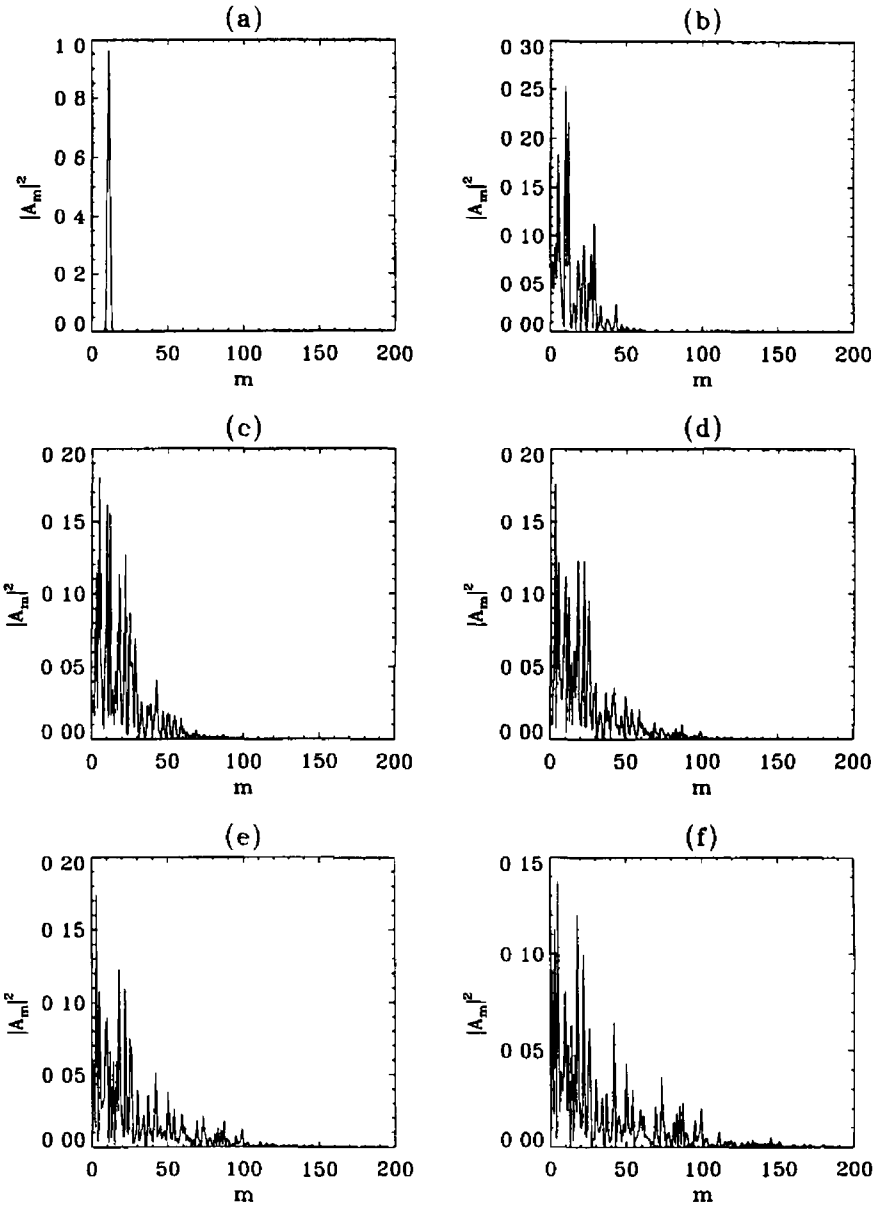

Fig 6 3 The amphtude spectrum for the same initial state in fig 6 1 but with $\mu_q = 1\ 5$ and the time between successive plots being 4 time steps The spread over the states is apparent and boundary saturation occurs soon after (f) at around 40 time steps

and see obvious differences as some changes from iteration to iteration can be very subtle but nevertheless important It is clearer to examine the energy of the system as a function of the iterations to see just how substantial a change can occur a fixed time interval We perform this task in the next section with an examination of the wavefunctions' structures

as well

6 2 Energy, Quasi-Energy Levels & Wavefunction Evolution

As with any quantum system, once you know the probability amplitudes and you have a complete set of eigenfunctions, then obtaining such quantities as the energy, wavefunction *probabilities* in space and constructing quasi-phase spaces in relatively straightforward In this section, the energy as a function of the time steps is examined and the wavefunctions at each step calculated We will also show that stable energy levels exist, for moderate kick strengths Depending on the initial state of the system, one of these levels is approached by the energy of the system We will try, within the bound specified by the finite size of U i e 350 eigenfunctions, to calculate some energy level statistics as is done for most of the time-independent non-linear quantum system examined in the journals (Berry at al (1986), Robnik et al (1986), Lewenkopf (1990) Tanner et al (1991))

For neghglibly small kicking the effect on the system's energy is very small if at all noticeable In the previous section figs 6 1$(a)-(f)$ showed how the initial state changed almost adiabatically with little discernible change in its profile We present in fig 6 4 the energy corresponding to the amplitudes in fig 6 1 showing how little the change in energy is over the time interval The kick strength for this case is $\mu_q = 0\ 00005$ This case corresponds to the limit as $\mu_q \to 0$ and is included as a test to confirm that the system is behaving properly or to put it succintly *to check that the numerics are correct*

Artificial boundary effects, caused by the imposition of the finite eigenfunction set, can be seen clearly in those energy curves where μ_q is large enough to diffuse the initial state sufficiently so that it *collides* with the boundary of 350 eigenfunctions These boundary effects manifest themselves as *bend overs* in the energy curves, for both the off and on resonance cases, and all observed energy saturations have to be checked and thoroughly examined to exclude any such artificial effects The primary reason for this scrutiny, also the reason why we don't employ a blanket masking out of all observed saturations, is that it has been hypothesised (Chirikov et al (1981)) that energy saturations are an indication of a suppression of *quantum chaos*, as has been observed in the kicked rotator system

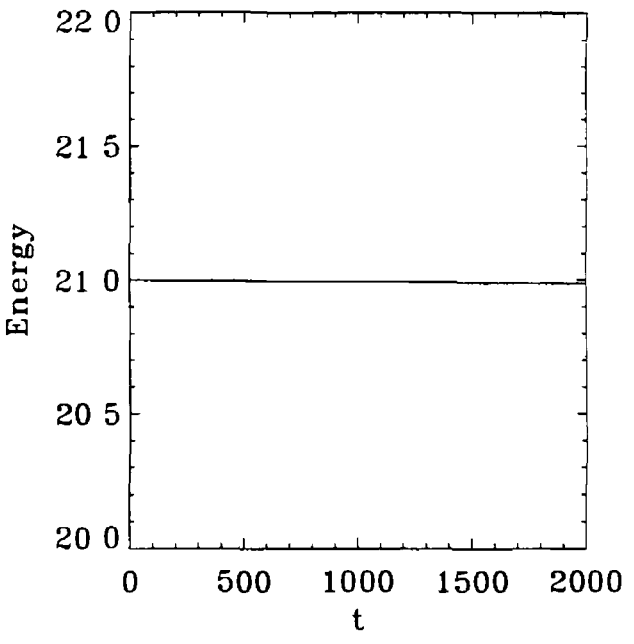

Fig 6 4 The energy evolution for the quantum system corresponding to the probability amplitudes in fig 6 1 The near constant energy confirms the almost perturbative effect the kicking is having on the system at $\mu_q =$ 0 00005

(Casati et al (1979)), bistable systems (Ray (1990)) and simple linearly quantised systems (Scharf & Sundaram (1991)) This is still a subject for contention with some (Berman et al 1991) arguing that these systems are non-physical and that the inclusion of an extra time scale (such as in our kicked oscillator) is sufficient to counter the suppression seen in these other systems (Shepelyansly (1983) & Adachi et al (1988)) The kicked harmonic oscillator model, on the other hand, is a realistic system and thus any saturation, and related localisation, in energy could be considered indicative of *chaos suppression*

Unfortunately as with everything in life there is a catch, namely we need to increase the size of our matrix to eliminate the possibility of saturation Strictly speaking the size should be infinite to be absolutely positive that no saturation occurs and this is numerically impossible To date with a test matrix of 450×450 (we couldn't and wouldn't trust MathLink for orders any higher than 450 due to its inability to handle some of the numbers Mathematica was sending it) we found no evidence of saturation In fig 6 5 we

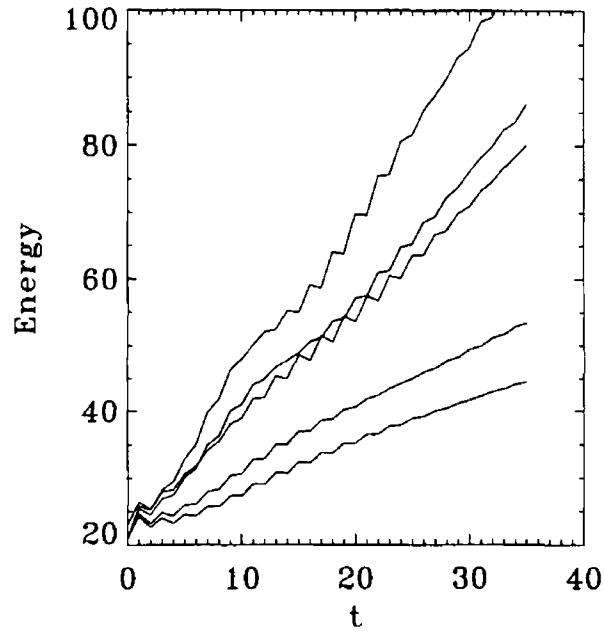

Fig 6 5 Five energy curves for the mixed state at m=10 The curves correspond to (from top to bottom) μ_q = 1 7,1 6,1 5,1 4 & 1 3 Though not perfect for calculating the quantum diffusion coefficient, D_q, we will fit straight lines to them to estimate D_q at each of the values The result in shown in fig 6 6

give a composite plot of five different kick strengths over a specified time We omit some of the energy points at higher kick strengths due to boundary saturation of the energy at these higher levels

The linear nature of these energy curves, we found the energy to scale as

$$E(\mu_q, n) = B(\mu_q)n \tag{6 2 1}$$

suggest it might be possible to evaluate a quantum diffusion coefficient, $D_q(\mu_q)$ The problems associated with this exercise are, the small time interval over which the energy doesn't saturate by impinging on the boundary, the requirement to calculate a new evolution matrix for each value of the kick strength and the need to average over a set of states which is further limited by the finite size of the unitary matrices However we do have a number of matrices of size 350 $\times$ 350 calculated and for these matrices with linear

energy increases we attempted to calculate a quantum diffusion coefficient, $D_q(\mu_q)$ where we define this diffusion coefficient to be the partial derivative of the energy with respect to time for a fixed kick strength

$$D_q(\mu_{q_o}) = \left\{ \frac{\partial E(\mu_q, t)}{\partial t} \right\}_{\mu_q \equiv \mu_{q_o}} \tag{6 2 2}$$

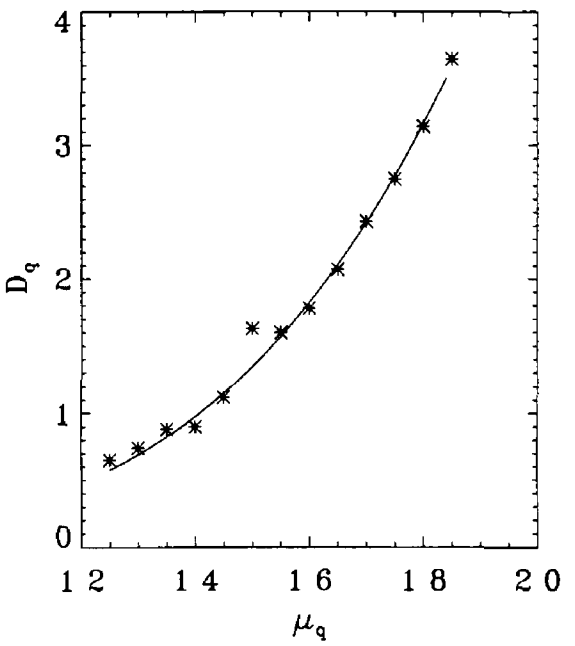

Fig 6 6 The quantum diffusion coefficient, $D_q \equiv \frac{\partial E(t)}{\partial t}$, vs μ_q The increase is certainly non-linear and found generally to increase as $A(\mu_q)^b$ where A=0 2 and b=4 68 The solid line is the fit associated with A & b above and fits the data very well The bump is not a glitch and was found to occur at $\mu_q = 1\ 5$

The result is presented in fig 6 6 We found a glitch to occur at $\mu_q = 1\ 5$ and at finer resolution we found the neighbouring points to be well behaved (in the sense they followed the general trend of the curve) but the slope of the energy at $\mu_q = 1\ 5$ took a definite jump This occurance at close to $\frac{\pi}{2}$ cannot be discarded and may be a kind of enhancement similar to the Resonantly Enhanced Diffusion in Chapter 4 One of the methods this glitch will

be examined in the future is to examine the elements of the evolution matrix at specific kick strengths, their limits, as the matrix size tends to infinity, and their influence on the momentum (and hence diffusion) It should be possible to do this *hand in hand* with the future analysis proposed for the quasi-energy levels described later

This finishes our examining of those diffuse states with apparently boundless energy increase Such states may exist the kind of hypersensitivity referred to by Schack & Caves (1993) as these states are responsible to the extended structure we shall see in the the Wigner distributions in Chapter 7 These states are (over our limited range of scrutiny) de- localised and do not give us any information on possible stable energy levels within our kicked system To do this we need to examine localised states

The final set of energy curves dealt with those which saturate naturally (those which don't impinge on the finite boundary dicatated by the numerics) and saturate at different levels for different initial conditions These levels are steady state solutions for the quantum mapping at a specific value of μ_q They are also reffered to as *Quasi-Energy* levels because the wavefunctions are periodic w r t the kick duration Therefore at each kick the wavefunction returns to its value at the previous kick and the energy stays constant The wavefunction has become localised in terms of the kicks Israilev (1990) introduces such levels in the kicked rotator where he refers to the quasi-energies first introduced by Zeldovich (Israilev (1990)) and Ritus (Israilev (1990)) back in 1966 We use his notation here We introduce a set of quasi-energies ϵ determined by the relationships

$$\psi_\epsilon(q,t) = e^{-\iota\epsilon t/T}\phi_\epsilon(q,t) \tag{6 2 3}$$

where

$$\phi_\epsilon(q,t+T) = \phi_\epsilon(q,t) \tag{6 2 4}$$

In this sense the $\phi_\epsilon(q,t)$ are eigenfunctions of the evolution operator matrix U for the specific value of $\mu_q$we are dealing with The diagonalisation of the evolution matrix U for any kicked system should present us with a complete set of these eigenfunctions (Berry et al (1986)) but as U is an infinite square matrix we need to be sure that the decay of off diagonal terms to zero is rapid enough so that their contribution to the calculation of the eigenvalues of U is negligible On examination of the necessary matrix data files for

the real and imaginary components at $\mu_q = 0\,5$ and $\beta = (\sqrt{5}+1)/2$, which is the case we considered, we found that the off diagonal terms decay to more 15 orders of magnitude less than the principle diagonal terms within 170 terms of the principle diagonal If we set this limit to 10 orders less then the limit is 100 terms to the diagonal and reduces to 50 if the limit is set at 5 orders below the principle diagonal term So the question is *what accuracy do we require to determine the cut-off for the off-diagonal terms?* This cut-off will also determine how many eigenvalues we can calculate from a fixed 350×350 matrix This is only one of several considerations necessary for the solving of the matrix, U To date we have not yet attempted this beyond a brief trial using the routines in Mathematica (which crashed) yet despite this the idea does provide an interesting direction in which this research can proceed in the near future such as obtaining the energy level statistics (Berry et al (1986), Lewenkopf (1991)) However, as shown by Lewenkopf (1991), these statistics are not conclusive evidence of chaos We continue now with the quasi-energy levels which we obtained from the evolution matrices

When investigating the existence of steady state levels (quasi-energy levels) we found that not all initial states give unique steady state levels and so we have degeneracy present We found these steady state levels to exist in the system at a kick strength of $\mu_q = 0\,5$ for an off resonance case ($\beta = (\sqrt{5}+1)/2$) From the plot of the results, in fig 6 7, one can see quite clearly the three levels attained by the four starting states The lowest state (that of a gaussian distribution of probability amplitudes centered on the lowset state $m = 0$) evolved to the same steady state level as that for a state with gaussian distribution centred on $m = 11$ This was included to illustrate the degeneracy present and also to highlight that this steady state level is probably the lowest level in the system We can see that the levels do not appear to be equally spaced but, with the matrix size available to us, we do not have enough levels present to construct a relationship between them With the future diagonalisation of the evolution matrix, U, we should be capable of relating levels (or groups of levels) together

Our final discussion in this section is centered about the structure of the wave-functions themselves and how the probability in Q is related to the diffuse or localised nature of the system at the values of the kick strength being considered

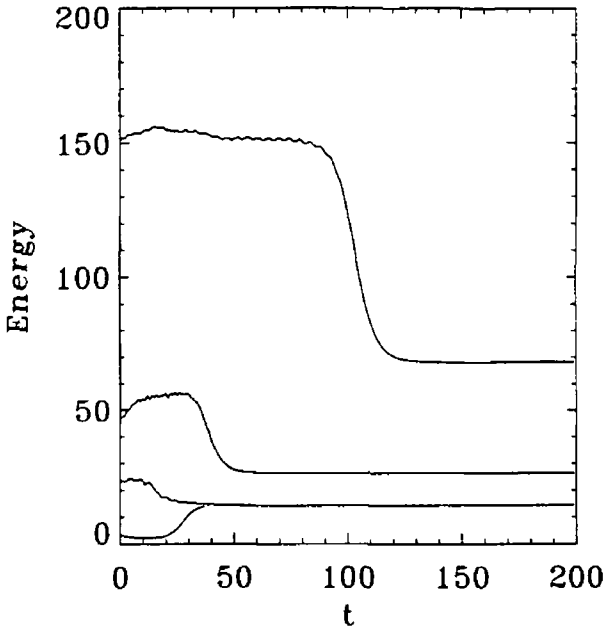

Fig 6 7 The three lowest levels obtained for $\mu_q = 0\,5$ and $(\beta = (\sqrt{5}+1)/2)$ The levelling off is obvious and indicative of a stable solution of the evolution matrix These levels are the quasi-energy levels discussed in the text

Any wavefunction which satisfies Schrodinger's wave equation (eq (5 1 3)) for the undriven system, whose Hamiltonian is given by eq (5 1 2), can be expressed as a linear combination of the eigenfunctions of that system, *c f* eq (5 1 4) For the kicked system (eq (5 1 1)) the wavefunctions are related to the undriven system's eigenfunctions with time dependent amplitudes given by the relationship in eq (5 1 30) So once we have the amplitudes we can calculate what the wavefunction would look like at each time step The importance of examining the wavefunctions is principally to see how the evolution of system affects the existence probabilities of the system at different Q values As the eigenfunctions themselves have an $\exp(-\frac{1}{2}Q^2)$ term present they will tend to zero as Q tends to infinity The higher the order of the eigenfunction, the further out along the $\pm Q$ axes the wavfunction will exist for Thus for a finite set of amphtudes (as we have here with our 350×350 matrix) the wavefunctions will tend to zero as Q increases beyond a critical value dependent on the highest eigenfunction order present in the evolution matrix with non-zero probability amplitude Therefore we expect that, for those states which diffuse

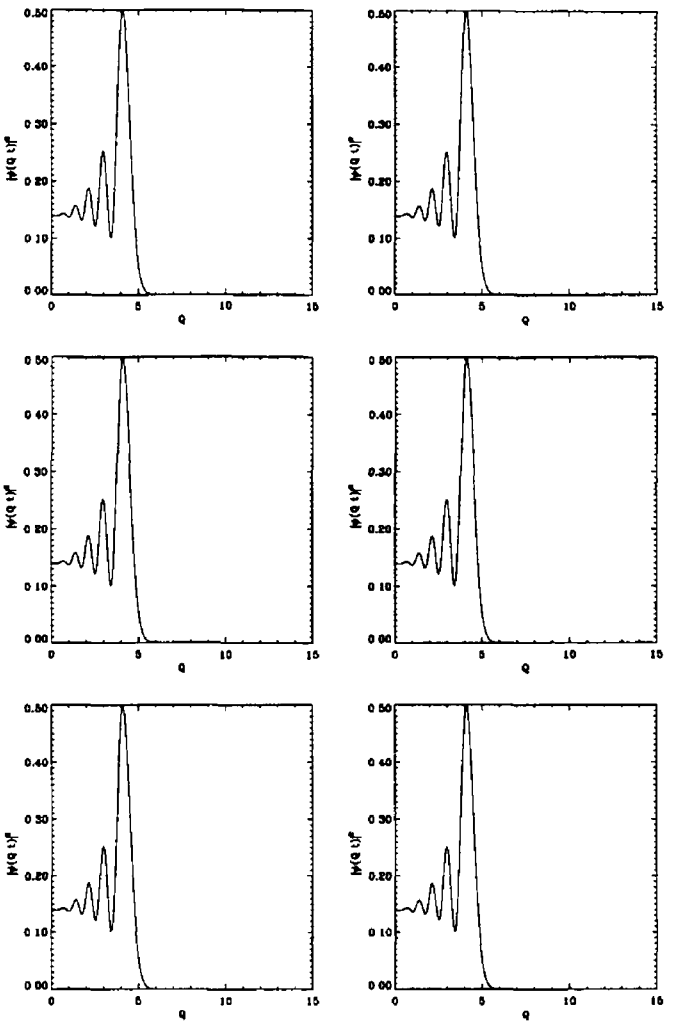

Fig 6 8 The wavefunction, $\psi(Q)$, for the system when the kick strength, μ_q, is so small as to be negligible The system is on resonance and $\beta = \frac{\pi}{2}$ The time interval between plots is 300 iterations The wavefunction is symmetric about the origin ($Q = 0$) so only the positive half is shown

rapidly up through the orders of the eigenfunctions, the wavefunctions would be the most spread out (diffuse) in a given time scale Those which saturate naturally at a given energy *above* their initial state would be less spread out whereas those whose energy stays approximately constant and equal to their initial state would have little or no spreading at all The degree of spreading out over the eigenfunctions orders would also determine the degree of *diffusivity* and lack of structure present in the wavefunction To illustrate these three cases we present the wavefunctions for the three cases considered so far for the

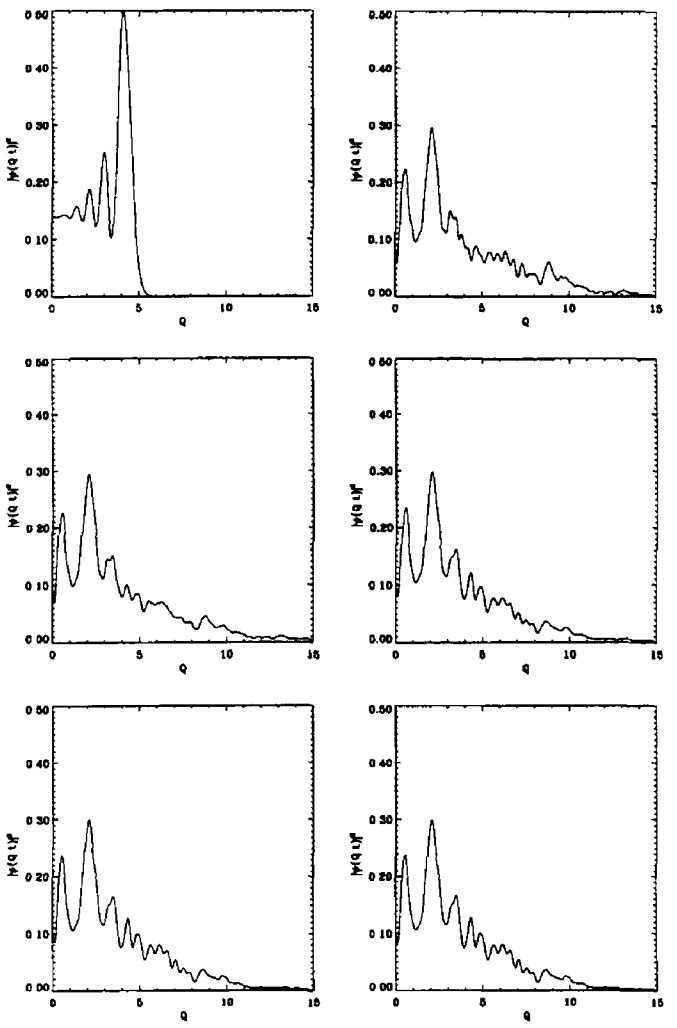

Fig 6 9 The wavefunction, $\psi(Q)$, for when the kick strength, $\mu_q = 0\,5$ and $\beta = \frac{(\sqrt{5}+1)\pi}{2}$ The time interval between plots is 300 iterations The system has saturated naturally and the wavefunction can be seen to be time independent in the final 3 plots supporting this natural saturation, c *f* fig 6 7

energy evolution and the probability amplitude evolution

The initial state we choose for the following set of three figures is the mixed state consisting of a gaussian distribution of probability amplitudes centred on the $m = 10$ eigenstate The figures 6 8 – 6 10 show $|\psi(Q, \mu_q, t)|^2$ vs Q at specified times of the system's evolution The wavefunction is defined according to eq 5 1 4 and the dependence of the probability amphtudes on time and μ_q is given by the evolution equation, eq (5 1 30)

The figures show just the positive half of the Q axis but due to the property that $H_{-n}(Q)$ $= (-1)^n H_n(Q)$, and as we're plotting $|\psi(Q,\mu_q,t)|^2$, the resultant figures are symmetric about the origin because $(H_{-n}(Q))^2 = (H_n(Q))^2$

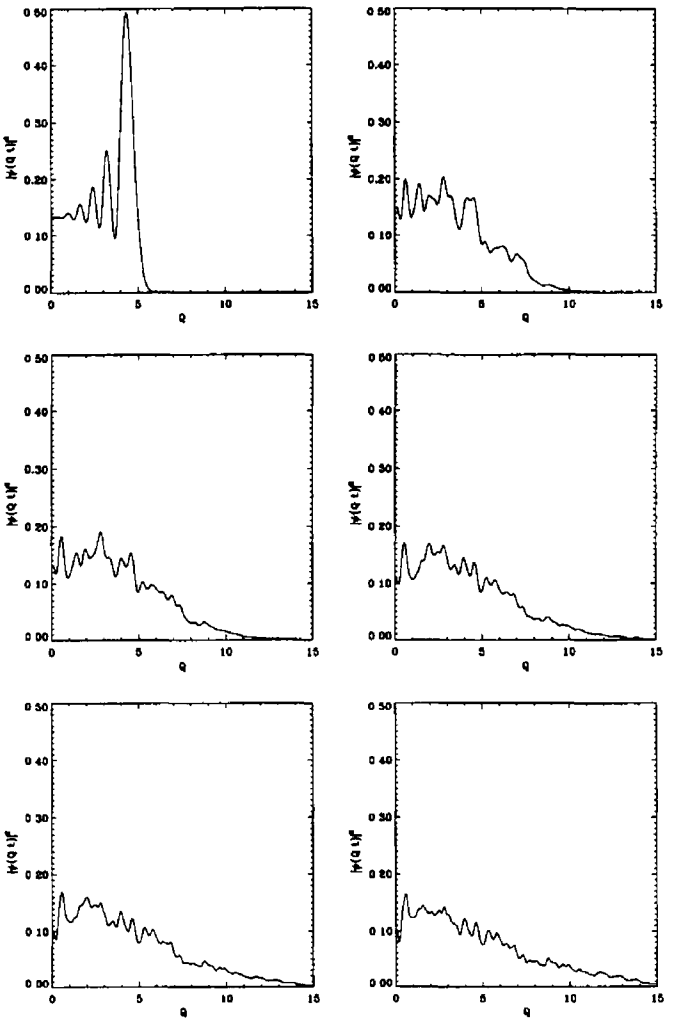

Fig 6 10 The wavefunction, $\psi(Q)$, for when the kick strength, $\mu_q = 1\ 5$ and $\beta = \frac{\pi}{2}$ The parameter values correspond to the unbounded growth we discussed and presented in fig 6 5 The time between each plot is 6 time steps of the mapping Even over such a short period of time the spread over Q and the increasing lack of structure indicates a significant diffusion for this state

As before we begin with the case where the kick strength is so small as to be a perturbation of the undriven system We use this case as a test to ensure that in the limit

$\mu_q \rightarrow 0$ the system reverts to the undriven case This is what figs 6 1 & 6 4 illustrate for the probability amplitudes and energy respectively The corresponding figure for the wavefunction itself is shown is fig 6 8 The change is negligible, if at all, and the system is behaving like the undriven oscillator as we would expect This limit is important as it ensures a continuity from the undriven to the driven systems and, as the undriven oscillator has been well studied, it serves as a test to ebsure the numerics are functioning properly

The plots presented in fig 6 9 are those for the wavefuntion evolution when the kick strength is 0 5 and *the system is off resonance*, *i e* $\beta = \frac{(\sqrt{5}+1)\pi}{2}$ This corresponds to the system in fig 6 7 where we illustrated the natural saturation of the system and the existence of quasi-energy levels The initial state chosen for the wavefunctions in fig 6 9 corresponds to the lowest energy level in fig 6 7 The temporal periodicity of the wavefunction, $\psi(Q)$, which ensures its steady state behaviour at each time step makes this wavefunction a eigenfunction of the driven system The energy corresponding to this eigenfunction would constitute one of the qausi-energy levels we discussed previously One of the more interesting observations that can be made of the probability distributions in fig 6 9 is the structure which exists in the wavefunction in the last three plots The peaks near the origin in the second plot (300 time iterations after the start) remain right through the time evolution up to 2000 iterations These, plus the smaller and less prominent peaks, indicate that certain eigenfunction are preferred over others and these preferential eigenfunctions are those with the greatest overlap with the peaks seen Such stable structures in the wavefunction is important as it is proof that the wavefunction is *not* going to spread out over the complete basis of eigenfunctions but will remain essentially restricted to a subset of the basis Thus the evidence of stable structure in the wavefunction can be used as a method for determining the *diffusiveness* of an initial state for a given set of parameters

The unbounded like spread in the probability amplitudes in fig 6 3 and the corresponding unsaturating energy increases in fig 6 5 suggest that the wavefunction for such a class of state would diffuse from the initial bounded (in Q) state and tend to a state which was spread out near uniformly over the whole Q axis This tendency to spread out over Q would necessitate the inclusion of higher (and higher) order eigenfunctions, $u_n(Q)$, of the undriven oscillator as these eigenfunctions are themselves bounded m a finite section of the

Q axis for a finite order This to spread over the full axis (or even tend to such a spreading) the initial state would have to diffuse over all the eigenfunctions of the undriven system which would subsequently lead to an unbounded increase in the wavfeunction's energy We present, in fig 6 10, the closest we can come to such an unbounded diffuse state Our size of matrix (350×350) limits our analysis and the number of iterations we can perform on the state before the state reaches the limit imposed by our finite matrix and our results become meaningless Therefore the time duration of our analysis of such diffuse states is, on average, about 40 iterations (depending on the kick strength and whether we're on or off resonance) The wavefunction evolution shown in fig 6 10 is of such a diffuse state with an interval of 6 time steps between each plot, it is trivial for one to work out the total evolution illustrated encompasses 30 interations The kick strength, μ_q, is set equal to 1 5, about mid-way along the curves shown in fig 6 5, and the system is on resonance with $\beta = \frac{\pi}{2}$ The plots show how, after a short time, the initial well-structured state becomes more diffuse and spreads out over Q with increasing time and how the wavefunction itself is losing any structure and tending to a flat distribution across the Q axis The origin has a still somewhat high probability but even this is decreasing with increasing time and we would expect, on this evidence and trend, for the probability, $|\psi(Q)|^2$, to tend to become independent of Q (*i e* a flat distribution)

CHAPTER 7
THE WIGNER DISTRIBUTION OF THE QUANTUM MAPPING

In this chapter we derive a form for the Wigner distribution (Wigner (1932), Hillery et al (1984)) and use it to construct a quasi-phase space for the quantum mapping By using this Wigner distribution we hope to compare like with like (the observed structures in the quantum quasi-phase space with those in the classical phase space) The principle aim here is to develop a correspondence between the quantum and the classical structures with the intention of using this correspondence to argue the existence of quantum chaos

7 1 The Wigner Distribution

The effect of classical orbits *scarring* the quantum wavefunctions can be best examined using those distributions which generate a quasi phase space for the system When we use the term *scar*, we refer to the correspondence in the quantum eigenfunctions and quasi-phase space of a classical periodic orbit (Heller (1989)) By quasi we refer to the fact that trajectories as we understand them in the classical regime have no meaning in the corresponding quantum regime Therefore we use a specific form of distribution whose task is to represent the quantum wavefunction in a momentum and position space (P & Q in our case) The most widely used of this type of distribution is that attributed to Wigner (1932) He proposed a distibution, denoted $P_W(p,q)$ whose form is given by

$$P_W(q,p) = \frac{1}{\pi\hbar}\int_{-\infty}^{\infty} dy < q-y|\hat{\rho}|q+y > \exp\left(2\imath py/\hbar\right) \qquad (7\,1\,1)$$

which for a pure state, ψ, becomes (Hillery et al (1984))

$$P_W(q,p) = \frac{1}{\pi\hbar}\int_{-\infty}^{\infty} dy\psi^*(q+y)\psi(q-y)\exp\left(2\imath py/\hbar\right) \qquad (7\,1\,2)$$

To proceed with this derivation we follow the steps that Hillery et al use in their calculation of the Wigner distribution for a pure eigenstate of the harmonic oscillator (Hillery et al (1984)) The eigenstates of the harmonic oscillator are given by

$$\phi_n(q) = \left(\frac{\alpha^2}{\pi}\right)^{1/4} \left(\frac{1}{2^n n!}\right)^{1/2} \exp\left(-\alpha^2 q^2/2\right) H_n(\alpha q) \qquad (7\,1\,3)$$

where $\alpha = \sqrt{m\omega_o/\hbar}$ Therefore any time-dependent wavefunction can be expressed as a linear combination of the eigenstates

$$\psi(q,t) = \sum_{n=0}^{\infty} a_n(t)\phi_n(q) \qquad (7\,1\,4)$$

The Wigner distribution of this mixed state is thus

$$P_W(q,p) = \int_{-\infty}^{\infty} dy \exp\left(\imath 2py/\hbar\right) \psi^*\left(q+y\right) \psi\left(q-y\right) \qquad (7\,1\,5)$$

Expanding $\psi(q,t)$ (writing $a_n^*(t)$ as just a_n^* and similarly for $a_m(t)$) we get

$$P_W(q,p) = \sum_{n=0}^{\infty}\sum_{m=0}^{\infty} \frac{\alpha}{\sqrt{2^n 2^m n! m! \pi}} a_n^* a_m$$

$$\int_{-\infty}^{\infty} dy \exp\left(\imath 2py/\hbar\right) \exp\left(-\alpha^2(q^2+y^2)\right) H_n\left(\alpha(q+y)\right) H_m\left(\alpha(q-y)\right) \qquad (7\,1\,6)$$

where we have replaced the $\exp(-\alpha^2(q-y)^2/2) * \exp(-\alpha^2(q+y)^2/2)$ term arising from the $\exp(-\alpha^2 q^2/2)$ part of the eigenfunctions, $U_n(\alpha q)$, by the more compact $\exp(-\alpha^2(q^2+y^2))$ Removing all terms not dependent on y from the integral, we obtain

$$P_W(q,p) = \sum_{n=0}^{\infty}\sum_{m=0}^{\infty} \frac{\alpha \exp(-\alpha^2 q^2)}{\sqrt{2^n 2^m n! m! \pi}} a_n^* a_m$$

$$\int_{-\infty}^{\infty} dy \exp\left(\imath 2py/\hbar\right) \exp\left(-\alpha^2 y^2\right) H_n\left(\alpha(q+y)\right) H_m\left(\alpha(q-y)\right) \qquad (7\,1\,7)$$

To be consistent with the other derivations we have for the Harmonic Oscillator problem we now replace p & q with their dimensionless cousins P & Q where

$$Q = \alpha q$$

$$P = p/(\alpha\hbar)$$

and we replace y with a dimensionless form $Y = \alpha y$ so that $dY/\alpha = dy$ Our expression for $P_W(q,p)$ changes to $P_W(Q,P)$ given by

$$P_W(Q,P) = \sum_{n=0}^{\infty}\sum_{m=0}^{\infty} \frac{\exp(-Q^2)}{\sqrt{2^n 2^m n! m! \pi}} a_n^* a_m$$

$$\int_{-\infty}^{\infty} dY \exp(\iota 2PY) \exp(-Y^2) H_n(Q+Y) H_m(Q-Y) \qquad (7\,1\,8)$$

Noting that $\exp(\iota 2PY - Y^2)$ can be written as $\exp(-(Y-\iota P)^2)\exp(-P^2)$ we find that the expression for $P_W(Q,P)$ takes the form

$$P_W(Q,P) = \sum_{n=0}^{\infty}\sum_{m=0}^{\infty} \frac{\exp(-(Q^2+P^2))}{\sqrt{2^n 2^m n! m! \pi}} a_n^* a_m$$

$$\int_{-\infty}^{\infty} dY \exp(-(Y-\iota P)^2) H_n(Q+Y) H_m(Q-Y) \qquad (7\,1\,9)$$

We now define the new variable $z = Y - \iota P$ so that the $dz = dY$ The arguments inside the Hermite polynomials become $Q + z + \iota P$ instead of $Q + Y$ and $Q - z - \iota P$ instead of $Q - Y$ The argument for the H_m is thus depending negatively on the variable z so we use the identity that $H_m(-z) = (-1)^m H_m(z)$ With these two changes, noted $P_W(P,Q)$ becomes

$$P_W(Q,P) = \sum_{n=0}^{\infty}\sum_{m=0}^{\infty} \frac{\exp(-(Q^2+P^2))}{\sqrt{2^n 2^m n! m! \pi}} a_n^* a_m (-1)^m$$

$$\int_{-\infty}^{\infty} dz \exp(-z^2) H_n(z+\iota P+Q) H_m(z+\iota P-Q) \qquad (7\,1\,10)$$

We now invoke that well used (by us anyhow) identity in Gradshteyn and Ryzhik (1965) (eq 7 377 pg 838) which gives an analytical solution for the integral above with a certain restriction, namely it exists for $n \leq$m However (as will be shown later) the order in the integral can be swapped **keeping the arguments the same** (the order they appear in the integral changes but the arguments of H_m and $H_n$are the same as above) so we can obtain a solution for the case $m \leq$n Using the identity from Gradshteyn and Ryzhik (1965) we obtain the following solutions for the case $n \leq m$

$$P_W(Q,P) = \sum_{n=0}^{\infty}\sum_{m=0}^{\infty} \frac{\exp(-(Q^2+P^2))}{\sqrt{2^n 2^m n! m! \pi}} a_n^* a_m$$

$$(-1)^m 2^m \sqrt{\pi} n! (\iota P - Q)^{m-n} L_n^{m-n}(2(Q^2+P^2)) \qquad (7\,1\,11)$$

This simplifies to

$$P_W(Q,P) = \exp(-(Q^2+P^2))$$

$$\sum_{n=0}^{\infty}\sum_{m=0}^{\infty}\sqrt{\frac{2^m n!}{2^n m!}}a_n^* a_m(-1)^m(\iota P-Q)^{m-n}L_n^{m-n}\left(2(Q^2+P^2)\right) \qquad (7\,1\,12)$$

which of course has the restriction that $n \leq$m For the case $m \leq n$ we swap the order in the integral for H_n and H_m, i e

$$\int_{-\infty}^{\infty} dz \exp\left(-z^2\right) H_n\left(z+\iota P+Q\right) H_m\left(z+\iota P-Q\right) \equiv$$

$$\int_{-\infty}^{\infty} dz \exp\left(-z^2\right) H_m\left(z+\iota P-Q\right) H_n\left(z+\iota P+Q\right)$$

in our case the above holds but in general the swapping of functions within an integral like the above depends on the individual properties of the functions (or operators) being considered In this case the expression takes on the slightly different form

$$P_W(Q,P) = \exp(-(Q^2+P^2))$$

$$\sum_{n=0}^{\infty}\sum_{m=0}^{\infty}\sqrt{\frac{2^n m!}{2^m n!}}a_n^* a_m(-1)^m(\iota P+Q)^{n-m}L_m^{n-m}\left(2(Q^2+P^2)\right) \qquad (7\,1\,13)$$

which can be changed to a more comparable form for the case of $n \leq m$ by noting that the $(-1)^m(\iota P+Q)^{n-m}$ can be replaced by $(-1)^n(-\iota P-Q)^{n-m}$ Grouping all real components together and separating out and grouping those elements containing **both** real and complex parts we get for $P_W(Q,P)$

$$P_W(Q,P) = \exp(-(Q^2+P^2))$$

$$\sum_{m=0}^{\infty}\sum_{n=0}^{m}\sqrt{\frac{2^m n!}{2^n m!}}(-1)^m L_n^{m-n}\left(2(Q^2+P^2)\right)\left\{a_n^* a_m(-Q+\iota P)^{m-n}\right\} \qquad n \leq m \quad (7\,1\,14)$$

$$P_W(Q,P) = \exp(-(Q^2+P^2))$$

$$\sum_{n=0}^{\infty}\sum_{m=0}^{n}\sqrt{\frac{2^n m!}{2^m n!}}(-1)^n L_m^{n-m}\left(2(Q^2+P^2)\right)\left\{a_n^* a_m(-Q-\iota P)^{n-m}\right\} \qquad m \leq n \quad (7\,1\,15)$$

It is quite straightforward to see that when $m = n$ the two expressions are the same All terms outside the {} brackets on the R H S in both cases are equal in value when m in the first equals n in the second If we think of each element outside the {} (and exclusive of the summations) as a matrix element A_{nm} of some matrix A, i e

$$A_{n+1,m+1}(Q,P) = \exp(-(Q^2+P^2))\sqrt{\frac{2^m n!}{2^n m!}}(-1)^m L_n^{m-n}\left(2(Q^2+P^2)\right) \qquad (7\,1\,16)$$

then what we're stating here is that $A_{i,j} = A_{j,i}$ or that $A^T = A$ where T signifies transpose What follows from this is that if the pairs of elements $A_{j,i}$ and $A_{i,j}$ are summed together first, and then all these pairs added for the complete sum, then the terms in the {} brackets (for each of these pair additions) are complex conjugates of each other and the complex parts subsequently cancel leaving a real valued distribution which is one of the more important properties of Wigner distributions A proof of how these terms give rise to complex conjugates can be found in Appendix C as well as how the P and Q values in each of the four quadrants in the $2D$ position-momentum plane are related

It is also worth adding here that as the matrix A is equal to its transpose then we only have to calculate all of the elements $A_{i,j}$ on one side of the principle diagonal Thus the equation for the Wigner distribution is

$$P_W(Q,P) =$$

$$2\sum_{m=0}^{\infty}\sum_{n=m}^{\infty} A_{n+1,m+1}(Q,P) * (a(Q,P) * \gamma(Q,P) - b(Q,P) * \delta(Q,P)) \qquad (7\ 1\ 17)$$

where we have used eq $(C\ 3)$ obtained in Appendix C in substituting for the complex terms This is the expression we numerically evaluate to obtain the Wigner distribution

Most of the literature today quote using the Husimi distribution as the source of their quasi-phase space portraits (Radons & Prange (1990), Balazs (1990), Scharf & Sundaram (1991), Kuś et al (1991)) The Husimi distribution (Husimi (1940)) is a special case of the scheme proposed by Cohen (Hillery et al (1984)) for generating distribution functions Cohen proposed the use of the expression

$$P_g(q,p) = \int_{-\infty}^{\infty} dq' \int_{-\infty}^{\infty} dp' \tilde{g}(q-q', p-p') P_W(q',p') \qquad (7\ 1\ 18)$$

for calculating distributions other than the Wigner distribution One can see from the above expression that the distribution function P_W is simply *smeared* by the function $\tilde{g}$ (Hillery et al (1984)) The Husimi distribution is such that this smearing function g has a form similar to the coherent state representation used by investigators analysing systems with E-M radiation playing a major role (lasers etc) The explicit form of $\tilde{g}$ is

$$\tilde{g}(q,p,\alpha) = \frac{1}{\pi\hbar} \exp(-q^2/\alpha) \exp(-\alpha p^2/\hbar^2) \qquad (7\ 1.19)$$

which leads to a distribution P_H (H for Husimi) which is positive for all p and q The corresponding smearing function, $\tilde{g}$, for P and Q is

$$\tilde{g}(Q,P) = \frac{1}{\pi\hbar} \exp(-Q^2) \exp(-P^2) \tag{7 1 20}$$

so that the Husimi distribution becomes

$$P_H(Q,P) = \frac{1}{\pi} \int_{-\infty}^{\infty} dQ' \int_{-\infty}^{\infty} dP' \exp(-(Q-Q')^2) \exp(-(P-P')^2) P_W(Q',P') \tag{7 1 21}$$

This is all very nice on paper but implementing the above is another matter Our exact analytical expression for $P_W(Q,P)$ allows us to choose any point (Q_o, P_o) on the phase space and calculate its P_W at that point For the Husimi distribution, however, we have a problem Following a search of as many textbooks as we could find on the subject, we couldn't come up with an analytical form for eq (7 1 21) and its integrals contained within Therefore the calculation of P_W rests solely on approximating the double integral over the phase space by a crude summation over the P_W for the points we considered This is acceptable if the number of calculated P_W values is quite large but our calculated P_W consisted of a 64×64 grid over a square of side 25 Q & P units centered on $(0,0)$ So we, with the time available and the computing power at our disposal, decided to use the Wigner distribution as our guide to the quantum phase space

Now that we have our expression for P_W we will now present some of the results obtained by numerically evaluating the expression for P_W in *eq* (7 1 17) We would hope for a correspondance to exist between the regions of high probability in the quantum space and those of high densities in the classical space This *scarring* of the quantum quasi-phase space by classical orbits is considered by many to be the signature of a quantum correspondance to classical chaos

7 2 The Quasi-Phase Space

The almost overwhelming diversity of choice for the initial conditions for the quantum mapping presented us with many dilemmas up to now but this was no preparation for

the problems we faced here in evaluating the wigner distributions for the quantum phase space Each 64 × 64 grid of distribution values for one time step for a specific set of parameters took 20 hours computing time! To examine even crudely the system's behaviour at various parameter values, at specific times and for various initial states we had to make some decisions regarding the extent of our examination at various parameter values, times etc In the following sets of figures we present seven pairs of phase spaces with each pair consisting of an *image* of the phase space with the corresponding contour below it The times, parameter values and intial states are given when appropriate and the reasons for their choices also explained

Our first pair of figures show the wigner distribution, $P_W(Q,P)$ for the chosen initial pure state By *pure* we refer to a state which is made up of a single eigenfunction of the undriven system The state chosen is the 10^{th} eigenfunction (m=10) of the harmonic oscillator, i e

$$(\psi(Q))_i = u_{10}(Q) = \frac{\iota^{10}}{\sqrt{2^{10}\sqrt{\pi}(10!)}} * H_{10}(Q)exp(-\frac{1}{2}Q^2) \qquad (7\ 2\ 1)$$

where the subscript i for the ψ indicates that its corresponds to the initial state of the system The image shown in fig 7 1 shows the circularly symmetric property of a pure eigenstate of the undriven system It is interesting to compare this figure (and its proceeding companion contour plot in fig (7 2)) with the phase space for the corresponding classical system when there is an absence of the driving potential, *c f* fig (2 1) The circular orbits of the classical system are strikingly similar to the pure eigenstates of the undriven system as we would expect The Husimi distribution for a 400 × 400 grid over the phase space of the Wigner distribution, which can be obtained because a pure state Wigner distribution requires many times less calculations then a mixed state distribution, shows a single smeared orbit circling a peak at the origin This is even more like a classical orbit which is normally a single circular orbit centered on the origin whose radius is the measure of its energy (*c f* chapter 2 section 2 and chapter 3 section 2)

So as expected we have a direct correspondence between the quantum and classical system's for the undriven harmonic oscillator The question remains as to the extent of the correspondence between the two when the kicking is present and beyond a perturbation

Fig 7 1 Image of $P_W(Q,P)$ for the initial system state corresponding to the 10^{th} eigenfunction of the undriven system One can clearly see the circular symmetry for this pure state and how this symmetry will be seen to contrast with the distributions for later times

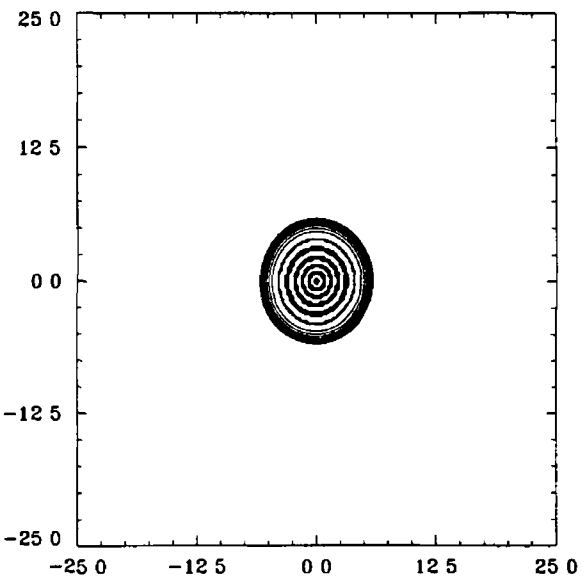

Fig 7 2 The corresponding contour plot of $P_W(Q,P)$ for the system as described for the image plot in fig (7 1) above

We make the note here that the scale used on the Q & P axes of all the following figures (both images and contours) is the same so comparisons can be made Furthermore each Wigner distribution is calculated at a specific time after the initial state The distribution is time dependent due to the time dependence of the probability amplitudes, $a_m(t)$, in constructing the wavefunctions, $\psi(Q,t)$, refer to eq (5 1 4) for the explicit definition Therefore the distribution will change in time, whether by a substantial amount or by a negligible amount depends on the system parameters and initial state Some change drastically such as the case for the on-resonance scenario with an intial pure state (compare fig (7 1) to fig (7 3)) Others change very little with the initial state's quasi-phase space being quite stable even after significant time periods (compare fig (7 11) with fig (7 13)) So we can expect the comparison of quantum to classical to be difficult but possible once the time dependence of these distributions is considered

The image and accompanying contour plot in figs 7 3 & 7 4 illustrate how the phase space has evolved from the intial state in figs 7 1 & 7 2 after a time lapse of 38 iterations of the quantum mapping for $\mu_q = 2\ 0$ In the natural time scale of the harmonic oscillator, τ_o where $\tau_o = \frac{2\pi}{\omega_o}$, this would correspond to 9 5 full period oscillations of the undriven oscillator This is so because for this resonance case the value of $\beta = \frac{\pi}{2}$ which by eq (3 1 1) makes the period between the kicks, τ, to be one-quarter the natural time period of the undriven system, τ_o The spread over first 110 eigenfunctions, (out of 350 for the matrix) used for calculating the Wigner distribution, from the initial single pure eigenstate is represented by the spreading out over the phase space and the obvious four-fold symmetry from the figures The dark regions represent higher probability areas while the light represent less probable zones There are four obvious ***islands*** surrounding the origin at 90 degree intervals which can be related back to the invariant islands of the classical phase space The regions joining such islands are probably related to the classical stochastic layer and exhibit a striking line type structure within them This could be a manifestation of the graphics package (I D L) joining regions of like probability as the number of calculated points for each of the figures presented in this chapter (except figs 7 1 & 7 2) is 6400 (an 80×80 grid) Whatever the answer is the symmetry is authentic and not a product of I D L 's management of the data

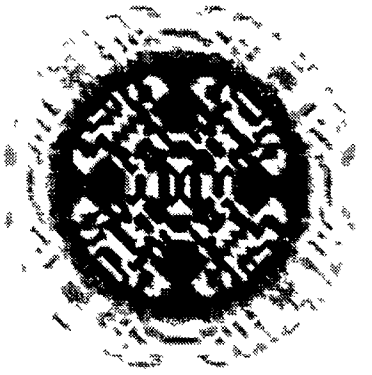

Fig 7 3 Image of $P_W(Q,P)$ for system 38 time steps after the initial state shown in figs (7 1) & (7 2) The system is on resonance with $\beta = \frac{\pi}{2}$ and $\mu_q = 2\,0$ The spreading out and 4−fold structure *scarring* the initial state is very evident

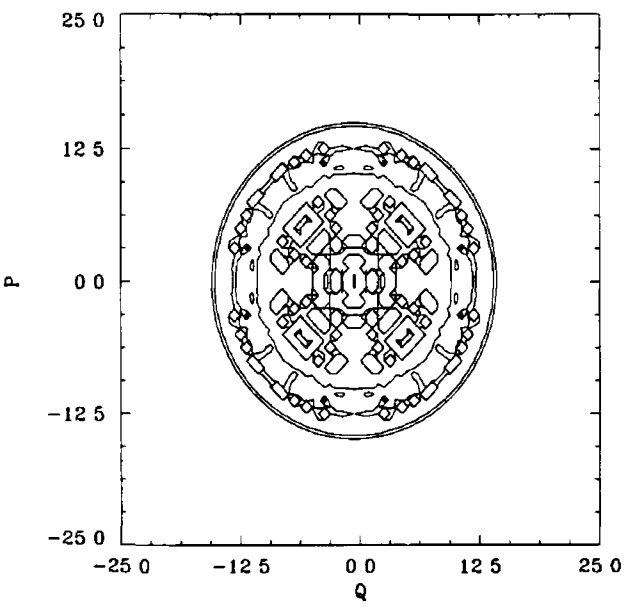

Fig 7 4 The corresponding contour plot of $P_W(Q,P)$ for the system as described for the image plot in fig (7 3) above

There is one obvious difference between the Wigner distribution illustrated in figs 7 3 & 7 4 and the resonant classical phase spaces in chapters 2 & 3 and that is the 45 degree orientation of the two w r t each other One possible reason why this could be is that the initial choice of a and $a^\dagger$ in chapter 2 relate the original basis (P & Q) to a new basis (a & $a^\dagger$) which is orientated 45 degrees to the original This could be just coincidence or, maybe, a factor in the orientation differences

The energy growth for the system with $\mu_q = 2\ 0$ and on resonance ($\beta = \frac{\pi}{2}$) is of a linear type increase similar to those shown in fig 6 5 Within a short time (around 40 interations) the spread of the initial state is such that the boundary of 350 eigenfunctions is hit and the energy curve saturates and bends over (refer to Chapter 6 sections 1 & 2) The rate of spreading can be related to the rate of increase in the energy curve with time (our quantum diffusion coefficient) and turns out to be higher than the rates plotted in fig 6 If the matrix was infinity large and we could iterate the mapping for an infinitely long time then we would expect the spread (from the trends given for the smaller matrix) to continue over all the eigenfunctions and the quasi-phase space for this case would extend over the whole $2D$ Q, P plane

Another method of checking the dynamics of the phase space, at specific points, would be to construct an asymmetric wavefunction in the Q, P plane and iterate it forward in time and examine its evolution By asymmetric, we mean a wavefunction which is not symmetric about the phase space origin like the harmonic oscillator's eigenfunctions but which is located at some point (Q, P) in the phase space and occupies some space about this point Unfortunately, to accomphsh this, we would need to know the probability amplitudes for this wavefunction and a *fourier* type expansion of the wavefunction in terms of a basis of the harmonic oscillator's eigenfunctions is required and to date we have not been able to obtain an analytical expression for the probability amplitudes of such a asymmetric wavefunction, if any exist This is one shortcoming of our technique but one which is outweighed by the importance and necessity of relating the probability amplitudes from one iteration to the next

The next pair of figures (figs 7 3 & 7 4) show the system for an off-resonance kicking The kick strength, μ_q, is kept constant at 2 0 and the number of iterations of the

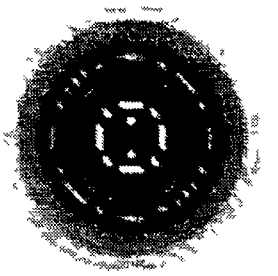

Fig 7 5 Image of $P_W(Q,P)$ for system 38 time steps after the initial state shown in figs (7 1) & (7 2) The system is off resonance this time with $\beta = \frac{(\sqrt{5}+1)\pi}{2}$ and $\mu_q = 2\ 0$ It is clear that the dominant symmetry is circular as we would expect (*cf* fig 2 4)

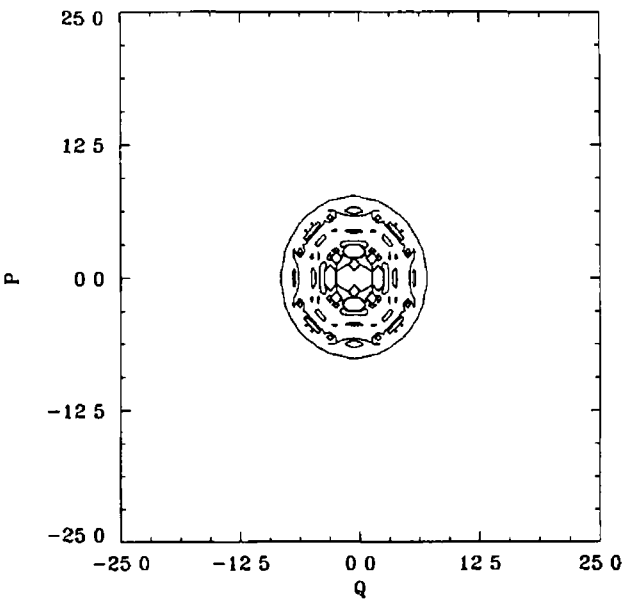

Fig 7 6 The corresponding contour plot of $P_W(Q,P)$ for the system as described for the image plot in fig (7 5) above

mapping is also the same as that for the previous pair of diagrams This is to facilitate comparisons between the off and on resonance cases For this pair the parameter β is set equal to $\frac{(\sqrt{5}+1)\pi}{2}$ which will exclude any commensurate resonance between τ, the kick period, and τ_o, the natural time period of the oscillator The differences between the Wigner distribution for this case and the distribution for the previous case in quite startling The symmetry of the distribution is definitely circular (except at the very origin which has a dumb-bell type shape) which makes it very like the off resonance classical phase space portrait in fig 2 4 The spread over the $2D$ plane is a lot less and an energy plot for this set of parameters would reveal it to saturate naturally in a manner similar to the cases shown in fig 6 7 This saturation occurs quite rapidly and the final time independent distribution is identical to that in the figure

From the last two pairs of figures the following conclusions can be made concerning the evolution of the quantum system with a pure initial state Firstly, the resonance case shows conclusively that the spreading over the eigenfunctions is significantly greater than the off resonance case The result is of this is that, secondly, the energy increase is correspondingly greater giving rise to a high diffusion coefficient for the resonance case (The off resonance case has a zero diffusion coefficient when it reaches saturation) Thirdly, the general symmetries of the quantum distributions correspond to the general forms of the classical phase space for both cases We conclude from this that correspondence between the quantum mapping and the classical one is very good and, further, that the observed energy increase on resonance, with the limited matrix size, points to possible unbounded growth in energy as we would expect in a classical phase space ensemble which includes some orbits in the stochastic layer

The success with the pure initial state prompted a further analysis with a mixed initial state The mixed state chosen is made up of a gaussian distribution of pure eigenstates and includes both even and odd parities As already mentioned previously in chapter 5 there is no interaction between odd parity states and even parity states While we expect this we have, up to now, only investigated an even pure eigenstate as our initial state so it could be argued that, without evidence to the contrary, the results for the Wigner distributions to date could be characteristic of the even states This is the reason why a

Fig 7 7 Image of $P_W(Q,P)$ for the initial state corresponding to the a gaussian distribution of the probability amplitudes centered on the 10^{th} eigenfunction of the undriven system Note the differences between this and fig (7 1)

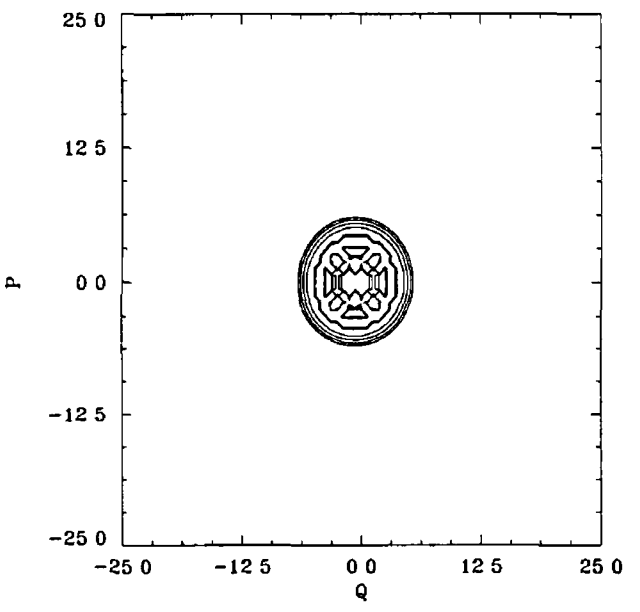

Fig 7 8 The corresponding contour plot of $P_W(Q,P)$ for the system as described for the image plot in fig (7 7) above

mixed state is now considered to allay these fears The evolution of this mixed state in time can be seen from the results presented in chapter 6 for the probability amplitudes, the energy evolution and the wavefunction evolution The initial state is identical to that chosen for the mixed state used in the chapter 6, a gaussian distribution of probability amplitudes centered on the 10^{th} eigenfunction The distribution of this initial state is illustrated in figs 7 7 & 7 8 The differences between it and the pure state in figs 7 1 & 7 2 are immediately apparent There is no obvious circular symmetry, except for the outer rim caused by the finite set of eigenfunctions, and the inner pattern is almost flower like in its form The only observable symmetry from these figures is 4−fold but the fine detail of the distribution is absent due to the restrictions placed on the size the grid of calculated points in this phase space can take In the analysis presented here all but the first pair of figures have a 80×80 grid of calculated distribution points spread over the same size section of phase space centered on the origin As a result, some of the smaller structures are absent because the grid's resolution is too course to pick them out

The result of iterating forward in time this mixed initial state when the kick strength, μ_q, is 1 5 and the parameter β is $\frac{\pi}{2}$ can be seen in figs 7 9 & 7 10 The time interval from initial state to the state shown is 20 iterations of the mapping (equivalent to 5 full periods of oscillation of the undriven oscillator as β, with its present value, gives a 1 4 ratio between τ_o and τ The similarity to the on resonance case for a pure even initial state is obvious with the four *islands* being more prominent than for the previous case in fig 7 3 Furthermore, as we shall highlight later in fig 7 13, there is evidence in fig 7 9 that four more islands could be present each situated on the corners of the sides the prominent islands make up Only half of these new islands exist but their presence would point to a possible continued (or extended) 4−fold structure in this quantum distribution The contour plot, in fig 7 10, too shows a half island type structure but it is not as clear as the image plot in fig 7 9 Thus we have some evidence to suggest a quantum periodic tiled structure existing in the Wigner distribution of the system of the order of the resonance we're considering

The absolute test would be to construct a very large evolution matrix (say 5000×5000) and check to see how far with this matrix this extended structure continues into the

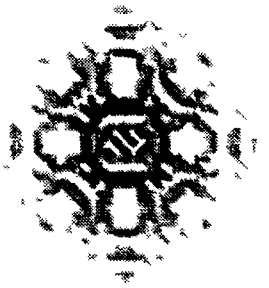

Fig 7 9 Image of $P_W(Q,P)$ for system 20 time steps after the initial state shown in figs (7 5) & (7 6) The system is on resonance with $\beta = \frac{\pi}{2}$ and $\mu_q = 1\ 5$ Some of the structure seen in figs 7 3 & 7 4 is not as clear but the dominant 4−fold symmetry is still very evident

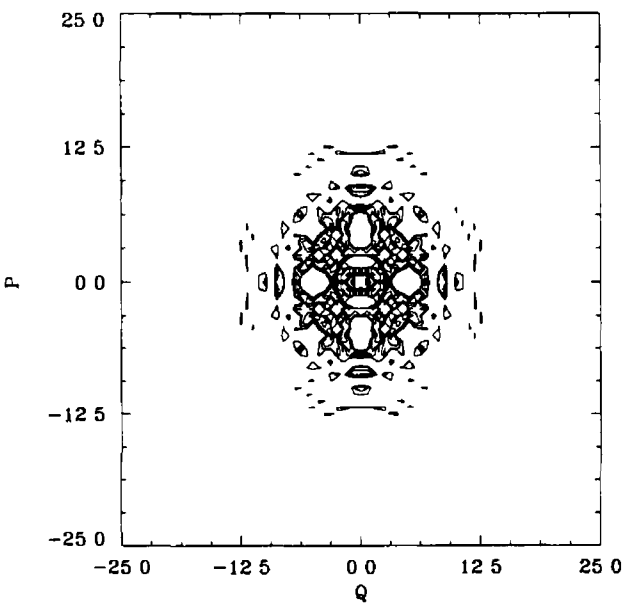

Fig 7 10 The corresponding contour plot of $P_W(Q,P)$ for the system as described for the image plot in fig (7 9) above

quantum *quasi* phase space At present this is beyond the computing and software limits available to us but with more powerful computers and a more efficient link to Mathematica to generate the Laguerre polynomials we should be capable of exploring the phase space more thoroughly and probing this apparent 4−fold structure

Serendipity in science is quite common and indeed we found something by accident which highlights the extended structure we have just mentioned The original distributions we obtained had a beautiful tiled structure up to the limit of the eigenfunctions extent in the phase space This structure was taken by us to be the proof we needed of a quantum like tiled phase space until we discovered the wrong file was used by the program The stunning similarity between these *results* and the classical phase space plagued us so much that we decided to incorporate the tiled structure as an initial condition and iterate the map forward, properly this time, and observe the evolution of the structure The next two pairs of figures show the initial state and then the result after 2000 iterations of the mapping The stability of the pattern is startling and leads us to beheve that the preferred distribution is close to that in the images in figs 7 11 & 7 13 So the mistake made initially has paid dividends in that it has highlighted the existence of an extended tiled structure, which appears quite stable, in the quantum quasi-phase space

We end our examination of the quantum phase space by highlighting the correspondence between the qauntum and classical and by briefly mentioning further improvements and research directions The correspondence can be considered quite strong between the quantum system and the classical The on resonance and off resonance cases yield phase spaces in both regimes which are definitely related The only *minus* is the rotation factor mentioned but a change of basis negates this The possible existence and stability of the extended tiled structure in the Wigner distribution for the resonance case when $\beta = \frac{\pi}{2}$ suggests that such a structure is a preferred by the system over others and that if the matrix was larger than its current 350×350 then we could possibly explore this more thoroughly As for future directions, a more detailed look at the finer structure of the Wigner distribution to check for further correspondences between the classical and quantum cases and an attempt to confirm, using large evolution matrices, the unboundedness of certain on resonance scenarios These results, though important, are only illuminating

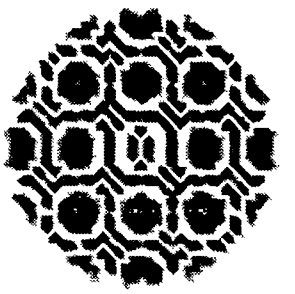

Fig 7 11 Image of $P_W(Q,P)$ for the initial state corresponding to the ***diffuse*** distribution of the probability amplitudes as discussed in the text Note the distinctive tiled structure and the close relationship between this type of pattern and the classical phase space tiled structure

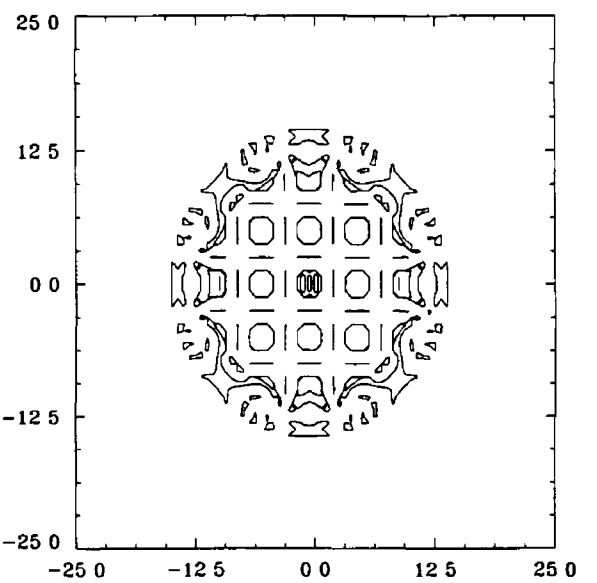

Fig 7 12 The corresponding contour plot of $P_W(Q,P)$ for the system as described for the image plot in fig (7 11) above

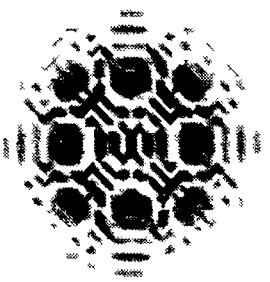

Fig 7 13 Image of $P_W(Q,P)$ for system 2000 time steps after the initial state shown in figs (7 11) The system is on resonance with $\beta = \frac{\pi}{2}$ and $\mu_q = 1\ 5$ The stability of the tiled pattern is evident from this images and contour plot below

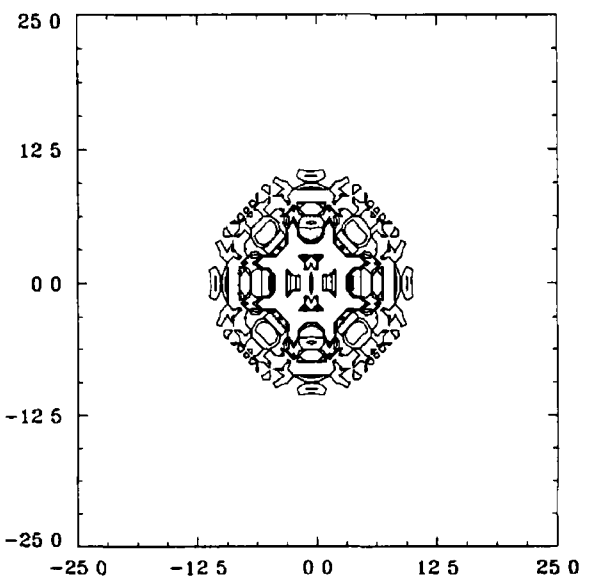

Fig 7 14 The corresponding contour plot of $P_W(Q,P)$ for the system as described for the image plot in fig (7 13) above.

a very small region of what could turn out to be a very rich and beautiful area of quantum mechanics

CHAPTER 8
CONCLUSIONS

The conclusions that can be drawn from the work presented in this thesis are many as are the number of routes further work can be persued The Harmonic Oscillator was chosen primarily because it is one of the most fundamental physical systems and not a mathematically-inspired mapping, such as the piecewise-linear standard map of Scharf & Sundaram (1991) Though some conclusions can be drawn from such unphysical systems they cannot be attributed as purely physical phenomena as such systems are physically unreal The harmonic oscillator is not and as such is an ideal candidate for analysis

In our classical analysis of the system's phase space we showed how the stochastic layer is the principle mechanism behind the diffuse transport and unbounded energy growth of certain orbits which he within the layer itself The principle directions of transport illustrated in fig 3 1 show the diffusing of orbits along the (stable and unstable) manifolds of the period four hyperbolic points whose separatrix net is the layer itself for infinitesimal kicking We have have found for the kicked oscillator, at resonance, that the existence of periodic orbits in or around the stochastic layer influences the breakup of the invariant orbits as would be expected from the K A M theorem As a result of this breakup, the boundary of the layer becomes increasingly complicated as the kick strength is increased Our analysis allows us to predict which resonances and hence which periodic orbits should be present in the system's phase space by means of a function obtained via a polynomial expansion of the kicking term The correlation between prediction and numerical results was found to be very good despite the practical problems in numerically locating complete sets of periodic orbits We further showed that the elliptic fixed points of period four at the center of the main invariant islands become hyperbolic for a kick strength of 10 0 causing these islands to break in two for kick strengths above 10 0 (*c f* table 3 1 & fig 3 2) This result holds the key to our quantum analysis, that being the origin becoming unstable above a certain kick strength allowing diffuse orbits to exist close to it for reasonable kick strengths Therefore we can analyse the quantum mapping using low order eigenfunctions knowing that if there is a correspondence between the quantum and classical we should be

able to observe diffuse type wavefunctions for reasonable kicking We do in fact see this and therefore can conclude the two limits do have a direct correspondence

The detailed study of the evolution of the stochastic layer as the kick strength is increased is of fundamental importance as it enables us to see the effect of increasing non-integrability on the system at large The most striking change in the layer is its variation in width with kick strength, which we studied in detail and compared to that predicted by perturbative analytical arguments (Chernikov et al 1989) We found that the width of the layer as a function of the kicking strength follows an exponential variation of the form ue^{-u}, where $u = 1/(\text{kick strength})$ This is the form predicted by Chernikov et al (1989) for kick strengths $\ll 1$ We find that this result is true for a range of kick strengths considerably in excess of the theoretical prediction This validity is surprising when one considers the increased complexity of the layer itself and the overall increase m structure at the layer boundary with increased kicking

The diffusion in the classical regime, analysed in chapter 4 based on the argument of Rechester & White (1980), was found to correspond exactly with that for the kicked rotator and this correspondence was put down to the dominance of the turbulent motion over the invariant periodic & restricted motion in the cells (refer to table 4 1 in chapter 4) This is important because such similarity, when the turbulent motion is dominant, is evidently generic of all one-dimensional hamiltonian systems when the kicking term is cosinusoidal Furthermore, the lower asymptotic limit was found to be identical to that found by Lichtenberg and Wood (1989) who constructed an approximate theory of diffusion on the stochastic web which is valid in the small μ_{cl} region Our results on the Resonance Enhanced Diffusion are unique in that no-one has yet shown the spikes in the diffusion coefficient to exist for the kicked harmonic oscillator (Ishizaki et al (1989) showed this diffusion to exist for the kicked rotator) or explicitly shown them to vary as the phase space's periodicity changes Our argument for this anomalous diffusion is based on strong correlations between successive points and follows on logically from the arguments of Rechester & White The main conclusion to be drawn from this diffusion analysis is that correlations do exist for reasonable kick strengths but *normally* die off when the kick strength tends to infinity However the anomalous diffusion has strong correlations

regardless of how strong the kick stength is once it equals a positive integer times the system's phase space

The quantum mapping we derived has not been, to our knowledge, used before Furthermore the approach we use, to obtain this mapping, based on the approach of Fox et al (1990 & 1994) has not been applied to this system either The approach is quite simple and was chosen for its directness, that of relating the probability amplitudes for successive kicks The success of this approach can be gauged from our ability to calculate energies, quasi-energy levels as well as wavefunctions and Wigner distributions From our analysis of the system we have been able to make some interesting conclusions about the quantum system We have seen certain states naturally saturate giving rise to quasi energy levels (Israilev 1990) in the kicked system The corresponding localisation in the wavefunction has also been examined and prominent peaks found to exist in these local states For larger kick strengths the wavefunctions spread out with an increasing rapidity with kick strength and their energy increase was found to be quite linear (up to the point they hit the boundary imposed by the finite matrix size) We used this linearity to calculate a quantum diffusion coefficient and found it to have a definite non linear form In fact we found the power-law to be of the form $0\ 2(\mu_q)^{4\ 7}$ The wavefunctions for these kick strengths were found to be quite diffuse with little structure on them except for a gradual fall off Q tends to ∞ (caused by the finite number of eigenfunctions used) We conclude from these latter results that the energy saturation is definitely artificial (caused by the finite matrix size) and that the energy was increasing linearly in a seemingly unbounded fashion and not following the nature of the suppresion of chaos in the kicked rotator

The Wigner distribution for the quantum phase space can be seen to have a definite four-fold symmetry when the system is on resonance ($\beta = \frac{\pi}{2}$) and, for a similar initial state and kick strength, the resonance case is more spread out and definitely of higher energy than its off resonance cousin The off resonance case also has a more circularly symmetric nature about it than the resonance case These point to a definite correspondence between the classical case (the off resonant & resonant phase space structures visible in chapter 2) and the quantum case (the Wigner distributions in chapter 7) Furthermore we observed from an mixed initial state, at a kick strength of 1 5, that the resonant structure formed

is very close to the tiled structure we used to test for the existence of a stable extended tiled structure (*re* figs 7 11 – 7 14) We found that this mixed initial state, at that kick strength, became diffuse as time evoloved (as shown in chapter 6) This, coupled with the similarity to the extended tiled structure, is indicative of continuing diffusion of this wavefunction over the phase space Our reasoning is quite simple, such an extended structure bears a striking resemblence to the classical tiled phase space structure and, as the wavefunction is spreading out without any indication of saturation, we conclude that this is proof that the system is behaving as if it has a quantum analog to the classical stochastic layer Therefore we conclude the existence of quantum chaos in this system as the quantum regime has wavefunctions which, from the results presented in chapters 6 & 7, mimic classical ensembles which have elements in the stochastic layer It is using ensembles like this that the classical phase space is constructed and to have quantum wavefunctions construct a tiled structure so close is proof that some correspondence exists between the dynamics of both limits

We have accomplished our main objective, that of showing the existence of quantum chaos in the kicked harmonic oscillator The research undertaken here has brought to light many unknowns about the system itself and we have also highlighted some of the ways in which future research on this system can proceed The kicked harmonic oscillator is a truly physical system, one whose properties should more fully increase our knowledge on this fledgling area of quantum chaos

APPENDIX A
EXPLICIT FORMULATION OF THE POTENTIAL TERM

The form of the equation that we have chosen for the potential is $V(p,q) = \mu_q(\cos(kq))$ (after Berman et al. (Berman et al. (1989)). This term is in effect the non-linearity in the system Hamiltonian and as such makes the integrable oscillator equations non-integrable. The degree of non-linearity depends on how many terms in the series expansion of $\cos(x)$ are required to accurately describe the potential term. As is well known, the larger the argument present in the cosine then the higher the number of terms needed to be accurate. Using the cosine series expansion we will show how the potential term in eq. (2.1.15) is arrived at. From the definitions in eqs. (2.1.3) and (2.1.4), for the operators $a(t)$ and $a^\dagger(t)$, we have for $q(t)$

$$q(t) = \frac{1}{\iota}\sqrt{\frac{\hbar}{2M\omega_0}}(a^\dagger(t) - a(t)) \tag{A.1}$$

So our equation for the potential becomes

$$V(a,a^\dagger) = \mu_q\left(\cos\left(\tfrac{k}{\iota}\sqrt{\hbar/(2M\omega_0)}(a^\dagger(t) - a(t))\right)\right) \tag{A.2}$$

For convenience we define K to be $(k\sqrt{\hbar/(2M\omega_0)})$. We show in chapter 2 how the $\hbar$ dependence is removed from K. Thus eq.(A.2) is simplified to

$$V(a,a^\dagger) = \mu_q\left(\cos\left(\tfrac{K}{\iota}(a^\dagger(t) - a(t))\right)\right) \tag{A.3}$$

To proceed further we have to change the compound argument of the cosine into simpler arguments of cosines and sine. This we accomplish using the well known trigonometric identity:

$$\text{Cos}(A - B) = \text{Cos(A)Cos}(B)+\text{Sin(A)Sin(B)}$$

Eq.(A.3) now becomes:

$$V(a,a^\dagger) = \mu_q\left(\cos\left(\tfrac{K}{\iota}a^\dagger(t)\right)\cos\left(\tfrac{K}{\iota}a(t)\right) + \sin\left(\tfrac{K}{\iota}a^\dagger(t)\right)\sin\left(\tfrac{K}{\iota}a(t)\right)\right) \tag{A.4}$$

We do not have any explicit rules for the commutation of a and $a^\dagger$with trigonometric functions whose arguments are either a or $a^\dagger$. To allow the commutation to proceed we

find it necessary to express the sines and cosines in terms of their series expansions These series expansions, for the sine and cosine functions, are well known and for our arguments break down to

$$\cos\left(\tfrac{K}{\iota}a^{\dagger}(t)\right)=\sum_{n=0}^{\infty}\frac{(-1)^{n}(K/\iota)^{2n}}{(2n)!}\left(a^{\dagger}(t)\right)^{2n} \qquad (A\ 5a)$$

$$\sin\left(\tfrac{K}{\iota}a^{\dagger}(t)\right)=\sum_{n=0}^{\infty}\frac{(-1)^{n}(K/\iota)^{2n+1}}{(2n+1)!}\left(a^{\dagger}(t)\right)^{2n+1} \qquad (A\ 5b)$$

So when expressed in this series form eq $(A\ 6)$ takes on the formidable but more useful appearance

$$V(a,a^{\dagger})=\mu_{q}\left\{\sum_{n=0}^{\infty}\frac{(-1)^{n}(K/\iota)^{2n}}{(2n)!}\left(a^{\dagger}(t)\right)^{2n}\sum_{n=0}^{\infty}\frac{(-1)^{n}(K/\iota)^{2n}}{(2n)!}\left(a(t)\right)^{2n}\right\}$$

$$+\mu_{q}\left\{\sum_{n=0}^{\infty}\frac{(-1)^{n}(K/\iota)^{2n+1}}{(2n+1)!}\left(a^{\dagger}(t)\right)^{2n+1}\sum_{n=0}^{\infty}\frac{(-1)^{n}(K/\iota)^{2n+1}}{(2n+1)!}\left(a(t)\right)^{2n+1}\right\} \qquad (A\ 6)$$

The next task is to commute this with $a(t)$ for the explicit form of $-\iota\left(a,V(a,a^{\dagger})\right)$ Eqs $(2\ 1\ 8a-d)$ will be put to good use here to simplify the equations immensely For the cosine terms we have a commutation of the form

$$\left(a(t),\sum_{n=0}^{\infty}(a^{\dagger}(t))^{2n}\sum_{n=0}^{\infty}\left(a(t)\right)^{2n}\right)$$

$$=\left(a(t),\textstyle\sum_{n=0}^{\infty}(a^{\dagger}(t))^{2n}\right)\displaystyle\sum_{n=0}^{\infty}\left(a(t)\right)^{2n}+\left(a(t),\textstyle\sum_{n=0}^{\infty}\left(a(t)\right)^{2n}\right)\displaystyle\sum_{n=0}^{\infty}(a^{\dagger}(t))^{2n} \qquad (A\ 7)$$

using the relation in eq $(2\ 1\ 8c)$ Taking the summation after the commutation makes no difference so for the first half of the right hand side in eq $(A\ 7)$ we have

$$\left(a(t),\textstyle\sum_{n=0}^{\infty}\left(a^{\dagger}(t)\right)^{2n}\right)\displaystyle\sum_{n=0}^{\infty}\left(a(t)\right)^{2n}\equiv\sum_{n=0}^{\infty}\left(a(t),\left(a^{\dagger}(t)\right)^{2n}\right)\sum_{n=0}^{\infty}\left(a(t)\right)^{2n} \qquad (A\ 8)$$

whereas for the latter half we get

$$\left(a(t),\textstyle\sum_{n=0}^{\infty}\left(a(t)\right)^{2n}\right)\displaystyle\sum_{n=0}^{\infty}\left(a^{\dagger}(t)\right)^{2n}\equiv\sum_{n=0}^{\infty}\left(a(t),\left(a(t)\right)^{2n}\right)\sum_{n=0}^{\infty}\left(a^{\dagger}(t)\right)^{2n} \qquad (A.9)$$

The parts to be commuted with $a(t)$ consist now of an operator to the power of 2n There is one problem, however, and that is the $n = 0$ term of the summation This gives $(a(t), 1)$ which is zero So the summation should be performed from $n = 1$ to $n = \infty$ with the $n = 0$ term separate Noting that, using eq (2 1 8d), $(A, B^{2n}) = 2n (A, B) B^{2n-1}$ we get for eq (A 8)

$$(a(t), \sum_{n=0}^{\infty} (a^{\dagger}(t))^{2n}) \sum_{n=0}^{\infty} (a(t))^{2n} \equiv \sum_{n=1}^{\infty} 2n (a^{\dagger}(t))^{2n-1} \sum_{n=0}^{\infty} (a(t))^{2n} \qquad (A\ 10)$$

for eq (A 9) the story is different because $a(t)$ commutes with itself so that $(a(t), (a(t))^{2n})$ $\equiv 2n (a(t), a(t)) a(t)^{2n-1} \equiv 2n * 0 * a(t)^{2n-1} \equiv 0$ So substituting these identities into eq (A 7) we get

$$(a(t), \sum_{n=0}^{\infty} (a^{\dagger}(t))^{2n} * \sum_{n=0}^{\infty} (a(t))^{2n}) = \sum_{n=1}^{\infty} 2n (a^{\dagger}(t))^{2n-1} \sum_{n=0}^{8} (a(t))^{2n} \qquad (A\ 11)$$

So the complete cosine term from eq (A 6) becomes

$$\sum_{n=1}^{\infty} \frac{(-1)^n (K/\iota)^{2n}}{(2n)!} 2n (a^{\dagger}(t))^{2n-1} * \sum_{n=0}^{\infty} \frac{(-1)^n (K/\iota)^{2n}}{(2n)!} (a(t))^{2n} \qquad (A\ 12)$$

The summation from 1 to ∞ presents no problem as by introducing a new dummy variable $u = n - 1$ we get

$$\sum_{n=1}^{\infty} \frac{(-1)^n (K/\iota)^{2n}}{(2n)!} 2n (a^{\dagger}(t))^{2n-1} \rightarrow -\frac{K}{\iota} \sum_{u=0}^{\infty} \frac{(-1)^u (K/\iota)^{2u+1}}{(2u+1)!} (a^{\dagger}(t))^{2u+1} \qquad (A\ 13)$$

which is just $-\frac{K}{\iota} \sin (\frac{K}{\iota} a^{\dagger}(t))$ So the $\cos (\frac{K}{\iota} (a^{\dagger}(t))) \cos (\frac{K}{\iota} (a(t)))$ term becomes $-\frac{K}{\iota} \sin (\frac{K}{\iota} (a^{\dagger}(t))) \cos (\frac{K}{\iota} (a(t)))$ following the commutation with $a(t)$

For the sine terms we have a similar argument with the commutation being of the form given below in eq (14)

$$(a(t), \sum_{n=0}^{\infty} (a^{\dagger}(t))^{2n+1} * \sum_{n=0}^{\infty} (a(t))^{2n+1}) =$$

$$(a(t), \sum_{n=0}^{\infty} (a^{\dagger}(t))^{2n+1}) \sum_{n=0}^{\infty} (a(t))^{2n+1} + (a(t), \sum_{n=0}^{\infty} (a(t))^{2n+1}) \sum_{n=0}^{\infty} (a^{\dagger}(t))^{2n+1} \qquad (A\ 14)$$

Taking the approach we used for the cosine terms we get

$$\left(a(t), \sum_{n=0}^{\infty}\left(a^{\dagger}(t)\right)^{2n+1} * \sum_{n=0}^{\infty}\left(a(t)\right)^{2n+1}\right) = \sum_{n=0}^{\infty}(2n+1)\left(a^{\dagger}(t)\right)^{2n} \sum_{n=0}^{\infty}\left(a(t)\right)^{2n+1} \tag{A 15}$$

The term modified $(a^{\dagger}(t))$ by the commutation with $a(t)$ affects the total sine sum as follows

$$\sum_{n=0}^{\infty} \frac{(-1)^n (K/\iota)^{2n+1}}{(2n+1)!}(2n+1)\left(a^{\dagger}(t)\right)^{2n} \rightarrow \frac{K}{\iota}\sum_{n=0}^{\infty} \frac{(-1)^n (K/\iota)^{2n}}{(2n)!}\left(a^{\dagger}(t)\right)^{2n} \tag{A 16}$$

which is just $\frac{K}{\iota}\cos\left(\frac{K}{\iota}a^{\dagger}(t)\right)$ Thus the term, $\sin\left(\frac{K}{\iota}\left(a^{\dagger}(t)\right)\right)\sin\left(\frac{K}{\iota}\left(a(t)\right)\right)$, becomes $\frac{K}{\iota}\cos\left(\frac{K}{\iota}\left(a^{\dagger}(t)\right)\right)\sin\left(\frac{K}{\iota}\left(a(t)\right)\right)$ after the commutation

So we have now obtained expressions for both the cosine product term and the sine product term after commuting with $a(t)$ What remains now is to combine these results to obtain an expression for the potential after commutation (i e the term $f(a, a^{\dagger})$) We find that, in its final form , the potential term satisfies

$$-\iota\left(a(t), V\left(a(t), a^{\dagger}(t)\right)\right)$$
$$= \mu_q\left\{K\sin\left(\frac{K}{\iota}\left(a^{\dagger}(t)\right)\right)\cos\left(\frac{K}{\iota}\left(a(t)\right)\right) - K\cos\left(\frac{K}{\iota}\left(a^{\dagger}(t)\right)\right)\sin\left(\frac{K}{\iota}\left(a(t)\right)\right)\right\}$$

or more succintly

$$f(a(t), a^{\dagger}(t)) = -\iota\left(a(t), V\left(a(t), a^{\dagger}(t)\right)\right) = \mu_q\left\{K\left(\sin\left(\frac{K}{\iota}\left(a^{\dagger}(t) - a(t)\right)\right)\right)\right\} \tag{A 17}$$

This is the substitution we make for $f(a, a^{\dagger})$ in chapter 2

APPENDIX B
THE ANNIHILATION & CREATION OPERATORS

In eqs (5 1 7) and (5 1 8) we defined the a & $a^\dagger$ operators in terms of Q and $\frac{d}{dQ}(\equiv P)$ The eigenfunctions of the hamiltonian can be found without using the operator technique, previously, by explicitly solving the differential equation with trial solutions This way the solutions found are identical to those found using the more direct operator approach The eigenfunctions found $u_n(Q)$ have the form

$$u_n(Q) = \frac{1}{\sqrt{2^n\sqrt{\pi}(n!)}}\left(Q - \tfrac{d}{dQ}\right)^n \exp\left(-\tfrac{1}{2}Q^2\right) \qquad (B\ 1)$$

where $u_o(Q) = \frac{1}{\sqrt{\sqrt{\pi}}}\exp\left(-\frac{1}{2}Q^2\right)$ and $u_1(Q) = \frac{1}{\sqrt{2}}\left(Q - \frac{d}{dQ}\right)u_o(Q) \equiv a^\dagger u_o(Q)$ Likewise it can be shown that for any n

$u_{n+1}(Q) =$

$$\frac{1}{\sqrt{2^{n+1}\sqrt{\pi}((n+1)!)}}\left(Q - \tfrac{d}{dQ}\right)^{n+1}\exp\left(-\tfrac{1}{2}Q^2\right) = \frac{1}{\sqrt{(n+1)2}}\left(Q - \tfrac{d}{dQ}\right)u_n(Q) \qquad (B\ 2)$$

thus

$$u_{n+1}(Q) \equiv \frac{1}{\sqrt{n+1}}a^\dagger u_n(Q) \qquad or \qquad \sqrt{n+1}u_{n+1}(Q) \equiv a^\dagger u_n(Q) \qquad (B\ 3)$$

The annihilation operator $a = \frac{1}{\sqrt{2}}\left(\frac{d}{dQ} + Q\right)$ does the opposite of the $a^\dagger$ operator by taking a polynomial of order n down to a polynomial of order $n-1$ with a $\sqrt{n}$ coefficient How this comes about is by looking at the commutation properties of a and $a^\dagger$, i e

$$\left(a, a^\dagger\right) = aa^\dagger - a^\dagger a = 1$$

so that if we operate on u_n then

$$\left(a, a^\dagger\right)u_n(Q) = aa^\dagger u_n(Q) - a^\dagger a u_n(Q) = u_n(Q) \qquad (B\ 4)$$

Hence $\sqrt{n+1} * au_{n+1}(Q) - a^\dagger a u_n(Q) = u_n(Q)$ Assuming the operator a changes $u_n(Q)$ to $\sqrt{n+r}u_{n+p}(Q)$ then we have that

$$\sqrt{n+1}\sqrt{n+1+r}u_{n+p+1}(Q) - \sqrt{n+r}\sqrt{n+p+1}u_{n+p+1}(Q) = u_n(Q) \qquad (B\,5)$$

As the $u_n(Q)$ form an othogonal basis then $n+p+1 = n \Leftrightarrow p = -1$ Furthermore $\sqrt{n+1}\sqrt{n+1+r} - \sqrt{n+r}\sqrt{n+p+1} = 1 \quad n+p+1 = n$ so $\sqrt{n+1}\sqrt{n+1+r} - \sqrt{n+r}\sqrt{n} = 1 \Leftrightarrow r = 0$ Thus $au_n(Q) = \sqrt{n}u_{n-1}(Q)$ as stated earlier in this section

This ends our brief justification of the a & $a^\dagger$ definitions Though not very elegant, this justification serves for me as a way to visualise how these operators manipulate eigenfunctions of the quantum system

APPENDIX C
SIMPLIFICATION OF THE COMPLEX TERM IN $P_W(Q,P)$

Here we want to simplify the complex terms contained within the {} brackets in eqs (6 2 14-15) so that we can show the Wigner distribution, $P_W(Q,P)$, to be real valued (if not always positive) To do this we shall split the complex term into two parts the first will be the product $a_n^* a_m$ while the second will deal with the $(-Q+\imath P)^{m-n}$ term

Let the complex probability amplitude $a_k = a_k^{(r)} + \imath a_k^{(im)}$ then the expression for $a_n^* a_m$ becomes

$$a_n^* a_m = \left(a_n^{(r)} a_m^{(r)} + a_n^{(im)} a_m^{(im)}\right) + \imath\left(a_n^{(r)} a_m^{(im)} - {}_n^{(im)}\, a_m^{(r)} a\right) \equiv \alpha + \imath\beta \qquad (C\,1)$$

For the case when m and n are interchanged we get $\alpha - \imath\beta$ Furthermore for any complex number z taken to the power m we find that it still has a complex conjugate relationship to its complex conjugate taken to the same power

$(x+\imath y)^n =$

$$x^n + \imath n x^{n-1} y + (\imath)^2 \binom{n}{2} x^{n-2} y^2 + \quad + (\imath)^{n-2} \binom{n}{2} x^2 y^{n-2} + (\imath)^{n-1} n x y^{n-1} + (\imath y)^n \quad (C\,2a)$$

and

$(x-\imath y)^n =$

$$x^n - \imath n x^{n-1} y + (-\imath)^2 \binom{n}{2} x^{n-2} y^2 + \quad + (-\imath)^{n-2} \binom{n}{2} x^2 y^{n-2} + (-\imath)^{n-1} n x y^{n-1} + (-\imath y)^n \quad (C\,2b)$$

As $(\imath)^{2m}$ is equal to $(-\imath)^{2m}$ $\forall m \in \mathbf{Z}$ and $(\imath)^{2m+1} = -(-\imath)^{2m+1}$ again for $m \in \mathbf{Z}$ then the above two equations give a real part which is identical but imaginary parts which are the negative of each other thus making $(x-\imath y)^n$ the complex conjugate of $(x+\imath y)^n$ Therefore $(-Q+\imath P)^{m-n}$ is complex conjugate to $(-Q-\imath P)^{m-n}$ or, in our case when m and n are interchanged, $(-Q-\imath P)^{n-m}$ Therfore we have the sum of the product of two complex number with the product of their complex conjugates below $a_n^* a_m$ is denoted $(a+\imath b)$ and $(-Q+\imath P)^{m-n}$ is replaced by $(\gamma+\imath\delta)$ so that the complete complex term, $a_n^* a_m (-Q+\imath P)^{m-n}$, is

$$a_n^* a_m(-Q+\imath P)^{m-n} = (a+\imath b)(c+\imath d) \qquad (C\,3)$$

$$(a+\imath b)(\gamma+\imath\delta) = (a\gamma - b\delta) + \imath(b\gamma + a\delta)$$
$$(a-\imath b)(\gamma-\imath\delta) = (a\gamma - b\delta) - \imath(b\gamma + a\delta)$$

which when summed gives a real number, $2(a\gamma - b\delta)$ Thus the distribution is real
To numerically evaluate the equation(s) leading to the Wigner distribution would require an immense amount of computing power so any *tricks* to reduce this cost in time would be welcome The phase space of P & Q is split into four quadrants but here we shall restrict our argument to just two of them (1 and 3) and then apply the results to the other two (we can do this because any point (a,b) in the quadrant 1 is just $(-1)(a,b)$ in 3 and likewise for 2 and 4)

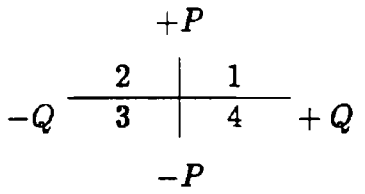

Schematic of the four quadrants constituting the phase space

The distributions for the respective quadrants are

$$P_W^1(Q,P) = \sum_{m=0}^{\infty}\sum_{n=0}^{m} A_{n+1,m+1}\left\{a_n^* a_m(-Q+\imath P)^{m-n}\right\} \qquad n \le m \qquad (C\,4a)$$

$$P_W^1(Q,P) = \sum_{n=0}^{\infty}\sum_{m=0}^{n} A_{n+1,m+1}\left\{a_n^* a_m(-Q-\imath P)^{n-m}\right\} \qquad m \le n \qquad (C\,4b)$$

for quadrant 1 (note the superscript 1 on $P_W(Q,P)$ and

$$P_W^3(Q,P) = \sum_{m=0}^{\infty}\sum_{n=0}^{m}(-1)^{m-n} A_{n+1,m+1}\left\{a_n^* a_m(-Q+\imath P)^{m-n}\right\} \qquad n \le m \qquad (C\,4c)$$

$$P_W^3(Q,P) = \sum_{n=0}^{\infty}\sum_{m=0}^{n}(-1)^{n-m} A_{n+1,m+1}\left\{a_n^* a_m(-Q-\imath P)^{n-m}\right\} \qquad m \le n \qquad (C\,4d)$$

for quadrant 3 where we have defined $A_{n+1,m+1}$ to be the matrix element

$$\exp(-(Q^2+P^2))(-1)^m\sqrt{\frac{2^m n!}{2^n m!}}L_n^{m-n}\left(2(Q^2+P^2)\right) \qquad n \leq m$$

or

$$\exp(-(Q^2+P^2))(-1)^n\sqrt{\frac{2^n m!}{2^m n!}}L_m^{n-m}\left(2(Q^2+P^2)\right) \qquad m \leq n$$

It is clear from eqns $(C\ 4\ a-d)$ that for $m-n$ $(n \leq m)$ even, the terms in the third quadrant equal that in the first whereas for $m-n$ odd the terms are of equal magnitude but opposite signs The same is true for $n-m$ when $m \leq n$ To illustrate things lets restrict m and n to values less than 4 The matrices would be as follows

$$\begin{pmatrix} A_{11} & A_{12} & A_{13} & A_{14} \\ A_{12} & A_{22} & A_{23} & A_{24} \\ A_{13} & A_{23} & A_{33} & A_{34} \\ A_{14} & A_{24} & A_{34} & A_{44} \end{pmatrix} \text{ for quadrant 1} \qquad \begin{pmatrix} A_{11} & -A_{12} & A_{13} & -A_{14} \\ -A_{12} & A_{22} & -A_{23} & A_{24} \\ A_{13} & -A_{32} & A_{33} & -A_{34} \\ -A_{14} & A_{24} & -A_{34} & A_{44} \end{pmatrix} \text{ for quadrant 3}$$

In general these two matrices are very different however we will now show that if we restrict the initial condition to a PURE eigenstate then the matrices for both quandrants one and three are the same To see this refer back to chapter 5 where we derive the quantum mapping In eq (5 1 31), we show that there is included in the expression for $A_m((N+1)\tau)$, a term contained within $\{\}$ which forces the expression to zero if $p-m$ is odd Therefore if the initial state is a *pure odd* numbered state then, m order for $p-m$ to be even, only odd states exist in the resulting system (similarly if we begin with a *pure even* numbered state) Thus we end up in eqs $(C\ 4c-d)$ with the same expression for P_W as we have in eqs $(C\ 4a-b)$ The importance of this is to allow us to cut down on time when calculating the phase space itself by obtaining two quandrants while only calculating one

REFERENCES

Adachi S , Toda M & Ikeda K , 1988, Phys Rev Lett **61**, 659

Arrechi F T , Muecci R , Puccioni G & Tredicce J , 1982, Phys Rev Lett **49**, 1217

Auerbach D , Cvitanovic P , Eckmann J , Gunaratne G and Procaccia I , 1987, Phys Rev Lett **58**, 2387

Balazs N L , in *Quantum Chaos*, edited by H Cerdeira, R Ramaswammy, M Gutzwiller and G Casati, (World Scientific, Singapore, 1990), p 296

Berge P , Pomeau Y & Vidal V , Order Within Chaos (Wiley, New York, 1987)

Berman G P , Rubaev V Yu and Zaslavsky G M , 1991, Nonlinearity **4**, 543

Berry M V , 1984, Physica **10D**, 369

Berry M V & Robnik M , 1986, J Phys A **19**, 649

Blumel R & Esser B , 1994, Phys Rev Lett **72**, 3658

Cary J R , Meiss J D & Bhattacharjee A , 1981a, Phys Rev A **23**, 2744

Cary J R & Meiss J D , 1981b, Phys Rev A **24**, 2664

Casati G , Chirikov B V , Israilev F M & Ford J , in *Stochastic Behaviour in Classical and Quantum Hamiltonian Systems*, edited by G Casati and J Ford, Lecture Notes in Physics Vol 93 (Springer, Berlin,1979),p 334

Chernikov A A , Sagdeev R Z , Usikov D A , Zakharov M Yu & Zaslavsky G M , 1987, Nature **326**, 559

Chernikov A A , Sagdeev R Z , Usikov D A & Zaslavsky G M , 1987, Phys Lett A **125**, 101

Chernikov A A , Sagdeev R Z , Usikov D A & Zaslavsky G M , 1989, Sov Sci Rev C Math Phys **8**, 83

Chirikov B V , 1979, Phys Rep **52**, 265

Chirikov B V Israilev F M & Shepelyansky D L , 1981, Sov Sci Rev C **2**, 209

Chirikov B V in *Reviews of Plasma Physics*, Vol **13**, edited by B B Kadomtsev (Consultants Bureau, New York, 1987), p 1

Cleary P W , 1990, Phys Rev A **41**, 2924

Cohen D , 1991, Phys Rev A **43**, 639

Cvitanovic P , Universality in Chaos (Springer-Verlag, New York, 1990)

D'Ariano G , Evangelista L & Saraceno M , 1992, Phys Rev A **45**, 3646

Daly M V & Heffernan D M , 1994, Submitted to Journal of Physics A

Devaney R L , An Introduction to Chaotic Dynamical Systems 2*ed* (Addison-Wesley, Massachusetts, 1989)

Duhem P , La Théorie Physique Son Objet et sa Structure (Chevalier et Rivière, Paris, 1906)

Feigenbaum M , 1978, J Stat Phys **19**, 25

Feigenbaum M , 1979, J Stat Phys **21**, 669

Feigenbaum M , Jensen M and Procacca I , 1986, Phys Rev Lett **56**, 1503

Fishman S , Grempel D R & Prange R E , 1984, Phys Rev Lett **49**, 509

Fox R F & Edison J C , 1987, Phys Rev A **36**, 4321

Fox R F & Lan B L , 1990, Phys Rev A **41**, 2952

Fox R F & Elston T C , 1994, Phys Rev E **49**, 3683

Gerry C C & Schneider T , 1990, Phys Rev A **42**, 1033

Goggin M E , Sundaram B & Milonni P W , 1990, Phys Rev A **41**, 5705

Gradshteyn I S & Ryzhik I M , Table of Integrals, Series and Products 4*ed* (Academic Press, New York, 1965)

Grempel D R , Prange R E & Fishman S , 1984, Phys Rev A**29**, 1639

Guevera M R , Glass L & Shrier A m *Universality in Chaos* 2*ed*, edited by P Cvitanovic (Adam Hilger, Bristol, 1989), p 178

Gutzwiller M , Chaos in Classical and Quantum Mechanics (Springer-Verlag, New York, 1990)

Hadamard J , 1898, J Math Pure Appl **4**, 27

Hannay J H & Berry M V , 1980, Physica **1D**, 267

Heffernan D M , Jenkins P , Daly M V , Hawdon B J & O'Gorman J , 1992, Int Jour Theor Phys **31**, 1345

Helleman R H G , in *Fundamental Problems in Statistical Mechanics*, vol **5**, edited by E G D Cohen, (North Holland, Amsterdam, 1980), p 165 also in *Universality in Chaos* 2*ed*, edited by P Cvitanovic, (Adam Hilger, Bristol, 1989), p 37

Heller E J in *Chaos and Quantum Physics*, edited by M J Giannoni, A Voros and J Zinn-Justin, (North-Holland, Amsterdam, 1991), p 547

Hillery M , O' Connell R F , Scully M O & Wigner E P , 1984, Phys Rep **106**, 121

Hogg T & Huberman B A , 1983, Phys Rev A **28**, 22

Hudson J L & Mankin J C in *Universality in Chaos* 2*ed*, edited by P Cvitanovic (Adam Hilger, Bristol, 1989), p 157

Husimi K , 1940, Proc Phys Math Soc Japan **22**, 264

Ishizaki M , Horita T , Kobayashi T & Mori H , 1991, Prog Theor Phys **85**, 1013

Israilev F M , 1990, Physics Reports **196**, 299

Jensen R V , 1992, Nature **355**, 311

Karney C F F , Rechester A B & White R B , 1982, Physica **4D**, 425

Kervorkian J , Partial Differential Equations (Wadsworth & Brooks, California, 1990)

Kimball J , Singh V & D'Souza M , 1992, Phys Rev A **45**, 7065

Kus M , Zakrzewski J & Zyczkowski K , 1991, Phys Rev A **43**, 4244

Lewenkopf C H , 1990, Phys Rev A **42**, 2431

Libchaber A & Maurer J in *Universality in Chaos* 2*ed*, edited by P Cvitanovic (Adam Hilger, Bristol, 1989), p 109

Lichtenberg J & Wood P B , 1989, Phys Rev A **39**, 2153

Louisell W , Radiation and Noise in Quantum Electronics (McGraw-Hill, New York, 1964)

Lowenstein J H , 1991, Phys Rev A **43**, 4104

Lu Zi-Min, Heagy J , Vallieres M & Yuan Jian-Min, 1991, Phys Rev A**43**, 1118

Mandelbrot B B , The Fractal Geometry Of Nature (Freeman, San Francisco, 1982)

May R M , 1976, Nature **261**, 459

Messiah A , Quantum Mechanics Vol 1 (North-Holland, Amsterdam, 1976)

Milburn G J & Holmes C A , 1991, Phys Rev A **44**, 4704

Ott E , Chaos in Dynamical Systems (Cambridge University Press, Cambridge, 1993)

Poincaré H , Science et Méthode (Ernest Flammarion, Paris, 1908)

Press W H , Teukolsky S A , Vetterling W T & Flannery B P , Numerical Recipes in C 2*ed* (Cambridge University Press, Cambridge, 1992)

Radons G & Prange R E , in *Quantum Chaos*, edited by H Cerdeira, R Ramaswammy, M Gutzwiller and G Casati, (World Scientific, Singapore, 1990), p **333**

Ray D S , 1990, Phys Rev A **42**, 5975

Rechester A B & White R B , 1980, Phys Rev Lett **44**, 1586

Reulle D & Takens, F, 1971, Math Phys **20**, 167

Robnik M & Berry M V , 1986, J Phys A **19**, 669

Saraceno M , 1990, Ann Phys **199**, 37

Schack R & Caves C M , 1993, Phys Rev Lett **71**, 525

Scharf R & Sundaram B , 1991, Phys Rev A **43**, 3183

Scharf R & Sundaram B , 1992, Phys Rev A **45**, 3615

Schmera G , Jung P & Moss F , 1992, Phys Rev A **45**, 5462

Shepelyansly D , 1983, Physica **8D**, 208

Shepelyansly D , 1993, Phys Rev Lett **70**, 1787

Tanner G , Scherer P , Bogomonly E B , Eckhardt B & Wintgen D , 1991, Phys Rev Lett **67**, 2410

Testa J , Perez J & Jefferies C , 1982, Phys Rev Lett **48**, 714

Wigner E , 1932, Phys Rev **40**, 749

Zaslavsky G M & Filonenko N N , 1968, Zh Eskp Teor Fiz **54**, 1590

Zaslavsky G M , Zakharov M Yu , Sagdeev R Z , Usikov D A & Chernikov A A , 1986, Zh Eksp Teor Fiz **91**, 500

Zhang Wei-Min, Yuan Jian-Min, Feng Da Hsuan, Pan Q & Tjon J , 1990, Phys Rev A **42**, 3646